VOLUME 39 APRIL 1953 NUMBER 4

PROCEEDINGS
OF THE
NATIONAL ACADEMY OF SCIENCES
OF THE
UNITED STATES OF AMERICA

EDITORIAL BOARD

LINUS PAULING, *Chairman* EDWIN B. WILSON, *Managing Editor*
ALEXANDER WETMORE, *Home Secretary* ROGER ADAMS, *Foreign Secretary*
WILLIAM W. RUBEY, *Chairman of the National Research Council*

J. W. BEAMS
R. E. CLELAND
W. W. RUBEY
HARLOW SHAPLEY
F. E. TERMAN
G. W. BEADLE
E. A. DOISY
G. C. EVANS
C. H. GRAHAM
J. T. PATTERSON
GREGORY BREIT
L. C. DUNN
W. F. LIBBY
J. VON NEUMANN
PAUL WEISS

Publication Office: Mack Printing Company, Easton, Pa.
Editorial Office and Home Office of the Academy
2101 Constitution Avenue, Washington 25, D. C.

Entered as Second-Class matter, June 21, 1920, at the Post-office at Easton, Pennsylvania, under the Act of August 24, 1912. Accepted for mailing at a special rate of postage provided for in section 1103, act of October 3, 1917. Authorized June 18, 1920.

Published Monthly Price per Annum, $7.50

OFFICERS OF THE ACADEMY

PRESIDENT ..... DETLEV W. BRONK
VICE PRESIDENT ..... EDWIN B. WILSON
FOREIGN SECRETARY ..... ROGER ADAMS
HOME SECRETARY ..... ALEXANDER WETMORE
TREASURER ..... WILLIAM J. ROBBINS

INFORMATION TO SUBSCRIBERS

Checks covering subscriptions to the PROCEEDINGS OF THE NATIONAL ACADEMY OF SCIENCES at the rate of $7.50 per annum should be made payable to the National Academy of Sciences, and sent to the Treasurer, National Academy of Sciences, 2101 Constitution Ave., Washington 25, D. C. Single numbers $0.75. These prices effective January, 1951.

Microfilm copies of the PROCEEDINGS are available to subscribers to the paper edition. The microfilm is a positive, furnished on metal reels, suitably labeled, and is distributed at the end of the volume year. Inquiries concerning purchase should be directed to University Microfilms, 313 N. First St., Ann Arbor, Michigan.

Past publications of the NATIONAL ACADEMY OF SCIENCES from 1863 to 1926 and of the NATIONAL RESEARCH COUNCIL from 1916 to 1925 are listed in the Index to the First Ten Volumes of these PROCEEDINGS. This Index appeared as Part 2 of Volume 13, No. 1, January, 1927, and is for sale separately at the price of $1.50. Orders should be sent to the Home Secretary, National Academy of Sciences, 2101 Constitution Ave., Washington 25, D. C.

Past volumes of the PROCEEDINGS may be obtained at five dollars per volume unless the sale of the volume would break a complete set of Volumes I to XXX. Single numbers may be obtained for fifty cents except where the sale of such numbers would break up a complete volume. Beginning with Volume 37 (1951), complete volumes are $7.50, and single numbers $0.75. Only forty complete sets of the PROCEEDINGS are available for sale —Volumes I to XXX price $200.00. Orders should be sent to the Home Secretary, National Academy of Sciences, 2101 Constitution Ave., Washington 25, D. C.

THE NATIONAL ACADEMY OF SCIENCES-NATIONAL RESEARCH COUNCIL also issues technical publications reviewing and correlating recent research. The *Bulletin* and *Reprint and Circular Series* have been replaced by a single publication series, available individually, or by subscription at 25% discount. For a list of available publications, with prices and ordering procedures, address the Publications Office, National Academy of Sciences-National Research Council, 2101 Constitution Avenue, Washington 25, D. C.

PROCEEDINGS
OF THE
NATIONAL ACADEMY OF SCIENCES

Volume 39 April 15, 1953 Number 4

*OXIDATION OF INTERMEDIATES OF THE TRICARBOXYLIC ACID CYCLE BY EXTRACTS OF AZOTOBACTER AGILE**

By Roy Repaske† and P. W. Wilson

Institute for Enzyme Research and Department of Bacteriology, University of Wisconsin, Madison

Communicated by E. B. Fred, February 19, 1953

Investigating the terminal carbohydrate metabolism of *Azotobacter vinelandii* 0, Stone and Wilson[1, 2] demonstrated by manometric and isotopic methods that the tricarboxylic acid (TCA) cycle is a primary path of oxidation. Karlsson and Barker[3] concluded from the results of simultaneous adaptation and isotopic dilution experiments with whole cells of *A. agile* 4.4 that acetate is not oxidized by any of the conventional metabolic pathways. As two organisms so closely related would not be expected to possess completely different terminal oxidative mechanisms, the oxidation of intermediates of the TCA cycle by *A. agile* has been reinvestigated using cell-free extracts as well as whole cells.

Methods.—*Azotobacter agile* 4.4 was grown on Burk's nitrogen-free mineral salts medium with 2% sucrose as the source of carbon. The cultures were grown in 500-ml. Erlenmeyer flasks containing 100 ml. of medium that had been inoculated with 5% of an active 24-hr. culture and incubated for 15 hrs. at 30°C. on a rotary shaker; both the quantity of inoculum and the incubation time were selected to give a large yield of young cells with a high protein content—about 12 grams of wet cells per liter containing 5–6% protein. The stock culture was maintained by 24-hr. serial transfer.

Details of the methods for harvesting the cells and for preparing the cell-free extracts are described by Wilson and Knight.[4] Several methods for making the enzyme preparations were tested, including grinding in a Booth-Green mill, with glass beads and with alumina, but none was as satisfactory as breaking in a Raytheon 10 Kc sonic oscillator.

Twelve grams of wet cells were suspended in a total volume of 40 ml. with cold 0.1 *M* $KHCO_3$, pH 8.4, and exposed for 10 minutes in the sonic oscillator cooled by circulating ice water. The endogenous respiration of

such a suspension is usually 100–200 μl O_2 per hr. per mg. N, but after dialyzing 5 hrs. against two changes of 0.04 *M* phosphate buffer, pH 7 (two liters), the endogenous activity drops below 50 μl. The preparations contained 1.4 to 2.2 mg. biuret protein nitrogen per ml.; extracts with less than 1.2 mg. N per ml. are unsatisfactory. In the experiments reported

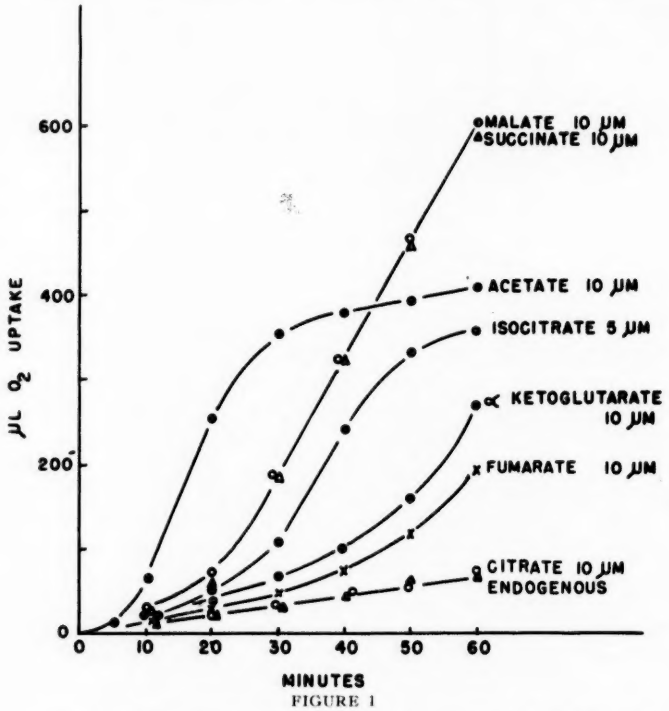

FIGURE 1

Oxidation of intermediates of tricarboxylic acid cycle by whole cells of *Azotobacter agile* 4.4. Flask contents: substrate as indicated; 6 μM. Mg phosphate; 40 μM. PO_4, pH 7; 1 ml. of cell suspension (0.179 mg. N/ml.) and H_2O to 3.0 ml.; 0.2 ml. 20% KOH in center well. Temperature of bath 33°C.

here the extracts were tested the same day as prepared; they can be kept overnight at −10°C. without appreciable loss in activity.

All experiments were made by conventional manometric procedures; oxygen uptake was measured at 33°C., the initial reading was made after 5 minutes of equilibration after which the substrate was tipped. Details of contents of the flasks are supplied in the tables and figures. The re-

agents were commercial products with the exception of the CoA (20% pantothenic acid) kindly supplied by Dr. Helmut Beinert and the TPN (triphosphopyridinenucleotide) prepared by the method of Kornberg and Horecker.[5]

Results.—Figure 1 illustrates typical results obtained with whole cells of *Azotobacter agile* 4.4. A period for adaptation was required to oxidize all members of the TCA cycle except acetate, which was immediately oxidized, and citrate, which was not oxidized even after an hour. An

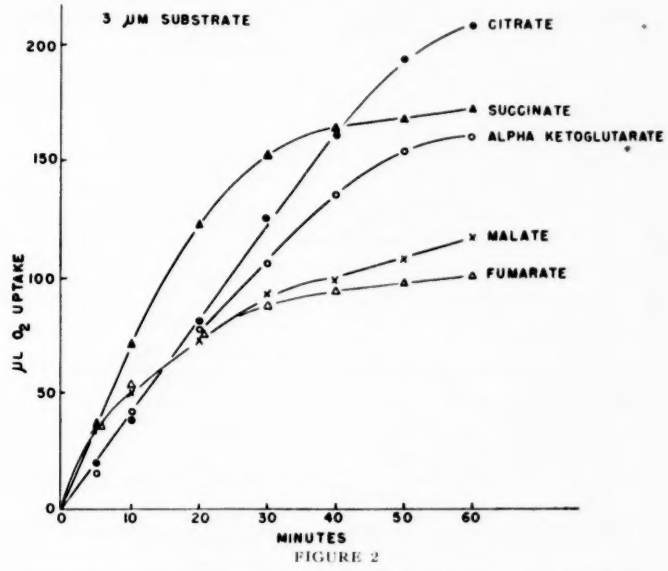

FIGURE 2

Oxidation of intermediates of tricarboxylic acid cycle by cell-free extracts of *Azotobacter agile* 4.4. Flask contents: 2 μM. $MgCl_2$, 500 μg. DPN, 16 μg. TPN, 19 μg. CoA, 30 μM. glutathione, 1 ml. enzyme (RD11; 2.09 mg. N/ml.), 3 μM. substrate and water to 3.0 ml.; 0.2 ml. 20% KOH in center well. Temperature of bath 33°C. Corrected for endogenous (16 μl. O_2/hr.).

entirely different result is obtained, however, when cell-free enzyme preparations are used (Fig. 2). Although the whole cells required adaptative periods of 15 to 60 minutes before the maximum rate of oxidation of various substrates is reached, extracts from these cells immediately oxidized all the TCA intermediates tested. This is most strikingly demonstrated with citrate; oxidation of isocitrate occurred at an even greater rate (not shown).

The dialyzed extracts must be supplemented with certain coenzymes for

maximum rates of oxidation with citrate, α-ketoglutarate and acetate. The quantities required under the conditions of our experiments are indicated in the captions for figures 2 and 3. The oxidation of isocitrate by enzymes from animal and yeast cells requires TPN. Extracts of *A. agile* slowly oxidize citrate in the presence of 500 μg. DPN (table 1), but when as little as 4 μg. TPN is also added the $Q_{O_2}(N)$ is increased almost threefold; 16 μg. TPN per vessel caused a slightly higher rate of oxidation. Although

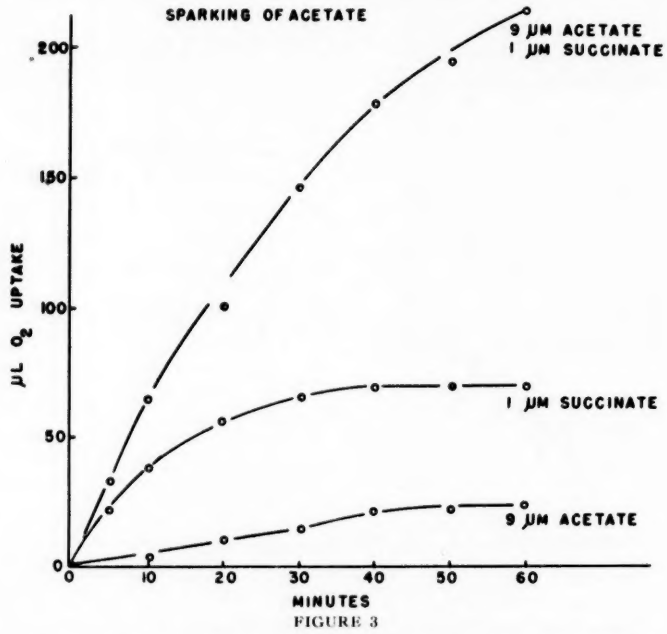

FIGURE 3

Oxidation of acetate by cell-free extracts of *Azotobacter agile* 4.4. Flask contents: 1 ml. extract (RD9; 1.78 mg. N/ml.), 2 μM. $MgCl_2$, 500 μg. DPN, 16 μg. TPN, 19 μg. CoA, 30 μM. glutathione, 4 μM. ATP, substrate as indicated, and water to 3.0 ml.; 0.2 ml. 20% KOH in center well. Temperature of bath 33°C. Corrected for endogenous (18. μl. O_2/hr.).

experiments were conducted with citrate as substrate, isocitric dehydrogenase activity had been demonstrated, and it is probable that it is the isocitric dehydrogenase of *A. agile* that is TPN-linked. Coenzyme A also stimulated the oxidation of citrate, but the effects may arise from the CoA requirement for oxidation of α-ketoglutarate, presumably the product of citrate oxidation.

DPN, CoA and Mg^{++} were all found to increase the rate of oxidation of

α-ketoglutarate (table 2). Lindstrom[6] has demonstrated these same requirements for oxidation of this compound by a soluble α-ketoglutaric oxidase from *Aztobacter vinelandii*, and Sanadi and Littlefield[7] found CoA and DPN are required for the oxidation of α-ketoglutarate by a soluble preparation from animal tissue. The dialyzed extract from *A. agile* oxidizes α-ketoglutarate slowly without added DPN; if 50 μg. DPN is

TABLE 1

OXIDATION OF CITRATE BY EXTRACTS OF *Azotobacter agile*

PREPARATION	SYSTEM	μl. O_2 UPTAKE[b]		
		$Q_{O_2}(N)$	30 min.	60 min.
RD9	Complete[a]	249	215	340
	4 μg. TPN	191	157	256
	Minus TPN	69	63	133
RD10	Complete	156	144	200
	Minus TPN	47	45	54
	Minus CoA	56	62	111

[a] Complete system contains 16 μg. TPN; for other constituents see figure 2.
[b] Figures in all tables corrected for endogenous respiration.

RD9 1.78 mg. N/ml.; 10 μM. citrate per vessel; endogenous, 18 μl. O_2/hr.
RD10 1.86 mg. N/ml.; 3 μM. citrate per vessel; endogenous, 21 μl. O_2/hr.

TABLE 2

OXIDATION OF α-KETOGLUTARATE BY EXTRACTS OF *A. agile*

PREPARATION	SYSTEM	μl. O_2 UPTAKE		
		$Q_{O_2}(N)$	30 MIN.	60 MIN.
RD8	Complete[a]	199	140	174
	50 μg. DPN	85	58	82
	Minus DPN	42	32	55
RD10	Complete	137	117	136
	Minus DPN	51	47	75
	Minus CoA	50	43	75
	Minus Mg^{++}	83	79	127

[a] Complete system contains 500 μg. DPN; for other constituents see figure 2.

RD8 1.70 mg. N/ml.; endogenous, 17 μl. O_2/hr.
RD10 1.86 mg. N/ml.; endogenous, 21 μl. O_2/hr.

added per vessel, the $Q_{O_2}(N)$ is increased slightly but still is only about 40% of that obtained with 500 μg. DPN per vessel. Since the reactive group of CoA is believed to be a sulfhydryl group, glutathione was used as a reducing agent (cysteine is itself oxidized and thus raises the apparent endogenous respiration). In the absence of added DPN or CoA the rate of α-ketoglutarate oxidation is one-third of maximum. CoA levels above 12–15 μg. per vessel did not increase the oxygen uptake.

Data in table 2 also demonstrate the stimulatory effect of Mg^{++}. The

over-all oxygen uptake per hour is about the same as in the complete system, but the rate of oxidation is more rapid with added Mg^{++}. ATP, cocarboxylase, and protogen have no effect on α-ketoglutarate oxidation.

Acetate alone, although immediately and rapidly oxidized by whole cells, is not oxidized to any extent by cell-free extracts (table 3). With the addition of small quantities of succinate (1 μM.), the net oxygen uptake in an hour corrected for oxidation of succinate alone is 5–6 times the uptake of acetate alone. As can be seen from figure 3, this "sparking" of acetate still continues at a rapid rate after the oxidation of the individual substrates has leveled off.

TABLE 3

ACETATE OXIDATION BY EXTRACTS OF *A. agile*

PREPARATION	SYSTEM	SUBSTRATE	$Q_{O_2}(N)$	μL. O_2 UPTAKE 60 MIN.
RD12	Complete[a]	9 μM. Acetate	11	20
		9 μM. Acetate + 1 μM. Succinate	104	158
		1 μM. Succinate	30	64
	No ATP	9 μM. Acetate	0	0
		9 μM. Acetate + 1 μM. Succinate	79	103
		1 μM. Succinate	89	81
RD9	Complete	9 μM. Acetate	17	24
		9 μM. Acetate + 1 μM. Succinate	187	215
		1 μM. Succinate	96	70
	No CoA	9 μM. Acetate	0	0
		9 μM. Acetate + 1 μM. Succinate	91	67
		1 μM. Succinate	67	45

[a] See figure 3 for complete system.

RD12 2.12 mg. N/ml.; endogenous, 18 μl. O_2/hr.
RD9 1.78 mg. N/ml.; endogenous, 21 μl. O_2/hr.

Discussion.—Two terminal oxidative cycles are generally postulated for bacteria, the dicarboxylic and the tricarboxylic,[8] although the data of Karlsson and Barker with whole cells of *Azotobacter agile* suggest that neither of these functions in this organism. The chief difference between the di- and tricarboxylic acid cycles is in the mechanism for formation of succinate: whether directly from two molecules of acetate or via citrate. One reason for rejecting the operation of the TCA cycle in *A. agile* has been the apparent inability of cells which immediately oxidize acetate to oxidize other members of the cycle without a period of adaptation (principle of simultaneous adaptation). However, this particular objection need no

longer be considered a serious handicap since such cells do possess the necessary enzyme systems, i.e., cell-free preparations readily oxidize the intermediates.

Further evidence supporting the existence of the TCA cycle in *A. agile* is the similarity of coenzyme and metal requirements for the oxidation of acetate, citrate, and α-ketoglutarate by extracts of these cells and these requirements in preparations from animal, yeast, and other bacterial species.

Finally, the "sparking" of acetate oxidation by succinate is strong evidence for the participation of a TCA cycle.[9] Either oxalacetate or a precursor must be available to condense with acetate; thereafter, oxalacetate is regenerated at each turn of the cycle. A requirement for a dicarboxylic acid would not be expected if two molecules of acetate condensed to form succinate. Also, it should be noted that Stern *et al.*[10] observed in 1950 that *A. agile* possesses the enzyme for condensing acetate with oxalacetate. Recently the reactions for formation of citrate from acetate have been clarified;[11, 12] in light of this work it seems significant that extracts of *A. agile* readily oxidize acetate only when ATP and CoA are present (table 3).

Although it is recognized that manometric experiments alone are not sufficient to demonstrate conclusively a metabolic pathway, it is emphasized that all results with cell-free extracts of *A. agile* are compatible with the view that the TCA cycle is a terminal oxidation pathway in this organism. These results do not agree with conclusions based on experiments with cell suspensions but do agree with analogous (and more extensive investigations) made with the closely related organism, *A. vinelandii*.

Summary.—The ability of unadapted cells of *Azotobacter agile* 4.4 and of cell-free extracts from such cells to oxidize intermediates of the tricarboxylic acid cycle has been compared. Adaptive periods were required before whole cells oxidize all substrates except acetate and citrate. Acetate was immediately oxidized; citrate was not oxidized even after an hour. Cell-free extracts, however, oxidized all these substrates immediately.

Dialyzed extracts of *A. agile* 4.4 had coenzyme requirements similar to those for the corresponding enzymes of the tricarboxylic acid cycle found in animal tissue. These included: TPN for citrate oxidation; CoA, DPN, and Mg^{++} for α-ketoglutarate oxidation; and Mg^{++}, CoA, and ATP for acetate oxidation. Acetate is not oxidized by these extracts unless it is "sparked."

All these findings are compatible with the conclusion that a tricarboxylic acid cycle functions in *A. agile* 4.4 as has been previously established for *A. vinelandii*.

Acknowledgment.—We wish to express our appreciation for the many helpful suggestions offered by Dr. D. E. Green.

* This work is supported in part by grants from the Rockefeller Foundation, Atomic Energy Commission, and the Research Committee of the Graduate School from funds provided by the Wisconsin Alumni Research Foundation.

† Atomic Energy Commission predoctoral fellow.

[1] Stone, R. W., and Wilson, P. W., *J. Bact.*, **63,** 605 (1951).

[2] Stone, R. W., and Wilson, P. W., *J. Biol. Chem.*, **196,** 221 (1951).

[3] Karlsson, J. L., and Barker, H. A., *ibid.*, **175,** 913 (1948).

[4] Wilson, P. W., and Knight, S. G., *Experiments in Bacterial Physiology*, 2nd ed., Burgess Publishing Co., Minneapolis, 1952, p. 42.

[5] Kornberg, A., and Horecker, B. L., unpublished method.

[6] Lindstrom, E. S., *J. Bact.* (in press), 1953.

[7] Sanadi, D. R., and Littlefield, J. W., *Science*, **116,** 327 (1952).

[8] Ajl, S. J., *Bact. Revs.*, **15,** 211 (1951).

[9] Green, D. E., Loomis W. F., and Auerback, V. F., *J. Biol. Chem.*, **172,** 389 (1948).

[10] Stern, J. R., Shapiro, B., and Ochoa, S., *Nature*, **166,** 403 (1950).

[11] Stern, J. R., Shapiro, B., Stadtman, E. R., and Ochoa, S., *J. Biol. Chem.*, **193,** 703 (1951).

[12] Stadtman, E. R., *Ibid.*, **196,** 535 (1952).

A BIOCHEMICALLY SPECIFIC METHOD FOR ENZYME ISOLATION

By Leonard S. Lerman*

Institute of Radiobiology and Biophysics, The University of Chicago

Communicated by Linus Pauling, January 29, 1953

It is at present accepted that the action of an enzyme requires as a first step the temporary combination of the substrate with a specific site on the enzyme, and that competitive inhibitors act by reversibly substituting for the substrate in combination with the specific site. If then, a specific competitive inhibitor or a suitable substrate of an enzyme is coupled to the surface of an inert solid, it may be expected that the enzyme will be reversibly bound to the solid through combination with the attached group, while enzymes with different specificities or other proteins will not be bound. The enzyme could later be released by a change in the medium to conditions unfavorable for combination, as, for example, change in pH or salt concentration. Alternatively, by the use of a solution of a competitive inhibitor (not necessarily the same as that coupled on the adsorbent) the enzyme will, according to the principle of mass action, be returned into solution by an additional specific process. Thus the isolation of the enzyme would depend directly on its catalytic specificity rather than, as in conventional procedures, its properties as a protein.

Mushroom tyrosinase was chosen for an experimental investigation because of convenience and the simplicity of the associated chemical proced-

ures. With suitable adsorbents a significant purification of the enzyme was achieved.

Experimental.—Tyrosinase: An aqueous extract of mushrooms minced in cold acetone was precipitated with ammonium sulfate, according to the procedure of Mallette, *et al.*,[1] the precipitate was redissolved and dialyzed thoroughly against distilled water. The resulting enzyme solution, usually diluted with malonate buffer, pH 5.8, was used in all experiments. For measurement of activity, aliquots of 0.05 ml. were incubated at 4°C. with 0.50 ml. of a solution containing 0.1 per cent catechol, 0.5 per cent gelatin, and 0.5 per cent piperidine in 0.1 *M* malonate buffer, pH 5.8. After twenty-four hours the mixture was diluted with 1.00 ml. of water,

TABLE 1

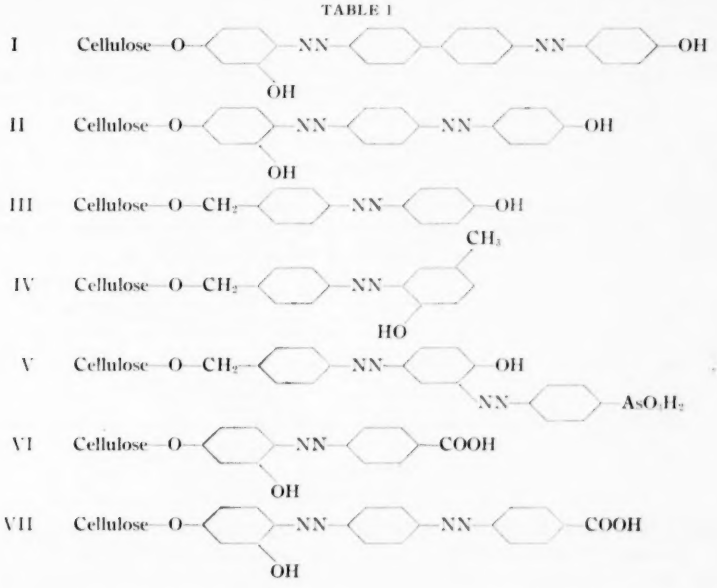

and the optical density of 390 mμ was measured in a 1.00 cm. cell. Because of the well-known reaction inactivation[2] of tyrosinase, the optical density reaches a stationary value, which remains unchanged for at least another day. Its dependence on the amount of enzyme was found to be linear up to a density of 0.92, with a standard error of estimate of less than 0.01. One unit of enzyme activity was arbitrarily defined as the amount which, under the above conditions, would yield a density of 42.4. Ludwig and Nelson[3] found a similar stationary value and proportionality to the amount of enzyme in the total oxygen uptake. Relative measurements of total protein concentrations were made by the colorimetric ninhydrin method of Kunkel and Ward.[4]

Adsorbents.—Since it was found that azodyes prepared by coupling an aromatic amine with phenol inhibit tyrosinase, various adsorbents, listed in table 1, containing *p*-azophenol groups and related groups were prepared from aromatic ethers of cellulose. Powdered cellulose (Solka-Floc BW200[5]) was partially etherified by one of two procedures: (*a*) refluxing in benzene with phosphorus tribromide, about two grams per hundred grams of cellulose, followed by refluxing in alcohol with an excess of sodium *m*-hydroxyphenoxide, or (*b*) refluxing with sodium ethylate and *p*-nitrobenzyl bromide, about two grams per hundred of cellulose, followed by reduction with sodium dithionite. The original fibrous character was not

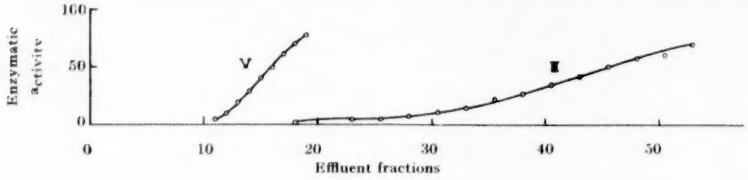

FIGURE 1

Frontal chromatograms obtained from the percolation of diluted crude tyrosinase through a 0.20-g. column of adsorbent III or a similar column of adsorbent V. The fractions were 0.05 ml. each, and the holdup volume was about 0.45 ml.

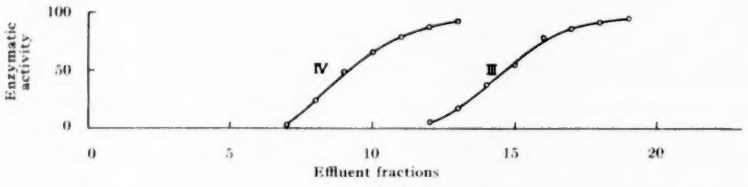

FIGURE 2

Frontal chromatograms from 0.12-g. columns of adsorbents IV and III. The fractions were 0.05 ml. each, and the holdup volume was about 0.35 ml.

appreciably changed. Coupling of the diazonium salts was indicated by the usual color changes; the colors were fast to washing with dilute acids, alkalis, etc. Similarly constituted dyes which were not bound through the ether linkage were found to be easily washed away.

Enzyme Adsorption.—Demonstration of adsorption by the cellulose derivatives, tests on specificity, and rough estimation of the capacity of the adsorbents were carried out by the technique of frontal analysis. As the enzyme solution percolated continuously through a column of the adsorbent, successive fractions of the effluent were collected and tested for activity. In the absence of adsorption the enzyme appeared immediately

after the interstitial fluid in the column (the holdup volume) was displaced by the entering solution. When adsorption occurred, the enzyme appeared later according to the capacity of the adsorbent. For quantitative experiments an aliquot of crude enzyme, usually just enough to saturate the adsorbent, was introduced into a column followed immediately by buffer of the same pH and later by the eluent.

Results.—Frontal chromatograms (Figs. 1 and 2) at pH 5.8 or 6.3 showed cellulose *p*-azophenol preparations I, II, and III to be effective adsorbents, while no retention of the enzyme by IV, V, VI, or VII was found except for the slight non-specific adsorption shown also by untreated cellulose. With certain of the crude tyrosinase preparations a small, well-defined shoulder in the frontal chromatograms previous to the emergence of the maximum concentration of the enzyme was noted, indicating the presence of at least a second catalytically active substance. Some dependence on salt concentration was found, in that dilution of the malonate to 0.001 *M*

TABLE 2

ADSORPTION OF 0.30 ML. CRUDE ENZYME SOLUTION ON FIVE GRAMS OF ADSORBENT III, THE COLUMN THEN WASHED WITH MALONATE AND ELUTED WITH PYROPHOSPHATE

	ACTIVITY PER ML. (ARBITRARY UNITS)	PROTEIN PER ML. (ARBITRARY UNITS)	VOLUME, ML.	FRACTION OF TOTAL ACTIVITY
Crude enzyme	1.00	122.4	0.30	1.00
Effluent from wash	...	...	..	0.03
Eluate fractions				
2 + 3	0.001	...	1.0	0.00
4 + 5	0.025	0.264	1.0	0.08
6 + 7	0.106	0.214	1.0	0.35
8 + 9	0.032	0.007	1.0	0.11
10 + 11	0.007	...	1.0	0.02
Total recovery in eluate				0.56

inhibited adsorption, and addition of sodium chloride to 0.5 *M* greatly increased non-specific adsorption. However, in the vicinity of 0.04 to 0.1 *M* near pH 6 malonate, phthalate, and chloride were satisfactory and interchangeable. The addition of considerable amounts of extraneous protein tended to inhibit adsorption.

On the passage through the column of a small sample of crude enzyme followed by buffer, nearly all of the original protein, now devoid of enzyme activity, was found in the effluent. The enzyme had remained on the adsorbent, and the enzyme was retained through protracted washing with malonate but was rapidly eluted by 0.02 *M* pyrophosphate at pH 8.3, 0.1 *M* glycine at pH 9.6, or other buffers of similar pH. Elution was also effected by a solution of sodium benzoate, a strong competitive inhibitor, at pH 6.3. Data on a single process of adsorption, washing and elution by pyrophosphate are given in table 2. Approximately 56 per cent of the

original enzyme was recovered in all fractions of the eluate; the most active fraction contained 62 per cent of the total recovered. The ratio of enzyme activity to protein concentration in that fraction was 61 times as great as in the original crude preparation. Since highly purified preparations of tyrosinase are more rapidly inactivated than crude preparations while acting on catechol,[2] a somewhat higher value might have been indicated by a different method of enzyme assay.

Continuing study of the method is directed toward determining its applicability to the purification of various enzymes, improving the capacity of the adsorbents, and achieving a degree of purification closer to that theoretically possible.

* Schenley Fellow, 1949–1951. Present address: Laboratory of Chemical Embryology, University of Colorado Department of Medicine, Denver, Colo.

[1] Mallette, M. F., *et al.*, *Arch. Biochem.*, **16**, 283 (1948).

[2] Nelson, J. M., and Dawson, C. R., *Advances in Enzymology*, **4**, 99 (1944).

[3] Ludwig, B. J., and Nelson, J. M., *J. Am. Chem. Soc.*, **61**, 2601 (1939).

[4] Kunkel, H. G., and Ward, S. M., *J. Biol. Chem.*, **182**, 597 (1950).

[5] Provided by the Brown Company, Chicago.

*THE SOLUBILITY OF THE DIMETHYLETHERATE OF ALUMINUM BROMIDE IN METHYL BROMIDE IN THE PRESENCE OF SATURATED HYDROCARBONS**

By Luther M. Foster and Charles A. Kraus

Metcalf Research Laboratory, Brown University

Communicated February 4, 1953

In the course of an investigation of the polymerization of ethylene in methyl bromide in the presence of aluminum bromide at −33°C., it appeared that the ethylene, or its polymerization products, did not complex with all the aluminum bromide present, although much more than one mole of ethylene reacted per mole of aluminum bromide.[1] At the same time, the hydrocarbon recovered on decomposing the complex with water was of higher molecular weight than expected, even though the proportion of ethylene to aluminum bromide was little greater than unity.

It was thought that the uncombined aluminum bromide might be separated out by adding dimethyl ether which forms the stable complex $AlBr_3 \cdot (CH_3)_2O$, whose solubility in methyl bromide is relatively low, particularly at lower temperatures. However, the solubility of the etherate was still rather high, even at −78°C. In a later investigation, propane was added to the methyl bromide solution of the etherate with a view to reducing its solubility. The solubility of the etherate in pure propane is negligible.

On carrying out some preliminary experiments, the expected large solubility decrease on addition of propane was not found and, moreover, singularities appeared in the solubility curve which could hardly be ascribed to experimental error. Accordingly, a series of careful measurements was carried out with the propane-methyl bromide mixtures at −78°C. These measurements established the correctness of the earlier observations. Measurements were then carried out at the same temperature with *n*-butane, isobutane and *n*-pentane as diluents.

All materials employed were carefully tested and, if necessary, purified. Aluminum bromide was distilled three times under reduced pressure; the product was colorless.

After purification, the vapor pressure of methyl bromide was measured over the temperature range −89.8° to +40°C. The experimental values are given to 0.25% by the empirical equation:

$$\log_{10} p = \frac{-588.517}{T} - 2.36660 \log_{10} T + 14.3997.$$

The boiling point as interpolated was found to be 3.66 ± 0.05°, in good agreement with 3.58 ± 0.05°, as reported by Egan and Kemp.[2] The freezing point was found to be −93.65 ± 0.05° in agreement with −93.66 ± 0.05° as reported by Egan and Kemp.

Dimethylether, said to have a purity of 99.9%, was passed over activated alumina. At 25° and 760 mm., the vapor was found to have a density of 1.918 g./l. in agreement with the value reported by Kennedy, Sagenkahn and Aston.[3] To establish the purity of the propane, its vapor pressure was measured between −95.50 and −42.00°. Experimental values are reproduced within 0.25% by the empirical equation

$$\log_{10} p = \frac{-1507.776}{T} - 5.02943 \log_{10} T + 21.2951.$$

By interpolation, the boiling point was found to be −42.12 ± 0.05° in agreement with Rossini's[4] value of −42.1°.

All solubility measurements were carried out at −78.08 ± 0.05°C. in a dry ice–acetone bath whose temperature was manually controlled. Temperatures were measured by means of a copper-constantan thermocouple, the tip of which was encased in a thin-walled glass tube and immersed in the solution. The thermocouple was calibrated by means of standard melting point samples and could be read to 0.02°.

The solutions were prepared in a tube having a capacity of approximately 150 cc.; it was provided with a magnetic stirrer which was operated manually. A weighed sample of aluminum bromide in a fragile bulb was introduced into the solubility tube and about 60 cc. of methyl bromide was condensed on the bromide. When the bromide was in solution, dimethyl

ether, in approximately 10% excess, was condensed in the solubility tube. The desired amount of hydrocarbon was then distilled into the system. Thereafter, the thermocouple was introduced.

The mixture was kept at $-78°$ for 20 hours (3 in the case of propane) and stirred from time to time. At the end of that period, a fritted filter was introduced. This filter was connected with a receiver of known volume and a quantity of solution was passed over into the receiver. Thereafter, the solution in the receiver was evaporated and the receiver was detached and weighed, thus yielding the weight of compound in a known volume of solution.

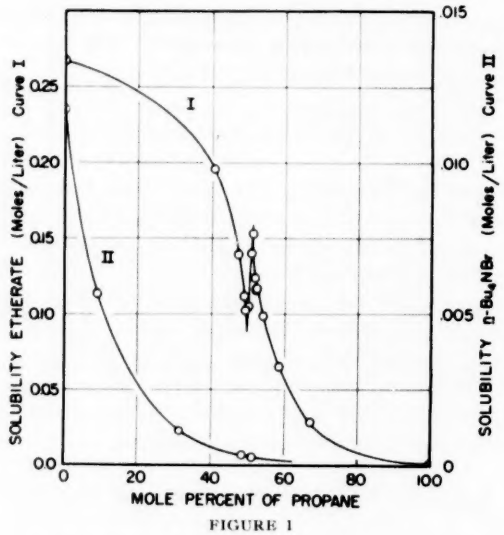

FIGURE 1

I. Solubility of $AlBr_3 \cdot (CH_3)_2O$ in propane-methyl bromide mixtures. II. Solubility of Bu_4NBr in propane-methyl bromide mixtures.

The product obtained on evaporation of the solute was shown to be the mono-etherate of aluminum bromide by analysis for aluminum and bromine. In the propane series, the residual product was evacuated for two minutes only and the results are slightly high by a few per cent in the methyl bromide-rich solutions (10% in pure methyl bromide). In the case of other hydrocarbons, the product was pumped for 30 minutes. With a solution containing 50.8 mole per cent propane, the weight obtained analytically was 98.6% of that obtained on weighing the residue. With the other hydrocarbons, the error was less than one per cent.

In the case of the isobutane mixtures, the receiver was provided with a pair of electrodes and the conductance of the solutions was measured as they were withdrawn.

The density of the liquids employed was determined at −81°C. as follows: methyl bromide, 1.9383; propane, 0.6263; *n*-butane, 0.6810; isobutane, 0.6681; *n*-pentane, 0.7148.

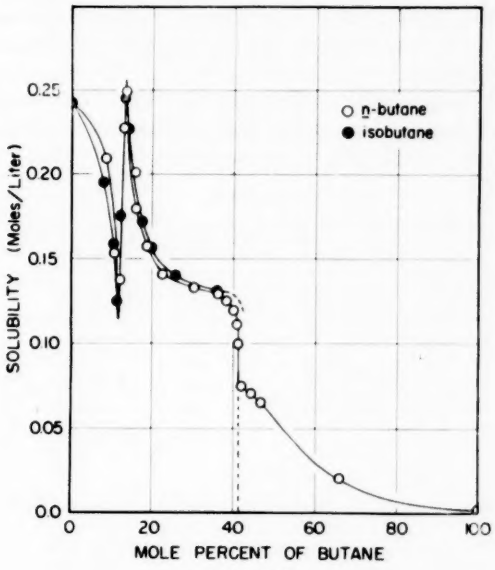

FIGURE 2

Solubility of $AlBr_3 \cdot (CH_3)_2O$ in mixtures of methyl bromide and *n*-butane and isobutane.

Measured values of the solubility of the dimethylether-aluminum bromide complex in propane-methylbromide mixtures are recorded in table 1 and are shown graphically in figure 1, curve I.

TABLE 1

SOLUBILITY OF $AlBr_3 \cdot (CH_3)_2O$ IN *n*-PROPANE-METHYL BROMIDE MIXTURES AT −78.08°

MOLE % PROPANE	SOLUBILITY, MOLES/L.	MOLE % PROPANE	SOLUBILITY, MOLES/L.	MOLE % PROPANE	SOLUBILITY, MOLES/L.
00.00	0.2668	49.96	0.1050	51.95	0.1163
40.65	0.1953	50.76	0.1397	52.33	0.1168
47.28	0.1396	51.22	0.1528	54.11	0.0983
48.85	0.1115	51.46	0.1244	58.56	0.0649
49.31	0.1021	51.69	0.1238	66.68	0.0280
				100.00	0.0000

The solubility curve consists of two branches; the first, at lower propane concentrations, is concave toward the axis of composition, the second is convex toward this axis. The two branches are joined by a nearly vertical section at a composition in the neighborhood of 50 mole per cent propane. At 49.3 mole per cent propane, the solubility reaches a value of 0.105 m./l. It then rises sharply to a value of 0.153 m./l. at a composition of 51.2 mole per cent propane. The solubility branch at higher propane concentrations is of normal form.

To check the experimental method, the solubility of tetrabutylammonium bromide was determined for the propane-methyl bromide mixtures. The results are shown graphically on curve II, figure 1. This curve is of the

TABLE 2

SOLUBILITY OF $AlBr_3 \cdot (CH_3)_2O$ IN *n*-BUTANE-METHYL BROMIDE MIXTURES AT $-78.08°$

MOLE % BUTANE	SOLUBILITY, MOLES/L.	MOLE % BUTANE	SOLUBILITY, MOLES/L.	MOLE % BUTANE	SOLUBILITY, MOLES/L.
0.00	0.2420	16.37	0.1794	40.23	0.1192
8.90	0.2094	18.97	0.1570	41.25	0.0996
11.31	0.1534	22.70	0.1406	42.24	0.0742
12.70	0.1374	30.58	0.1323	44.75	0.0703
13.28	0.2279	36.54	0.1292	46.80	0.0649
13.71	0.2492	38.60	0.1250	65.95	0.0194
				100.00	0.0000

TABLE 3

SOLUBILITY AND CONDUCTANCE OF $AlBr_3 \cdot (CH_3)_2O$ IN ISOBUTANE-METHYL BROMIDE MIXTURES AT $-78.08°$

MOLE % BUTANE	SOLUBILITY, MOLES/L.	SPEC. COND. $\times 10^6$	MOLEC. COND. $\times 10^3$	MOLE % BUTANE	SOLUBILITY, MOLES/L.	SPEC. COND. $\times 10^6$	MOLEC. COND. $\times 10^3$
0.00	0.2420	28.68	118.51	14.27	0.2272	3.984	17.53
8.00	0.1958	8.025	40.98	16.02	0.2011	3.235	16.08
10.67	0.1583	4.859	30.69	17.59	0.1720	2.269	13.19
11.49	0.1255	3.783	30.14	20.01	0.1562	...	...
12.28	0.1769	4.280	24.19	25.86	0.1408	0.578	4.11
13.22	0.2458	5.159	20.98	35.82	0.1319	0.149	1.13

expected form and the experimental values show no scatter. The observed discontinuities in the solubility curve of the aluminum bromide-ether complex cannot be accounted for on the basis of experimental error.

To eliminate the possibility of some unlooked-for interaction between methyl bromide and propane, the vapor pressure of mixtures of methyl bromide and propane was measured at $-78.08°$ from 0.0 to 43.5 mole per cent propane. The curve found was a regular one which was concave toward the axis of composition and which gave no evidence of any special type of interaction between the components.

The solubilities of aluminum bromide-dimethyletherate in *n*-butane-methyl bromide mixtures are presented in table 2 and those for the iso-

butane mixtures in table 3. The solubilities for both systems are shown graphically in figure 2, values in *n*-butane being represented by open circles, for isobutane by black circles. The solubility curves for the two systems appear to be identical. The slight differences found at higher concentrations of hydrocarbons are probably due to experimental error. It may be noted that the purity of the two butanes was established by means of their absorption spectra.

The solubility curve for the butane mixtures differs markedly from that of the propane mixtures. The solubility curve falls more rapidly with addition of butane than with that of propane and the first break comes in the

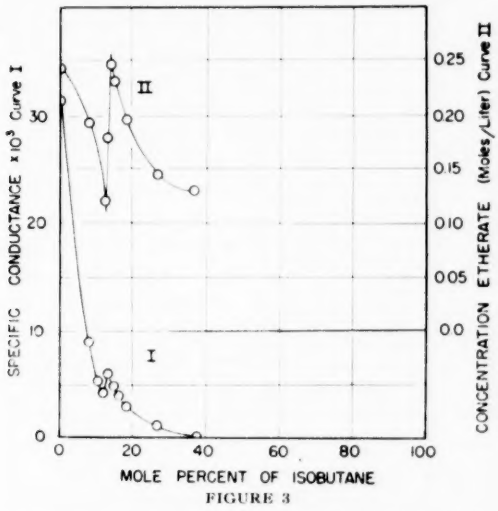

FIGURE 3

Solubility and conductance of $AlBr_3 \cdot (CH_3)_2O$ in isobutane-methyl bromide mixtures.

neighborhood of 10 mole per cent of hydrocarbon. The solubility then increases to a value of 24.9 as against 24.2 for pure methyl bromide. From the upper cusp of the solubility curve, the solubility begins to decrease in what might appear to be normal fashion but, on further addition of butane, the curve flattens out with a solubility in the neighborhood of 0.14.

In the neighborhood of 40 mole per cent butane, the solubility falls sharply from a value of 0.119 to 0.074. Thereafter, the solubility decreases in normal manner. This second discontinuity does not appear in the propane or the pentane mixtures.

In order to obtain a check on the measured solubilities in isobutane mixtures, the receptacle into which the solutions were withdrawn was provided

with a pair of electrodes and the resistance of the solutions was measured at $-78.08°$ prior to evaporation. This provided a value of the resistance from which the specific conductance and the molecular conductance of the solutions could be computed. In table 3, the composition of the mixture is given in column 1, the solubility of the etherate in column 2, the specific conductance of the solution in column 3 and the molecular conductance in column 4. The specific conductances are shown graphically in figure 3, curve I; the solubilities of the etherate are shown as curve II. The molecular conductances are shown in figure 4.

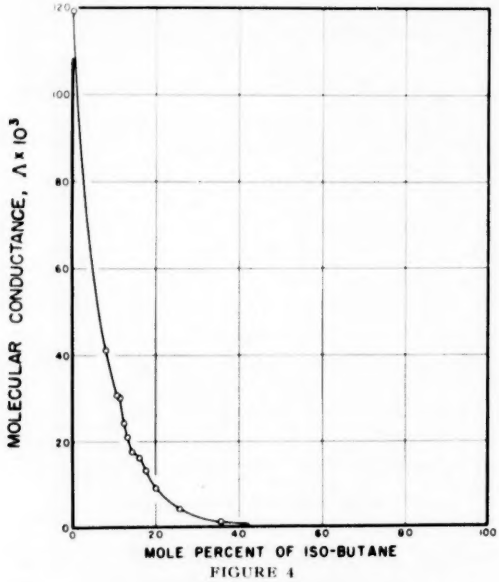

FIGURE 4

Molecular conductance of $AlBr_3 \cdot (CH_3)_2O$ in isobutane-methyl bromide mixtures.

As may be seen from figure 3, the curve of specific conductances closely parallels that of solubilities. At the lower cusp of the solubility curve, the specific conductance is 3.78×10^{-6}, at the upper cusp it is 5.16×10^{-6}; between the two cusps, the conductance increases in the ratio of 1.36:1. If the molecular conductance of the salt in the two mixtures were the same, then the salt concentration would have increased in that ratio. However, as many be seen from figure 4, as well as from table 3, the molecular conductance at the lower cusp is 30.1×10^{-3} while at the upper cusp it is 21.0×10^{-3}, a ratio of 1.43:1. If the solution at the upper cusp had the

same molecular conductance as at the lower cusp, the conductance ratios between the two cusps would be 1.95. In other words, on the basis of conductance measurements, we conclude that the concentration at the upper cusp is 1.95 times that at the lower cusp. Now the measured solubility at the lower cusp is 0.1255 and at the upper cups it is 0.2458 and the ratio is 1.96. Thus, the ratio of salt concentrations at the two cusps as determined by conductance measurements closely checks the measured solubility values.

A careful inspection of figure 4 will show that two small jogs occur in the curve of molecular conductance at compositions corresponding to the lower and upper cusps of the solubility curve. This indicates that a slight change is taking place in the strength of the electrolyte in solution which, if true, indicates that some change is taking place in the state of the electrolyte in solution.

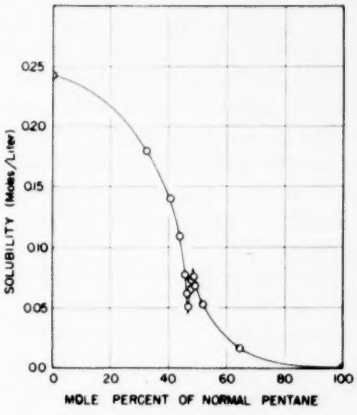

FIGURE 5

Solubility of $AlBr_3 \cdot (CH_3)_2O$ in *n*-pentane-methyl bromide mixtures.

Solubilities of the dimethyletherate of aluminum bromide in *n*-pentane-methyl bromide mixtures are presented in table 4 and are shown graphically in figure 5.

TABLE 4

SOLUBILITY OF $AlBr_3 \cdot (CH_3)_2O$ IN *n*-PENTANE-METHYL BROMIDE MIXTURES AT −78.08°

MOLES % PENTANE	SOLUBILITY, MOLES/L.	MOLE % PENTANE	SOLUBILITY MOLES/L.	MOLE % PENTANE	SOLUBILITY, MOLES/L.
32.58	0.1800	46.99	0.0509	52.06	0.0531
40.68	0.1400	47.60	0.0651	64.46	0.0160
43.92	0.1091	48.13	0.0733	100.00	0.0000
45.74	0.0776	48.72	0.0754		
46.45	0.0621	49.13	0.0686		

On addition of hydrocarbon, the solubility falls off somewhat more rapidly with pentane than with propane, but much less rapidly than with butane. The discontinuities in the solubility curve, with pentane, come at a slightly lower concentration of hydrocarbon (47 m. %) than with propane (49.3 m. %). The ratio of solubilities at the lower and upper cusps is 1.5 for both propane and pentane, but the actual solubilities with pentane are much lower (one half) than with propane. The solubility curve for the two butanes differs strikingly from those for propane and pentane.

Whenever a discontinuity occurs in the solubility curve of a solid compound, a change must be taking place in the state of the saturating phase. In the case of butane, for example, a phase change appears to set in at the composition of the lower cusp, which change is completed on reaching the composition of the upper cusp. With the butanes, there appears to be a second phase change at about 41 mole per cent butane in that the solubility drops precipitately from 0.169 to 0.074. This second discontinuity is absent with the other two hydrocarbons.

The etherate of aluminum bromide is a very stable compound and is always recovered without change on evaporation of its solutions. It would seem that, in some way, the etherate interacts with the hydrocarbon to form a compound much more soluble than the simple etherate. Presumably, at the lower cusp, a phase change takes place that leads to a higher solubility. In the case of the butanes, there appears to be a second phase change.

The small solubility change on initial addition of hydrocarbon is surprising and difficult to account for. The solubility of the etherate in pure hydrocarbons is negligibly small. On addition of hydrocarbon we should expect the solubility to fall off much as it does for tetrabutylammonium bromide or for the etherate at higher concentration of hydrocarbon.

It would seem that the solution of this problem lies in the characterization of the saturating phase which is in equilibrium with the solution along the different branches of the solubility curve. Separation of the solid phase from the supernatant solution at $-78°$ should not prove too difficult an operation.

* This paper is based on a portion of a thesis presented by Luther M. Foster to the Graduate School of Brown University, in partial fulfillment of the requirements for the degree of Doctor of Philosophy in June, 1947. Experimental details may be obtained by consulting this thesis which is on file in the library of Brown University.

[1] Morris, C. L., Thesis, Brown University (1941).

[2] Egan, C. J., and Kemp, J. D., *J. Am. Chem. Soc.*, **60**, 2097 (1938).

[3] Kennedy, R. M., Sagenkahn, M., and Aston, J. G., *Ibid.*, **63**, 2267 (1941)

[4] Rossini, F. D., *Chem. Eng. News*, **25**, 230 (1947).

THE POTENTIAL USEFULNESS OF NATURAL TRITIUM*

By W. F. Libby

Institute for Nuclear Studies and Department of Chemistry, University of Chicago

Communicated February 25, 1953

The production of tritium by the cosmic radiation in the earth's atmosphere[1-5] probably can now be taken as being established though many quantitative aspects remain unknown. Rainwater definitely contains tritium in amounts corresponding to between $5 \cdot 10^{-18}$ and $40 \cdot 10^{-18}$ tritium atoms per hydrogen atom. This is a small but definitely measurable quantity, requiring between one quart and five gallons of water as sample. The possible potential uses appear to be worth consideration.

A. Age of Rain and Agricultural Products.—In the first place it is clear that the tritium content of rain water will decrease with time elapsed after precipitation, since the cosmic ray source can introduce fresh tritium atoms only in the atmosphere where the new tritium atoms react with the atmospheric oxygen to form radioactive water. The time scale is set by the decay constant for tritium—12.5 years half life and 18.0 years average life. We expect therefore that whereas freshly fallen rain or snow will show a definite radioactivity due to tritium, old water will show none, and that the age of the water in the sense of the time elasped since precipitation may be determinable from the specific radioactivity. Further, agricultural products should be datable by the tritium content of their constituent hydrogen, the principle being that a considerable fraction of the hydrogen utilized in plant growth originates as rain water and is incorporated in the first few months after precipitation. The time of harvest therefore is close to the time of precipitation. Consequently, it seems possible that the age of agricultural products in the practical sense of the time elapsed since harvest probably can be measured by determination of the tritium content of the product itself. A series of tests is in progress in our laboratory using water of known age and wines of known vintage to test these postulates.

B. Hydrology and the Identification of Water Sources.—A second type of application occurs in the identification of water sources. The mean storage time of rain or snow water before it appears in a given water supply should be given directly by the tritium content of the given supply relative to that of average rain in the region involved. The determination of mean storage times of between about three and twenty-five years should prove possible, these times corresponding to between 15 and 75% loss of tritium due to radioactive decay. The determination of tritium in wells should reveal whether their ultimate supplies are closely connected to the rainfall and therefore are subject to seasonal fluctuations in rainfall.

C. Meteorology.—In the field of meteorology several possible applications seem to exist. The tritium production probably occurs at a steady rate independent of the weather. It seems likely that the production rate will vary strongly with altitude in about the same way that the production of neutrons and stars by the cosmic rays does.[6] This means that on the average the tritium is produced at an altitude of about 6 or 7 miles, and that a maximum in the production rate occurs at about 9 miles. Above this maximum the production rate will decrease with fall in atmospheric pressure, and below this maximum will decrease exponentially at a rate of about 50% for every meter of water increase in pressure.

1. Test of Vertical Mixing in Air Masses.—Direct sampling of the moisture in a given air mass at various altitudes should reveal whether vertical mixing has occurred. The determination of the extent to which vertical mixing occurs may be a matter of considerable interest. It seems not unlikely that the average air mass will be found to be mixed.

2. The Source of the Moisture in Air Masses.—It is clear that deep bodies of water will so dilute rain and snow water that the tritium content of the waters on the surface of the seas will be very small. Therefore, continental water sources such as rivers will be distinguishable from the sea, and it should be possible to determine whether an air mass acquires any considerable amount of moisture from the land masses as it travels over them. An air mass formed over the sea will contain no radioactive water except for the radioactivity acquired from the atmosphere. In fact, for such an air mass, assuming perfect vertical mixing and neglecting the variation of the tritium production rate with latitude,[7] we can write

$$\rho(T_\rho) = 470\, Qt, \qquad (1)$$

in which ρ is the moisture content of the air mass (g./cm.^{2}), T_ρ is the tritium content of the rain (10^{-18} T atoms/H atom), Q is the tritium production rate (T atoms/cm.^{2}/sec.), and t is the time (measured in years) spent by the moisture in the air mass in the air since it left the ocean. This equation should quite accurately represent the tritium content of the air mass so long as it has not acquired moisture from continental sources. Therefore, measurement of the tritium content of moisture in an air mass along its trajectory over the sea and over the continents may reveal to what extent it has acquired moisture from the land. Eq. (1) affords a possibility of determining the residence time of sea moisture in air, and it seems not unlikely that these determinations may be of some interest.

It is true, of course, that the production rate of tritium will probably vary with latitude rather strongly,[7] the production rate at 50° north geomagnetic latitude being some four times that at the equator. Consequently, the actual trajectory of the air mass must be used in the applica-

tion of Eq. (1), and a mean value of Q chosen according to the trajectory involved.

D. The Rate of Escape of He^3 from the Earth.—When the assay of natural tritium in the waters of the earth, now in progress in this laboratory, has been completed, a minimum value for the rate of production of He^3 will have been obtained, because He^3 is the isotope formed by tritium during its radioactive decay. This value is only a minimum because it would seem likely that He^3 could be produced in cosmic ray stars[8] just as tritium seems to be. If we dare assume that the cosmic ray intensity during the last 18 years has been the same as for the last 100 million years, we then can calculate an upper limit for the average residence time of a He^3 atom in the earth's atmosphere before it escapes from the earth.

* This research was supported in whole or in part by the United States Air Force under Contract No. AF 18(600)-564 monitored by the Office of Scientific Research, Air Research and Development Command.

[1] Libby, W. F., *Phys. Rev.*, **69**, 671 (1946).

[2a] Faltings, V. and Harteck, P., *Z. Naturforsch.*, **5a**, 438 (1950). [b] Harteck, P. and Faltings, V., *Nature*, **166**, 1109 (1950).

[3] Grosse, A. V., Johnston, W. H., Wolfgang, R. L., and Libby, W. F., *Science*, **113**, 1 (1951).

[4] Final Report to Air Research and Development Command (P. O. Box 1395, Baltimore 3, Maryland) for Contract AF 33(038)-18013 in 1951, "Sensitive Radiation Detection Techniques for Tritium . . .," W. F. Libby.

[5] Final Report to Air Research and Development Command (P. O. Box 1395, Baltimore 3, Maryland) for Contract AF 33(038)-18013 in 1952, "Natural Tritium Assay . . .," W. F. Libby.

[6] Yuan, Luke C. L., *Phys. Rev.*, **74**, 504 (1948); **76**, 1267 (1949); **76**, 1268 (1949); **77**, 728 (1950).

[7] Simpson, J. A., Jr., *Phys. Rev.*, **73**, 1389 (1948).

[8] Morrison, P. and Beard, D. B., *Phys. Rev.*, **75**, 1332 (1949).

TWO PLEATED-SHEET CONFIGURATIONS OF POLYPEPTIDE CHAINS INVOLVING BOTH CIS AND TRANS AMIDE GROUPS

BY LINUS PAULING AND ROBERT B. COREY

GATES AND CRELLIN LABORATORIES OF CHEMISTRY,* CALIFORNIA INSTITUTE OF TECHNOLOGY

Communicated January 30, 1953

In continuing our search for configurations of polypeptide chains with interatomic distances, bond angles, and other features as indicated by the known structures of crystals of amino acids, simple peptides, and related substances, we have investigated configurations involving both cis amide groups and trans amide groups, and have now discovered two pleated sheets

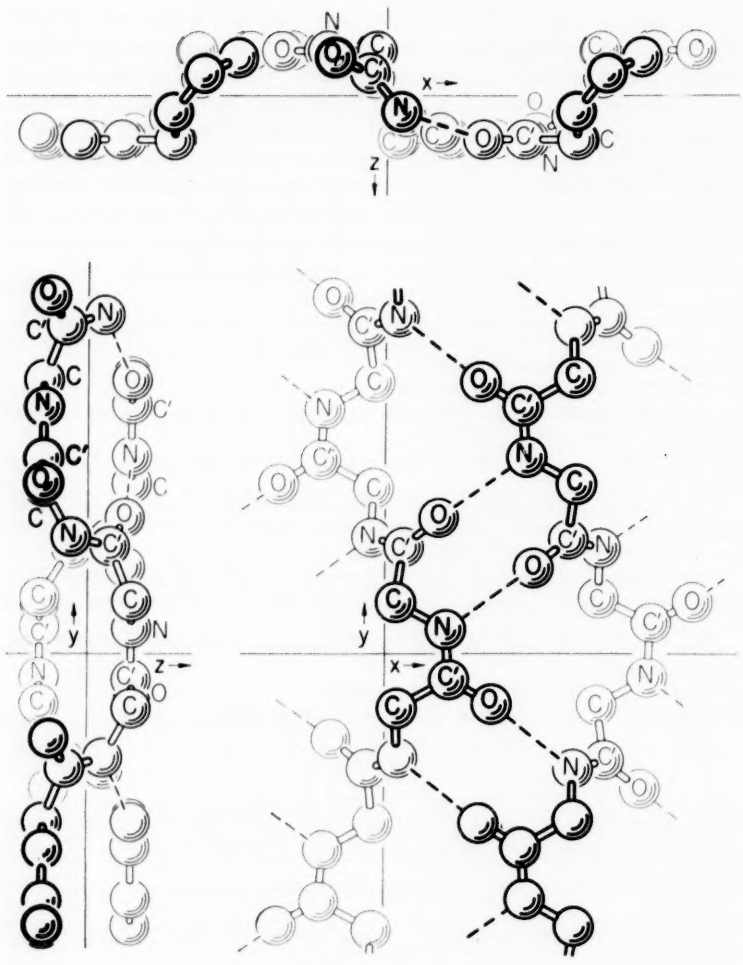

FIGURE 1

The vertically pleated cis-trans sheet of hydrogen-bonded polypeptide chains

composed of polypeptide chains with cis and trans amide groups in alternation.

The Vertically Pleated Cis-Trans Sheet.—The configuration shown in figure 1 results from the formation of diagonally directed hydrogen bonds between adjacent polypeptide chains in which cis amide groups and trans amide groups alternate. The cis amide groups have their C′—N axes nearly parallel to the fiber axis of the structure (the direction of the polypeptide chains), whereas the trans amide groups are nearly perpendicular to the fiber axis. The structure involves 10-membered rings containing two hydrogen bonds, and also 14-membered rings containing two hydrogen bonds. The topological features of the structure are represented in figure 2.

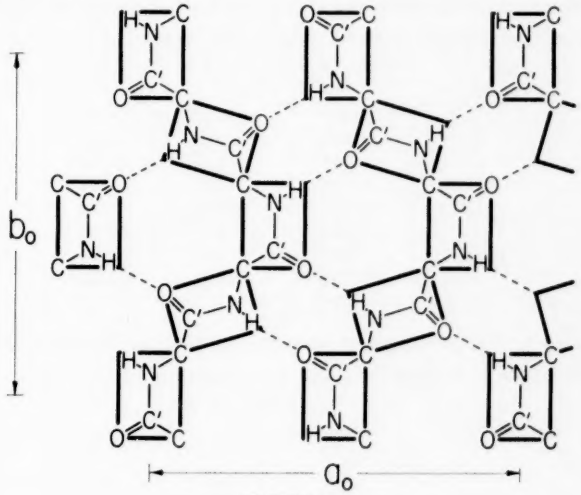

FIGURE 2

Diagram representing the topological features of both the vertically pleated cis-trans sheet and the horizontally pleated cis-trans sheet.

The symmetry of this sheet is orthorhombic, with vertical and horizontal twofold screw axes in the plane of the sheet, and twofold axes perpendicular to the sheet. The unit of structure, with dimensions $a_0 = 10.32$ A (perpendicular to the fiber axis) and $b_0 = 11.38$ A (parallel to the fiber axis), contains four cis amide groups, which are equivalent to one another, and four trans amide groups, which are equivalent to one another.

One of the atoms (other than N and C′) attached to each of the α carbon atoms lies in the plane of the sheet, and the other projects approximately perpendicular to the sheet. The first of these positions is unsuited for any group except the hydrogen atom, whereas the second is satisfactory for

any amino-acid side chain. The nature of the structure is such that a polypeptide composed exclusively of L amino-acid residues could have all of these residues in the second position, projecting out from the plane of the pleated sheet; this pleated-sheet configuration is accordingly, with respect to this consideration, a satisfactory one for proteins.

The coordinates of the atoms are given in table 1. These coordinates were obtained in part by calculation, and in part by the measurement of a set of models carefully constructed to the scale 10 cm. = 1 A. The assumed N—H · · · O distance is 2.77 A. The other interatomic distances and bond angles used are those previously reported.[1]

TABLE 1

ATOMIC COORDINATES FOR THE VERTICALLY PLEATED CIS-TRANS SHEET

$a_0 = 10.32$ A, $b_0 = 11.38$ A, $c_0 = 1.00$ A. Four atoms, at x, y, z; $\frac{1}{2} + x, \bar{y}, \bar{z}$; $\bar{x}$ $\frac{1}{2} + y, \bar{z}$; $\frac{1}{2} - x, \frac{1}{2} - y, z$

ATOM	x	y	z
C_1	0.029	−0.125	1.13
C_1'	0.160	−0.061	1.13
O_1	0.264	−0.116	1.13
N_1	0.150	0.055	1.13
C_2	0.025	0.117	1.13
C_2'	0.045	0.241	0.56
O_2	0.132	0.307	0.96
N_2	−0.034	0.263	−0.42

TABLE 2

ATOMIC COORDINATES FOR THE HORIZONTALLY PLEATED CIS-TRANS SHEET

$a_0 = 11.86$ A, $b_0 = 10.12$ A, $c_0 = 1.00$ A. Four atoms, at x, y, z; $\bar{x}$, $\frac{1}{2} + y, \bar{z}$; $\frac{1}{2} + x, \bar{y}, z$; $\frac{1}{2} - x, \frac{1}{2} - y, \bar{z}$

ATOM	x	y	z
C_1	0.099	−0.147	1.18
C_1'	0.208	−0.071	0.92
O_1	0.299	−0.130	0.76
N_1	0.194	0.058	0.89
C_2	0.085	0.122	1.07
C_2'	0.035	0.236	0.24
O_2	0.117	0.295	−0.25
N_2	−0.069	0.255	−0.20

The existence of pleats in the vertical direction can be seen from the vertical projection of the structure given in figure 1.

The Horizontally Pleated Cis-Trans Sheet.—A second pleated-sheet structure that differs from the first one in one essential feature is shown in figure 3; projections of the structure, also shown in figure 3, show that the pleats in this structure are horizontal, rather than vertical. The topological description of the structure is the same as for the other cis-trans sheet, and is given in figure 2.

This horizontally pleated cis-trans sheet involves cis-trans polypeptide chains and 10-membered and 14-membered rings, closely similar to the corresponding features of the vertically pleated cis-trans sheet. However the symmetry elements are different. The symmetry is monoclinic, rather than orthorhombic, and the sheet contains centers of symmetry, located in

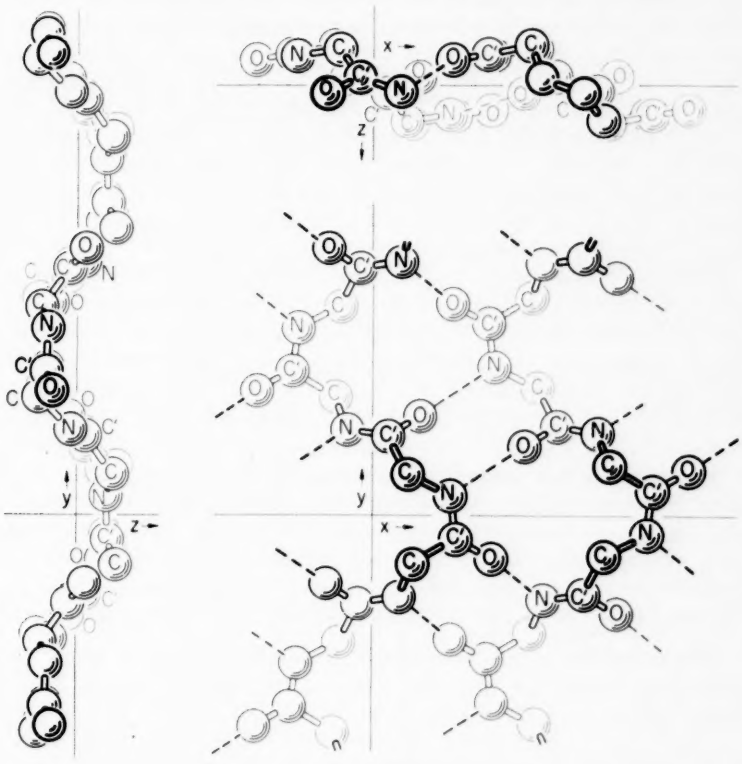

FIGURE 3

The horizontally pleated cis-trans sheet of hydrogen-bonded polypeptide chains.

the centers of the 10-membered rings, together with twofold screw axes parallel to the fiber axis of the sheet, and a horizontal glide plane of symmetry, which converts one cis-trans chain into an adjacent chain. In this structure, as in the other, adjacent chains alternate in direction.

The coordinates of the atoms are given in table 2. The value of a_0 (the identity distance perpendicular to the fiber axis) is 11.86 A and the value of b_0 (the identity distance in the direction of the fiber axis) is 10.12 A.

The feature of the structure that eliminates it as a possible structure for proteins is the presence of centers of symmetry. These symmetry elements require that half of the amino-acid residues have the L configuration, and the other half the D configuration. If it is not required that the side chains conform to the symmetry elements of the basic structure, and the side chains are introduced in the positions corresponding to the L configuration, half of the side chains are placed in positions that give rise to great steric hindrance, these being the positions from the α carbon atoms that are in the plane of the sheet. The horizontally pleated cis-trans sheet might accordingly be a possible structure for polyglycine, for a peptide in which the chains contain sequences of two L residues alternating with two D residues, or for polypeptides in which pairs of glycine residues alternate with pairs of L (or D) residues; it is not, however, acceptable for proteins, except for the unlikely case of a protein with pairs of glycine residues arranged in this sequence with pairs of L residues.

The Possible Occurrence of the Structures in Nature.—The only feature of the vertically pleated cis-trans sheet which seems unfavorable to its stability, in comparison with other polypeptide structures, is the presence of the cis configuration for half of the amide groups. There is some evidence that the cis configuration is less stable than the trans configuration; Mizushima and his collaborators[2] have emphasized this point. The amount of instability has not yet been evaluated. The only peptide that is definitely known to contain a cis amide group is diketopiperazine. Evidence of instability of cis amide groups is provided by the difficulty in synthesizing the corresponding cyclic anhydrides of other amino acids. No x-ray evidence has so far been reported that indicates the presence of the vertically pleated cis-trans sheet in proteins; in particular, the identity distance 11.38 A along the fiber axis has not been reported for any protein.

Acknowledgment.—This investigation was aided by grants from The Rockefeller Foundation and The National Institutes of Health, Public Health Service.

* Contribution No. 1770.

[1] Corey, R. B., and Pauling, L., *Proc. Roy. Soc.;* (in press).

[2] Mizushima, S.-I., and Shimanouchi, T., *J. Am. Chem. Soc.*, **74,** 5550 (1952).

TWO RIPPLED-SHEET CONFIGURATIONS OF POLYPEPTIDE CHAINS, AND A NOTE ABOUT THE PLEATED SHEETS

BY LINUS PAULING AND ROBERT B. COREY

GATES AND CRELLIN LABORATORIES OF CHEMISTRY,* CALIFORNIA INSTITUTE OF TECHNOLOGY

Communicated January 30, 1953

About a year ago, in the course of the consideration of configurations of polypeptide chains with favored orientations around single bonds, we described two pleated-sheet structures.[1] These structures are suited to polypeptide chains constructed entirely of L amino-acid residues or of D amino-acid residues. In one pleated sheet alternate polypeptide chains are antiparallel, and in the other they are parallel. The amide groups have the trans configuration.

We have observed that closely related structures can be constructed in which polypeptide chains of D and L amino-acid residues alternate. The configuration of these layer structures is such as to make it appropriate to call them rippled sheets.

The Antiparallel-Chain Rippled Sheet.—The antiparallel-chain rippled sheet, represented in figure 1, is closely similar to the antiparallel-chain

TABLE 1

ATOMIC COORDINATES FOR THE ANTIPARALLEL-CHAIN RIPPLED SHEET

$a_0 = 9.44$ A, $b_0 = 7.00$ A, $c_0 = 1.00$ A (assumed). Four atoms in x, y, z; $\frac{1}{2} - x, \frac{1}{2} + y, \bar{z}$; $\bar{x}, \bar{y}, \bar{z}$; $\frac{1}{2} + x, \frac{1}{2} - y, z$

	x	y	z
C	0.287	0.040	0.64
C′	0.200	0.216	0.28
O	0.068	0.220	0.45
N	0.275	0.359	−0.22

pleated sheet, and the diagrammatic representation given in figure 4 of the earlier paper[1] applies to both structures. One structure is converted into the other by the reflection of alternate chains into their enantiomers, in the plane of the sheet. The unit of structure was determined by measurement of a model constructed of units precisely built on the scale 10 cm. = 1A. The value of the lateral translation was found to be 9.44 A, and that of the translation in the direction of the polypeptide chains 7.00 A. Atomic coordinates are given in table 1.

The Parallel-Chain Rippled Sheet.—The parallel-chain rippled sheet, shown in figure 2, is closely similar to the parallel-chain pleated sheet, and has the same diagrammatic representation, shown in figure 5 of the previous paper.[1] The unit of structure was found by measurement of a model to have lateral identity distance $a_0 = 9.60$ A, and identity distance along the fiber axis $b_0 = 6.50$ A. Atomic coordinates are given in table 2.

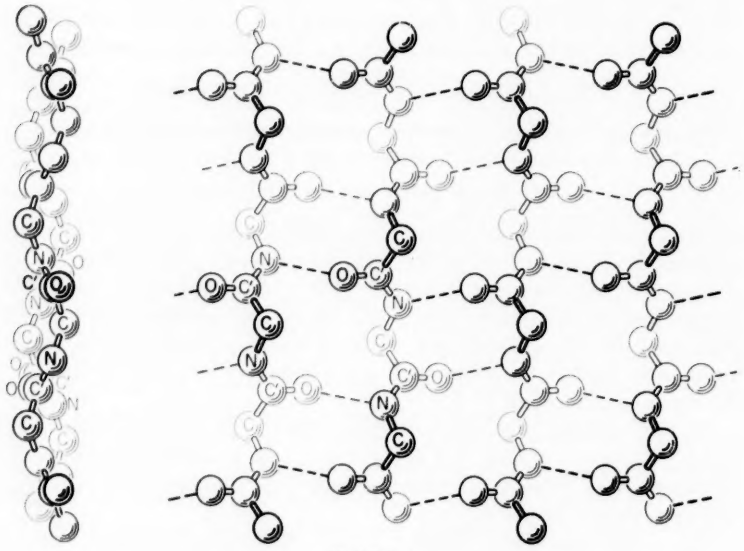

FIGURE 1

The antiparallel-chain rippled sheet of hydrogen-bonded polypeptide chains.

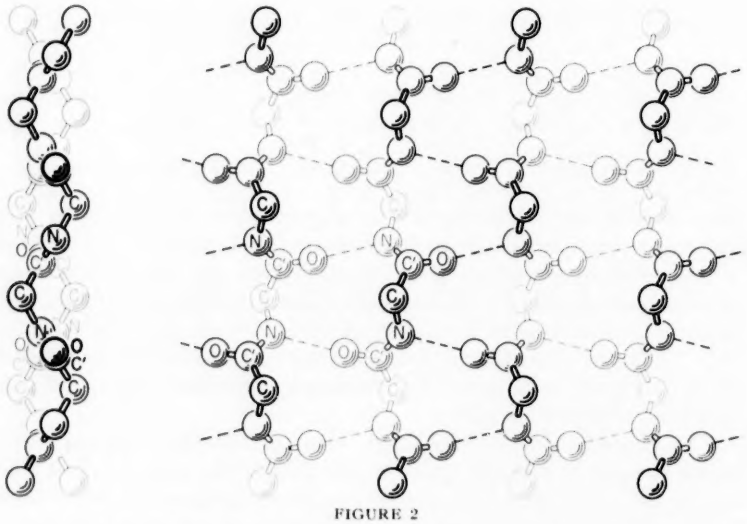

FIGURE 2

The parallel-chain rippled sheet of hydrogen-bonded polypeptide chains.

The antiparallel-chain rippled sheet and the parallel-chain rippled sheet are satisfactory structures, in that they involve linear hydrogen bonds, the interatomic distances and bond angles have the accepted values, and the amide groups are planar. The orientations of the bonds around the α carbon atoms are such that there is room for a side chain, projecting out nearly perpendicularly to the sheet, if alternate chains are constructed of D amino-acid residues and L amino-acid residues. These structures are accordingly satisfactory ones for equimolal mixtures of D polypeptides and L polypeptides.

Moreover, mixtures of D polypeptides and L polypeptides in which the enantiomeric polypeptide chains are present in unequal numbers can assume sheet structures which represent a mixture of a pleated-sheet configuration and a rippled-sheet configuration. Irregular sequences of polypeptide chains with positive and negative orientations can also lead to reasonably satisfactory hydrogen-bonded layer structures. The value of the identity distance in the fiber-axis direction would be intermediate between the value

TABLE 2

ATOMIC COORDINATES FOR THE PARALLEL-CHAIN RIPPLED SHEET

$a_0 = 9.60$ A, $b_0 = 6.50$ A, $c_0 = 1.00$ A (assumed). Four atoms in x, y, z; $\bar{x}$, $1/2 + y$, $\bar{z}$; $1/2 + x, y, \bar{z}$; $1/2 - x, 1/2 + y, z$

	x	y	z
C	−0.006	0.000	0.98
C′	0.059	0.185	0.28
O	0.188	0.205	0.25
N	−0.027	0.314	−0.26

7.00 A corresponding to linear hydrogen bonds for the antiparallel-chain sheets and the value 6.50 A corresponding to linear hydrogen bonds for the parallel-chain sheets. An intermediate value of this identity distance would require that all hydrogen bonds be somewhat bent, and presumably also somewhat strained.

A Note on the Pleated Sheets.—In the earlier discussion of the pleated-sheet configurations of the polypeptide chains[1] the assumption was made that certain orientations around the bonds between the α carbon atom and adjacent atoms in the amide group are favored over other orientations. The assumed favored orientations around these single bonds led to the predicted value 6.68 A for the identity distance in the fiber-axis direction (the direction of the polypeptide chains). Although the existence of a potential function causing certain orientations around these bonds to be favored is likely from *a priori* considerations, the magnitude of the effect is uncertain, and it may well be that very little strain (less than 0.1 kcal. mole^{-1} per residue) is involved in rotating the chain from favored to less favored configurations.

We have now found through the construction of large-scale models that other values of the identity distance in the direction of the polypeptide chains are indicated for the two pleated sheets, corresponding to slightly different orientations about the single bonds to the α carbon atom. The new configurations, described by the coordinates in tables 3 and 4, involve linear hydrogen bonds—that is, the angle N—H $\cdots$ O is equal to 180°. The fiber-axis identity distance for the antiparallel-chain pleated sheet is 7.00 A, and that for the parallel-chain pleated sheet is 6.50 A; these values are the same as for the corresponding rippled sheets.

The two pleated sheets provide satisfactory structures for proteins and for polypeptides composed exclusively of L amino-acid residues (or D amino-acid residues). We think that it is likely that silk fibroin, for which the

TABLE 3

ATOMIC COORDINATES FOR THE ANTIPARALLEL-CHAIN PLEATED SHEET

$a_0 = 9.50$ A, $b_0 = 7.00$ A, $c_0 = 1.00$ A (assumed). Four atoms in x, y, z; $\bar{x}, {}^1/_2 + y, \bar{z}$; ${}^1/_2 - x, \bar{y}, z$; ${}^1/_2 + x, {}^1/_2 - y, \bar{z}$

	x	y	z
C	0.034	−0.005	−0.70
N	−0.030	0.173	−0.20
C′	0.051	0.320	0.21
O	0.180	0.326	0.22
βC	0.024	−0.005	−2.24

TABLE 4

ATOMIC COORDINATES FOR THE PARALLEL-CHAIN PLEATED SHEET

$a_0 = 4.85$ A, $b_0 = 6.50$ A, $c_0 = 1.00$ A (assumed). Two atoms in x, y, z; $\bar{x}, {}^1/_2 + y, \bar{z}$

	x	y	z
C	0.012	0.000	−0.98
N	−0.066	0.186	−0.26
C′	0.118	0.315	0.28
O	0.371	0.295	0.25
βC	−0.093	0.014	−2.45

observed fiber-axis identity distance is 7.0 A, has the antiparallel-chain pleated-sheet structure, and that the β-keratin proteins, for which the observed fiber-axis identity distance is about 6.6 A, have the parallel-chain pleated-sheet structure, or a structure in which a considerable number of adjacent polypeptide chains have parallel orientations.

The atomic coordinates given in tables 3 and 4 differ only slightly from those previously reported.[1]

Acknowledgments.—This investigation was aided by grants from The Rockefeller Foundation and The National Institutes of Health, Public Health Service.

* Contribution No. 1771.

[1] Pauling, L., and Corey, R. B., these PROCEEDINGS, **37**, 729 (1951).

ON THE INCLINATION OF PLASTIC SLIP BANDS IN FLAT BARS IN TENSION TESTS

BY T. Y. THOMAS

GRADUATE INSTITUTE FOR APPLIED MATHEMATICS, INDIANA UNIVERSITY

Communicated January 21, 1953

1. Introduction.—In the following communication[1] we have applied the Hencky stress-strain relations for small plastic displacements, under the assumption of incompressibility,[2] to the problem of determining the inclination of the plastic slip bands which develop in flat bars subject to tension. This elastic-plastic problem is here shown to admit a simple *exact* solution which in a sense is analogous to the simple solution of the uniformly stressed bar in classical elasticity theory.

As the basic equations of this theory we have[3]

$$s_{\alpha\beta} = \varphi\eta_{\alpha\beta} \qquad \text{(stress-strain relations)}, \tag{1}$$

$$u_{\alpha,\,\alpha} = 0 \qquad \text{(equation of incompressibility)}, \tag{2}$$

$$\sigma_{\alpha\beta,\,\beta} = 0 \qquad \text{(equilibrium equations)}, \tag{3}$$

where the proportionality factor φ, which is assumed to be positive, is one of the initial unknowns of the system. The $\sigma_{\alpha\beta}$ are the components of the stress tensor and u_α the components of the plastic displacement. The tensors s and η are the stress and plastic strain deviations defined by

$$s_{\alpha\beta} = \sigma_{\alpha\beta} + p\delta_{\alpha\beta}; \quad \eta_{\alpha\beta} = e_{\alpha\beta} + q\delta_{\alpha\beta}, \tag{4}$$

where

$$e_{\alpha\beta} = \frac{1}{2}(u_{\alpha,\,\beta} + u_{\beta,\,\alpha}), \; p = \frac{-\sigma_{ii}}{3}, \; q = \frac{-e_{ii}}{3}. \tag{5}$$

The tensor e is the plastic strain tensor and is here identical with the strain deviation η since $q = 0$ on account of (2). These relations are referred to a rectangular coordinate system. The equations (1), (2), and (3) are $5 + 1 + 3 = 9$ in number and involve the 10 dependent variables $\sigma_{\alpha\beta}$, u_α, and φ. Another equation is provided by the yield condition of which two forms are commonly considered, namely

$$s_{\alpha\beta}s_{\alpha\beta} = 2k^2 \qquad \text{(von Mises yield)}, \tag{6}$$

$$s_1 - s_3 = 2k \qquad \text{(Tresca yield)}, \tag{7}$$

where k is a positive constant depending on the material. In the condition (7) the quantities s_1 and s_3 are the greatest and least of the principal values of the stress deviation.

Along the surface of separation of an elastic and plastic region the following general dynamical conditions of equilibrium must be satisfied[4]

$$\rho_1(v_{1n} - G) = \rho_2(v_{2n} - G),$$
$$[\sigma_{\alpha\beta}]\nu^\beta = \rho_1(v_{1n} - G)[v_\alpha],$$

where, as usual, the bracket denotes the discontinuity in the quantity enclosed. Furthermore v stands for the velocity of the flow and G is the normal velocity of the surface of separation whose unit normal vector is denoted by ν. The quantities ρ_1 and v_{1n} are the density and normal velocity on one side of the surface of separation while ρ_2 and v_{2n} are the corresponding quantities on the other side of this surface. Since we are here concerned with an equilibrium theory of elastic and plastic displacements we will have $v_\alpha = 0$ and $G = 0$. Hence the first of the above conditions is satisfied identically and the others reduce simply to

$$[\sigma_{\alpha\beta}]\nu^\beta = 0. \tag{8}$$

The conditions (8) can be expressed by saying that the stress vector, i.e., the vector having the components $\sigma_{\alpha\beta}\nu^\beta$, is continuous across the surface of separation. Other conditions which must be taken into account in this problem involve the vanishing of the stress vector on the outer boundaries of the plastic band.

Both under the von Mises and the Tresca yield conditions our solutions lead to an inclination angle of $\pm 35°16'$ for the slip bands. However in the case of the Tresca yield an inclination of $\pm 50°46'$ appears also as a possibility. Now the angle of $35°16'$ has been deduced by methods which seem to be more or less established in the literature and which have been presented in the book by A. Nadai.[5] My objection to these methods is the following. Apart from the fact that no plastic solution is exhibited, the conditions (8), which must be satisfied over the slip surface, as well as the outer boundary conditions are neglected. As a consequence it has been necessary to introduce an assumption, extraneous to the basic equations of the theory, which we find difficult to understand.[6] It may be mentioned, however, that such disregard for the basic requirements of theory appears to be a characteristic of the work of many of the professional writers in this area.

2. *The Ideal Flat Bar.*—To say that a rectangular bar is thin or flat implies that its thickness is small in comparison with its other dimensions, i.e., its width and length. Let us therefore define the *ideal flat bar* as one of finite thickness but whose flat sides are formed by two infinite parallel planes. By employing the concept of the ideal flat bar we can limit our attention to the boundary conditions on the two flat sides. Results obtained for such bars may be expected to be valid approximately in the interior, i.e., in a region removed from the narrow sides and the ends, of the flat bar of finite dimensions.

In figure 1 we have indicated a portion of an ideal flat bar. The lines

AB and CD are the intersections, with one of the flat sides of the bar, of parallel planes P_1 and P_2 perpendicular to the flat sides. Two coordinate systems x and y will be used in the following discussion. Both of these systems will be supposed, *for definiteness*, to have their origins at a point O mid-way between the flat sides of the bar and also mid-way between the planes P_1 and P_2. The x_3 and y_3 axes (not shown in Fig. 1) will be taken to

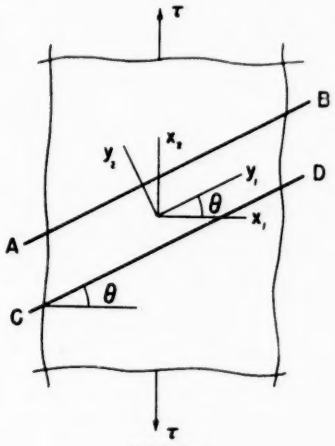

FIGURE 1

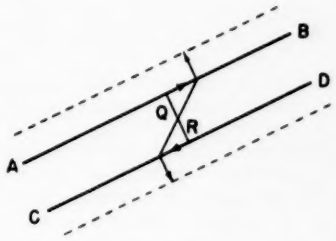

FIGURE 2

be identical and perpendicular to the flat sides. The y_2 axis is chosen perpendicular to the planes P_1 and P_2 and hence the y_1 axis will be parallel to these planes. Since the x_1, x_2 and y_1, y_2 coordinate axes are in the same plane it can be assumed that the y_1, y_2 axes are obtained from the x_1, x_2 axes by rotation through an angle θ (see Fig. 1). Hence the coordinates of these two systems will be related by the following transformation

$$x_1 = y_1 \cos\theta - y_2 \sin\theta;\ x_2 = y_1 \sin\theta + y_2 \cos\theta;\ x_3 = y_3. \quad (9)$$

Now suppose that the ideal flat bar is subjected to a uniform tension $\tau(>0)$ in the direction of the x_2 axis. Then if $\tau_{\alpha\beta}$ denotes the components of the stress tensor relative to the x system we shall have $\tau_{22} = \tau$ and $\tau_{\alpha\beta} = 0$ otherwise. Denoting the components of the stress tensor by $\mu_{\alpha\beta}$ in the y system the quantities $\mu_{\alpha\beta}$ can be determined from the values of the $\tau_{\alpha\beta}$ by the tensor transformation relating these two sets of components. Thus

$$\mu_{\alpha\beta} = \tau_{ij} \frac{\partial x_i}{\partial y_\alpha} \frac{\partial x_j}{\partial y_\beta} = \tau \frac{\partial x_2}{\partial y_\alpha} \frac{\partial x_2}{\partial y_\beta}.$$

Computing the derivatives in these relations from (9) we find that

$$\left.\begin{aligned} \mu_{11} &= \tau \sin^2\theta;\ \mu_{12} = \tau \sin\theta\cos\theta;\ \mu_{13} = 0, \\ \mu_{22} &= \tau \cos^2\theta;\ \mu_{23} = 0;\ \mu_{33} = 0. \end{aligned}\right\} \tag{10}$$

3. The Plastic Slip Band.—Suppose now that the value of τ is allowed to increase until the yield value is reached. It will then be assumed that the band or layer between the two parallel planes P_1 and P_2 becomes plastic in the sense that the displacements μ_α in this region satisfy the equations (1), (2), and (3) and one or the other of the yield conditions (6) or (7). In the case of the von Mises yield we shall have at the yield point $\tau = \sqrt{3}k$ and for the Tresca yield we shall have $\tau = 2k$. These relations between τ and k are an immediate consequence of the von Mises or Tresca yield condition and the values $\tau_{\alpha\beta}$ of the stress components given in §2. Outside this plastic band it is assumed that the material is in the elastic state.

Remark.—It is assumed that the plastic displacements u_α under consideration are relative to the natural or undeformed state. We therefore conceive of the material between the above planes P_1 and P_2 as in the undeformed state before determining its displacement u_α as a solution of the equations of §1. The possibility of realizing this condition can be seen as follows. After the tension in the bar has been brought to its yield value we transform the elastically deformed material between the planes P_1 and P_2 by the transformation inverse to that producing the elastic deformation. By this procedure the planes P_1 and P_2 will be transformed into parallel planes P_1' and P_2' which will be perpendicular to the flat sides of the bar and the material between these planes will be in the undeformed state. A rigid displacement or rotation of the undeformed layer between the planes P_1' and P_2' will now bring the plane P_1' into contact with the elastically deformed material which was previously along the plane P_1. Similarly a translation (rigid displacement) of the elastic material formerly in contact with P_2 will bring this material into contact with the plane P_2'. In the following we have omitted the primes and have denoted by P_1 and P_2 the planes separating the elastic material and the band which may be assumed to be placed symmetrically relative to the elastic portions of the bar.

After the plastic displacements u_α have been determined rigid displacements of the elastic portions of the bar may be allowed as well as rigid displacements of the plastic layer bounded by the planes P_1 and P_2 provided that these displacements do not produce a separation of material. In fact the elastic displacements and plastic displacements u_α under consideration can be determined at most to within such rigid displacements by the conditions of the problem.

We seek a simple solution μ_α of the equations (1), (2), and (3) in the plastic band satisfying the boundary conditions, i.e., for which the stress vector vanishes (after deformation) on the free surface of the band, and such that the conditions (8) are satisfied over the surfaces of separation of the elastic and plastic regions. It will be shown in fact that, relative to the y coordinate system of §2, such a solution is given by

$$u_1 = ay_2;\ u_2 = by_2;\ u_3 = -by_3, \tag{11}$$

where a and b are suitably chosen constants. In the first place it may be observed immediately that, regardless of the values of the constants a and

b, the equation of incompressibility (2) is satisfied by the displacements (11).

In consequence of (11) the planes P_1 and P_2 bounding the plastic band will be displaced into planes parallel to P_1 and P_2. This is illustrated in figure 2 where we have indicated the displacement, in a plane parallel to the flat side of the bar, of two points Q and R in the planes P_1 and P_2, respectively. This part of the displacement, which is determined by the first two relations (11), involves a shear followed by a movement in the y_2 direction proportional to the y_2 coordinate. From the third equation (11) it is seen that planes parallel to the flat sides of the bar remain parallel to the flat sides.

Since the displacement within the band, as above described, envolves a slip of material particles along the planes of separation P_1 and P_2, it is natural to refer to this band as a *plastic slip band*. In consequence of the displacement (11) within the plastic slip band the portions of elastic material on either side of the band will suffer a rigid displacement which will not effect their internal stresses. It is important to observe that these displacements can occur without separation of the material along the planes P_1 and P_2.

4. *Calculation of the Plastic Tensors.*—We shall now calculate the components of the stress tensor σ and its deviation s within the plastic slip band. This calculation will be carried out relative to the y coordinate system. Observe first that by differentiation of the equations (11) we have

$$\begin{aligned} u_{1,1} &= 0; \quad u_{1,2} = a; \quad u_{1,3} = 0, \\ u_{2,1} &= 0; \quad u_{2,2} = b; \quad u_{2,3} = 0, \\ u_{3,1} &= 0; \quad u_{3,2} = 0; \quad u_{3,3} = -b. \end{aligned}$$

From these relations we immediately determine the values of the stress components $e_{\alpha\beta}$ from (5). Thus

$$e_{11} = 0; \quad e_{12} = \frac{a}{2}; \quad e_{13} = 0,$$

$$e_{22} = b; \quad e_{23} = 0; \quad e_{33} = -b.$$

Hence from (1) and the fact that $\eta_{\alpha\beta} = e_{\alpha\beta}$ for the incompressible case under consideration we can write

$$\left.\begin{aligned} s_{11} &= 0; \quad s_{12} = \frac{a\varphi}{2}; \quad s_{13} = 0, \\ s_{22} &= b\varphi; \quad s_{23} = 0; \quad s_{33} = -b\varphi. \end{aligned}\right\} \tag{12}$$

Finally from (12) and (4) we obtain

$$\left.\begin{aligned} &\sigma_{11} = -p; \quad \sigma_{12} = \frac{a\varphi}{2}; \quad \sigma_{13} = 0, \\ &\sigma_{22} = b\varphi - p; \quad \sigma_{23} = 0; \quad \sigma_{33} = -b\varphi - p. \end{aligned}\right\} \tag{13}$$

5. *The Boundary Conditions.*—It follows from the third equation (11) that the quantity $-b$ is the plastic elongation in the y_3 direction. *We choose this quantity to be equal to the corresponding elastic elongation.* This amounts to taking the constant b equal to $\nu\tau/E$ where ν is Poisson's ratio and E is Young's modulus for the material. Since the value of b so defined is positive we see that the distance between the planes P_1 and P_2 of §2 will be increased by a plastic deformation (11) resulting from tension.

With the above value of the constant b the displacement in the y_3 direction of the sides of the bar, including the outer boundaries of the plastic band, will be determined entirely by the elastic deformation. The outer boundaries of the plastic band can therefore be made to lie, by the deformation (11), in the planes of the flat sides of the elastic portions of the bar. Hence the plastic boundary condition is given by $\sigma_{\alpha\beta}\xi^{\beta} = 0$ where ξ is a unit vector in the y_3 direction. In other words we must have $\sigma_{\alpha 3} = 0$ over the two outer boundaries of the plastic band. But from (13) we see that these equations are satisfied for $\alpha = 1, 2$. Taking $\alpha = 3$ it therefore follows that

$$p = -b\varphi \tag{14}$$

over the outer boundaries of the plastic band on account of the last equation (13). Now it is immediately seen from (12) and either of the yield conditions (6) or (7) that the quantity φ must be a constant in the plastic band. *We choose the quantity p to be the constant given by (14).* The actual value of p will not be needed in this discussion but it can be found from (14) and the value of the constant φ which is determined by the relations of §7 §8. With this choice of p the boundary conditions are thus automatically satisfied. *Moreover we see from (13) that the stress components $\sigma_{\alpha\beta}$ are constant throughout the plastic band and hence the equilibrium equations (3) are identically satisfied.*

6. *Conditions Along the Slip Planes.*—Let us now consider the conditions (8) which must be satisfied along the two planes separating the plastic band from the elastic portions of the bar. These will be the planes P_1 and P_2 of §2 or more precisely the planes into which P_1 and P_2 are displaced by the plastic deformation (11). In either case the planes of separation are perpendicular to the y_2 axis so that the vector ν in (8) has the components (0, 1, 0). Hence (8) reduces to

$$[\sigma_{\alpha 2}] = \mu_{\alpha 2} - \sigma_{\alpha 2} = 0, \tag{15}$$

where the values of the μ and σ are given by (10) and (13), respectively.

Making these substitutions and taking account of (14) the relations (15) give

$$\tau \sin\theta \cos\theta = \frac{a\varphi}{2}. \tag{16}$$

$$\tau \cos^2\theta = 2b\varphi. \tag{17}$$

Dividing corresponding members of (16) and (17) we now have

$$\tan\theta = \frac{a}{4b}. \tag{18}$$

This equation will determine the inclination θ of the slip band after the value of the constant a has been found. To determine a we first set up the relation obtained by the elimination of θ from the above equations. This elimination is accomplished quite simply by substituting for $\tan^2\theta$ and $\sec^2\theta$ ($= 1/\cos^2\theta$) in the identity

$$1 + \tan^2\theta = \sec^2\theta$$

the values of these quantities given by (17) and (18). Thus

$$1 + \frac{a^2}{16b^2} = \frac{\tau}{2b\varphi}, \text{ or } \frac{a^2 + 16b^2}{8b} = \frac{\tau}{\varphi}. \tag{19}$$

So far the yield conditions (6) and (7) have not been used explicitly. In the following sections the ratio τ/φ is found for each of the two yield conditions. Then the equation (19) will determine the value of the constant a and hence from (18) we can find the inclination θ of the slip band.

7. *Von Mises Yield.*—When we substitute the values of $s_{\alpha\beta}$ given by (12) into the condition (6) the following expression for φ is immediately obtained

$$\varphi = \frac{2k}{\sqrt{a^2 + 4b^2}} = \frac{2\tau}{\sqrt{3}\sqrt{a^2 + 4b^2}}, \tag{20}$$

where the plus sign is taken before the radical since it is assumed that φ is positive (see §1). Substituting the value of φ given by (20) into (19) we now find

$$a^2 + 16b^2 = 4\sqrt{3}\, b\sqrt{a^2 + 4b^2}. \tag{21}$$

Squaring both members of (21) we obtain a fourth degree equation in the quantities a and b which is seen to reduce immediately to the simple relation $a = \pm\sqrt{8}b$ by which the constant a is determined. Hence equation (18) becomes $\tan\theta = \pm 1/\sqrt{2}$. *It follows that the slip bands have an inclination of $\pm 35°16'$ under the von Mises yield condition.*

8. *Tresca Yield.*—The principal values of the stress deviation are given by the solutions s of the determinantal equation

$$|s_{\alpha\beta} - s\delta_{\alpha\beta}| = \begin{vmatrix} -s & \frac{a\varphi}{2} & 0 \\ \frac{a\varphi}{2} & (b\varphi - s) & 0 \\ 0 & 0 & (-b\varphi - s) \end{vmatrix} = 0.$$

Expanding this determinant and solving for s we find

$$s = -b\varphi, \; s = \left(\frac{b}{2} \pm \frac{1}{2}\sqrt{a^2 + b^2}\right)\varphi.$$

Let us denote these three values of s by s_1, s_2, and s_3 with the understanding that $s_1 \geqq s_2 \geqq s_3$. Assume for the moment that

$$s_1 = \left(\frac{b}{2} + \frac{1}{2}\sqrt{a^2 + b^2}\right)\varphi; \; s_2 = -b\varphi; \; s_3 = \left(\frac{b}{2} - \frac{1}{2}\sqrt{a^2 + b^2}\right)\varphi. \tag{22}$$

Then the Tresca yield condition (7) gives

$$s_1 - s_3 = \sqrt{a^2 + b^2}\,\varphi = 2k = \tau. \tag{23}$$

Substituting the value of the ratio τ/φ given by (23) into (19) we have

$$a^2 + 16b^2 = 8b\sqrt{a^2 + b^2}. \tag{24}$$

Now when we square both members of (24) we find that the resulting fourth degree equation in a and b leads to the following values of the constant a, namely

$$a = \pm\sqrt{8}\,b; \quad a = \pm\sqrt{24}\,b. \tag{25}$$

Substituting these values of a in turn into the equations (22) we find

$$s_1 = 2b\varphi; \; s_2 = -b\varphi; \; s_3 = -b\varphi,$$

and

$$s_1 = 3b\varphi; \; s_2 = -b\varphi; \; s_3 = -2b\varphi.$$

Hence the required inequalities $s_1 \geqq s_2 \geqq s_3$ are satisfied, since b and φ are both positive, for each of the two possible sets of values of the constant a given by (25).

Now it is evident that s_1 as given by (22) is the greatest of the principal values of the tensor s. If we suppose that the least of the principal values is given by $s_3 = -b\varphi$ and proceed as above it will be found that only the first set of relations in (25) is obtained. Hence (25) gives all relations possible between the constants a and b.

When we substitute the values of a given by (25) into the equation (18) we now have

$$\tan\theta = \pm\frac{1}{\sqrt{2}}, \pm\frac{\sqrt{3}}{\sqrt{2}}.$$

Hence $\theta = \pm 35°16'$ or $\theta = \pm 50°46'$. *In other words the plastic slip band has an inclination of* $\pm 35°16'$ *or* $\pm 50°46'$ *under the yield condition of Tresca.*

[1] Prepared for the Naval Research Laboratory, Washington, D. C.

[2] Cp. Prager and Hodge, *The Theory of Perfectly Plastic Solids*, Wiley & Sons, New York (1951), p. 36. Usually the equation of the classical elasticity theory relating the divergence of the displacement vector and the mean stress is assumed in this theory instead of the equation of incompressibility (2). See, for example, Hill, R., *The Mathematical Theory of Plasticity*, Oxford (1950), p. 46, and various articles by Russian writers in *Plastic Deformation*, Mapleton House, Brooklyn, N. Y. (1948). This modification of the above system of equations (1), (2), and (3) allows for the effects of compressibility in the determination of the inclination of the slip bands. We have also treated the compressible case and have found that under compressibility the inclination of the slip bands depends in a very simple manner on Poisson's ratio for the material. This result appears in these PROCEEDINGS, **39**, 266–273 (1953).

[3] Equations (1) are sometimes written in the form

$$\eta_{\alpha\beta} = \left(\frac{1+\phi}{2G}\right) s_{\alpha\beta},$$

and when so written they become identical with the corresponding elasticity relations for $\phi = 0$. However it has seemed advantageous to write these equations in the form (1) for the requirements of our discussion.

[4] See a forthcoming paper by Thomas, T. Y., "Singular Surfaces and Flow Lines in the Theory of Plasticity," to appear in the April issue of the *Journal of Rational Mechanics and Analysis* (1953). This paper contains a rather extended discussion of the flow equations of von Mises in connection with the occurrence of flow markings resulting from slip as well as those which result from a weaker form of discontinuity. Since the concept of velocity is involved in this discussion it was necessary to use the equations of motion, containing non-linear inertial terms, instead of the simpler equations of equilibrium (3). By making certain approximation assumptions the angle of 35°16′ was found to be the angle of inclination of slip lines on flat bars under tension although an exact solution of this flow problem, corresponding to the result of the present paper, was not obtained.

[5] Nadai, A., *The Theory of Flow and Fracture of Solids*, McGraw-Hill, New York, 1950, pp. 320–327.

[6] It is stated that $\epsilon_y = 0$ in the direction parallel to the edges of the oblique layer when it starts to neck down because the adjoining portions of non-yielding material do not participate in the deformation. In consequence of this assumption it follows that $\sigma_y = \sigma_x/2$ and by means of this relation the inclination of the slip bands is found. See Nadai, *loc. cit.*, p. 323.

THE EFFECT OF COMPRESSIBILITY ON THE INCLINATION OF PLASTIC SLIP BANDS I. FLAT BARS

By T. Y. Thomas

Graduate Institute for Applied Mathematics, Indiana University

Communicated February 2, 1953

1. Preliminary Remarks.—The condition of incompressibility used in our preceding note[1] in these PROCEEDINGS will now be replaced by the condition of the classical elasticity theory relating the divergence of the displacement vector and the mean stress. This leads to the usual form of the Hencky stress-strain relations for small plastic displacements which, for purposes of reference, we shall write as follows

$$s_{\alpha\beta} = \varphi\eta_{\alpha\beta}; \quad \sigma_{ii} = \frac{Eu_{i,\,i}}{1 - 2\nu}, \tag{1}$$

where E is Young's modulus and ν is Poisson's ratio for the material. To the stress-strain relations (1) we must add the equilibrium equations and either the von Mises or the Tresca yield condition. The notation employed in the above and following equations is the same as that in our previous note to which reference should be made.

The above system of equations will be applied to the problem of determining the inclination of plastic slip bands in an *ideal flat bar* in a state of simple tension.[2] The discussion in §2 and §3 of the previous note, involving the selection of the x and y coordinate systems and the planes P_1 and P_2 bounding the plastic slip band, is applicable and will be understood to apply in the following treatment. It will be shown that for suitable values of the constants a, b, and c the equations

$$u_1 = ay_2; \quad u_2 = by_2; \quad u_3 = cy_3, \tag{2}$$

will give an exact solution of the problem. This statement implies that the boundary conditions for the plastic band will be satisfied as well as the required conditions along the planes P_1 and P_2 separating the plastic band and the elastic portions of the bar.

In our previous note we obtained an angle of $\pm 35°16'$ for the inclination of the slip bands, both under the von Mises and the Tresca yield conditions, with the possibility of an additional inclination of $\pm 50°46'$ under the Tresca condition. The theoretically unacceptable attempts in the current literature, discussed briefly in §1 of the previous note, to solve this problem, have led also to an angle of $35°16'$ for the inclination of the slip bands in the bar.[3] Now these results are obtained under the hypothesis of incompressibility of the plastic material. The results of the present article, giving the inclination of the slip bands as a function of Poisson's ratio, depend

clearly on the effect of compressibility which is allowed by the stress-strain relations (1). In §4 and §5 we have deduced the inclination formulas under the von Mises and Tresca yield conditions, respectively. Formula (17), which is valid both for von Mises and Tresca yield, would appear at first sight to represent the most likely relationship between Poisson's ratio and the inclination of the slip bands. For a Poisson ratio of $1/3$ this formula gives an inclination angle of $\pm 30°$ which is the angle we have personally observed on specimens of aluminum alloy tested at the Naval Research Laboratory, Washington, D. C. It would be interesting to have exact experimental data for comparison with the theoretical relationship between Poisson's ratio ν and the inclination θ of the slip bands[4] contained in the table in §4.

2. *Formal Calculations.*—The components of certain of the plastic tensors will be needed and these will be calculated relative to the y coordinate system. By combining the quantities $u_{\alpha,\beta}$ resulting from differentiation of (2) we obtain the stress components $e_{\alpha\beta}$ as follows

$$e_{11} = 0; \quad e_{12} = \frac{a}{2}; \quad e_{13} = 0,$$
$$e_{22} = b; \quad e_{23} = 0; \quad e_{33} = c.$$

Using these values of the $e_{\alpha\beta}$ the strain deviation components $\eta_{\alpha\beta}$ can readily be found and hence, from the first of the equations (1), we obtain the components $s_{\alpha\beta}$ of the stress deviation. Thus

$$\left.\begin{aligned} s_{11} &= -\left(\frac{b+c}{3}\right)\varphi; \; s_{12} = \frac{a\varphi}{2}; \; s_{13} = 0, \\ s_{22} &= \left(\frac{2b-c}{3}\right)\varphi; \; s_{23} = 0; \; s_{33} = \left(\frac{2c-b}{3}\right)\varphi. \end{aligned}\right\} \tag{3}$$

From the formula relating the components of stress $\sigma_{\alpha\beta}$ and stress deviation $s_{\alpha\beta}$ we can now find the $\sigma_{\alpha\beta}$ in terms of the $s_{\alpha\beta}$ and the mean stress. But this latter quantity can be eliminated by the last equation (1). Hence we obtain

$$\left.\begin{aligned} \sigma_{11} &= -\left(\frac{b+c}{3}\right)\varphi + \frac{(b+c)E}{3(1-2\nu)}; \; \sigma_{22} = \left(\frac{2b-c}{3}\right)\varphi + \frac{(b+c)E}{3(1-2\nu)}, \\ \sigma_{33} &= \left(\frac{2c-b}{3}\right)\varphi + \frac{(b+c)E}{3(1-2\nu)}; \; \sigma_{12} = \frac{2\varphi}{2}; \; \sigma_{13} = \sigma_{23} = 0. \end{aligned}\right\} \tag{4}$$

3. *Boundary and Separation Conditions.*—The boundary conditions for the plastic band require the vanishing of the quantities $\sigma_{\alpha\beta}\xi^{\beta}$ over the free boundary of the band (after plastic deformation) where ξ is a vector normal to this boundary. But by choosing the constant c in (2) equal to $-\tau\nu/E$,

where $\tau(>0)$ is the yield value of the tension, the free boundaries of the plastic band will lie in the planes of the elastically deformed flat sides of the bar and hence the vector ξ will be parallel everywhere to the y_3 axis. This leads to the conditions $\sigma_{\alpha 3} = 0$ which are satisfied automatically for $\alpha = 1, 2$ on account of (4). The remaining condition becomes

$$(2c - b)\,\varphi + \frac{(b + c)E}{(1 - 2\nu)} = 0. \tag{5}$$

Now the quantity φ must be constant throughout the band in consequence of the yield condition. Hence the condition (5) can be viewed as a necessary relation between constants and not merely as a condition restricted to the outer boundaries of the plastic band. It may be mentioned also in this connection that the stress components $\sigma_{\alpha\beta}$ must be constant throughout the plastic band and hence the equilibrium equations will be satisfied identically.

We now consider the conditions which must be satisfied along the planes P_1 and P_2 separating the plastic band from the elastic portions of the bar. These conditions are expressed by the vanishing of the stress vector over the planes P_1 and P_2. In other words we must have

$$[\sigma_{\alpha\beta}]\nu^\beta = (\mu_{\alpha\beta} - \sigma_{\alpha\beta})\nu^\beta = 0,$$

where the ν^β are the components of the unit vector normal to the plane P_1 or P_2 and the $\mu_{\alpha\beta}$ are the stress components in the elastic part of the bar relative to the y coordinate system. The quantities $\mu_{\alpha\beta}$ were calculated in our previous note and are given by

$$\mu_{11} = \tau \sin^2\theta; \quad \mu_{12} = \tau \sin\theta\cos\theta; \quad \mu_{13} = 0,$$

$$\mu_{22} = \tau \cos^2\theta; \quad \mu_{23} = 0; \quad \mu_{33} = 0,$$

where τ is the yield value of the tension and θ the inclination of the slip band. But ν^β has the values (0, 1, 0) and hence the above condition becomes $\mu_{\alpha 2} = \sigma_{\alpha 2}$. These relations are satisfied automatically for $\alpha = 3$. For $\alpha = 1, 2$ they give

$$\tau \sin\theta\cos\theta = \frac{a\varphi}{2}, \tag{6}$$

$$\tau \cos^2\theta = (b - c)\varphi, \tag{7}$$

when use is made of the relation (5).

It will be found helpful to replace equation (6) by the relation resulting from (6) and (7) by elimination of the angle θ. To effect this elimination we may first set up the auxiliary equation

$$\tan \theta = \frac{a}{2(b - c)}, \tag{8}$$

obtained by dividing corresponding members of the two equations (6) and (7). Combining (7) and (8) in an obvious manner we can now obtain

$$a^2 + 4(b - c)^2 = 4(b - c)\frac{\tau}{\varphi}. \tag{9}$$

Let us also eliminate E from (5) by means of the relation $E = -\tau\nu/c$ used to define the constant c at the beginning of this section. This gives the following equivalent equation

$$\nu(b + c)\frac{\tau}{\varphi} = (1 - 2\nu)c(2c - b). \tag{10}$$

Equations (7), (9), and (10) are three equations for the determination of the four quantities a, b, θ, and φ. The remaining equation is furnished by the von Mises or the Tresca yield condition.

4. von Mises Yield.—Substituting the $s_{\alpha\beta}$ given by (3) into the von Mises yield condition we are led, after some reduction, to the following equation

$$\left(b^2 + c^2 - bc + \frac{3a^2}{4}\right)\varphi^2 = 3k^2 = \tau^2. \tag{11}$$

We now eliminate a^2 from (11) by means of (9). This gives a quadratic equation in the ratio τ/φ which can be written

$$(\tau/\varphi)^2 - 3(b - c)\tau/\varphi + 2b^2 + 2c^2 - 5bc = 0.$$

Solving this equation for the ratio τ/φ and labeling one of the solutions Case I, the other Case II, we have

$$\text{Case I, } \frac{\tau}{\varphi} = b - 2c, \tag{12}$$

$$\text{Case II, } \frac{\tau}{\varphi} = 2b - c. \tag{13}$$

Each of these cases must be treated separately.

Case I. Substitute the value of the ratio τ/φ given by (12) into (10); the resulting equation reduces to

$$b = \left(1 - \frac{1}{\nu}\right)c, \tag{14}$$

by which the constant b is determined. Hence

$$\frac{\tau}{\varphi} = -\left(1 + \frac{1}{\nu}\right)c, \tag{15}$$

from (12) and (14). Also from (14), (15), and (9) we obtain

$$a^2 = 4c^2/\nu, \text{ or } a = \pm 2c/\sqrt{\nu}. \tag{16}$$

Finally the inclination θ can be determined by substituting the values of b and the ratio τ/φ into the equation (7). This gives

$$\cos^2\theta = \frac{1}{1+\nu}, \quad \text{or} \quad \cos 2\theta = \frac{1-\nu}{1+\nu} \tag{17}$$

Case II. When we substitute the value of the ratio τ/φ given by (13) into (10) we obtained a quadratic equation in b. Solving this equation we find

$$\frac{b}{c} = \frac{-(1-\nu)}{4\nu} \pm \frac{1}{4\nu}\sqrt{1 + 14\nu - 23\nu^2}. \tag{18}$$

With b determined by (18) we obtain the equation determining the constant a by eliminating the ratio τ/φ from (9) and (13). This gives

$$a^2 = 4b(b-c). \tag{19}$$

Hence from (7), (13), and (18) we have

$$\cos^2\theta = \frac{-(1-\nu) \pm \sqrt{1 + 14\nu - 23\nu^2} - 4\nu}{-2(1-\nu) \pm 2\sqrt{1 + 14\nu - 23\nu^2} - 4\nu}. \tag{20}$$

The expressions for the determination of the angle θ can be simplified if we replace (20) by the equivalent equations for $\cos 2\theta$. We thus obtain

$$\cos 2\theta = \frac{2\nu}{1 + \nu \pm \sqrt{1 + 14\nu - 23\nu^2}}. \tag{21}$$

To consider the relations (21) more closely let us write

$$\cos 2\theta' = \frac{2\nu}{1 + \nu + \sqrt{1 + 14\nu - 23\nu^2}} \qquad \left(0 < \nu < \frac{1}{2}\right), \tag{22}$$

$$\cos 2\theta_1 = \frac{2\nu}{1 + \nu - \sqrt{1 + 14\nu - 23\nu^2}} \qquad \left(0 < \nu \leqq \frac{1}{4}\right), \tag{23}$$

where we have used θ' and θ_1 instead of θ to distinguish between these cases. It is easily seen that the equation (22) is valid for the entire range of permissible values of Poisson's ratio ν, as indicated, while in the relation (23) we must limit our attention to values of ν not exceeding $1/4$. The relation (22) corresponds to the selection of the minus sign and (23) to the plus

sign before the radical in (18). Also it is easily seen that if θ is determined by (22) or (23), and the corresponding value of b taken from (18), the value of a^2, given by (19), will not be negative. However the value of the constant φ given by (13) will be positive only for angles θ determined by the formula (22). Moreover the value of b will be negative for slip bands whose angle of inclination θ_1 is determined by (23) and hence there will be a contraction, in the y_2 direction, of the band from its undeformed state. Such slip bands would not appear to be realized in the case of actual materials.

It is seen from equation (17) that, corresponding to any value of ν, there will be two slip bands whose inclination angles θ are equal except for algebraic sign. A similar remark applies to the inclination angles θ' which are

TABLE 1

ν	θ	θ'	θ''
0.000	0	45°0′	54°44′
0.025	8°59′	44°21′	54°18′
0.050	12°36′	43°46′	53°57′
0.075	15°19′	43°15′	53°40′
0.100	17°33′	42°46′	53°24′
0.125	19°28′	42°19′	53°11′
0.150	21°10′	41°53′	52°58′
0.175	22°42′	41°27′	52°46′
0.200	24°6′	41°2′	52°35′
0.225	25°23′	40°37′	52°24′
0.250	26°34′	40°12′	52°14′
0.275	27°40′	39°47′	52°5′
0.300	28°43′	39°22′	51°55′
0.325	29°41′	38°56′	51°46′
0.350	30°37′	38°29′	51°37′
0.375	31°29′	38°2′	51°29′
0.400	32°19′	37°33′	51°20′
0.425	33°6′	37°2′	51°11′
0.450	33°51′	36°30′	51°3′
0.475	34°34′	35°54′	50°55′
0.500	35°16′	35°16′	50°46′

determined from the equation (22). The principal or first quadrant values of the angles θ and θ' have been listed in the second and third columns of table 1.

5. Tresca Yield.—The principal values of the stress deviation tensor, whose components $s_{\alpha\beta}$ are given by (3), are readily found to be

$$s_1 = \left(\frac{b - 2c}{6} + \frac{1}{2}\sqrt{a^2 + b^2}\right)\varphi; \quad s_2 = \left(\frac{2c - b}{3}\right)\varphi;$$

$$s_3 = \left(\frac{b - 2c}{6} - \frac{1}{2}\sqrt{a^2 + b^2}\right)\varphi. \qquad (24)$$

Let us assume that these values are ordered so that $s_1 \geqq s_2 \geqq s_3$; this assumption will later be verified. Then the Tresca yield condition gives

$$s_1 - s_3 = \sqrt{a^2 + b^2}\,\varphi = 2k = \tau, \tag{25}$$

where τ is the yield value of the tension. Eliminating the ratio τ/φ from (9) by means of (25) we obtain a quadratic equation in $(b - c)$, namely

$$4(b - c)^2 - 4\sqrt{a^2 + b^2}\,(b - c) + a^2 = 0.$$

When this equation is solved for $(b - c)$ in the usual manner the two relationships obtained can be written as follows

$$\text{Case I,} \quad \sqrt{a^2 + b^2} = b - 2c, \tag{26}$$

$$\text{Case II,} \quad \sqrt{a^2 + b^2} = 3b - 2c. \tag{27}$$

We shall examine each of these cases in turn.

Case I. On account of (25) and (26) the equation (10) reduces to (14) thus determining the constant b. Eliminating b from (10) by means of (14) the equation (15) for the ratio τ/φ is again obtained. Likewise we find (16) for the determination of the constant a when we make the substitutions (14) and (15) into the equation (9). Also, as before, we are led to the relation (17) for the determination of the inclination θ of the slip band. For this solution $s_1 > s_2 = s_3$ so that the required identities in the principal values of the stress deviation are satisfied. It is interesting to find that the results for this case are the same as those obtained for Case I under the von Mises yield condition.

Case II. From (25), (27), and (10) we find

$$2(1 - \nu)c^2 - (1 - \nu)bc - 3\nu b^2 = 0.$$

Solving this quadratic equation in c^2 we obtain

$$c = \frac{b}{4} \pm \frac{b}{4}\sqrt{\frac{1 + 23\nu}{1 - \nu}}. \tag{28}$$

The constant b is determined by (28). To determine a we have from (25), (27), and (9) that

$$a^2 = 4(b - c)(2b - c), \qquad \text{or} \qquad a = \pm 2\sqrt{(b - c)(2b - c)}. \tag{29}$$

Hence from (7), (25), and (27) we have

$$\cos^2\theta = \frac{b - c}{3b - 2c}, \qquad \text{or} \qquad \cos 2\theta = \frac{-b}{3b - 2c}. \tag{30}$$

Eliminating the constants b and c from the second of the relations (30) by means of the substitution (28) we find

$$\cos 2\theta'' = \frac{-2}{5 + \sqrt{\dfrac{1 + 23\nu}{1 - \nu}}} \qquad \left(0 < \nu < \frac{1}{2}\right), \tag{31}$$

$$\cos 2\theta_2 = \frac{-2}{5 - \sqrt{\dfrac{1 + 23\nu}{1 - \nu}}} \qquad \left(0 < \nu \leqq \frac{1}{4}\right), \tag{32}$$

where the range of permissible values of ν has been indicated and we have replaced θ by θ'' and θ_2 to distinguish between these two cases. It is to be observed that the relation (31) corresponds to the selection of the minus sign and the relation (32) to the selection of the plus sign before the radical in (28). In the case of the relation (32) neither the constant b nor the quantity in the right member of (27) will be positive as can easily be seen. Hence the possibility of having a slip band whose inclination θ_2 is given by (32) must be discarded. No such difficulty arises in the case of the relation (31); in fact for angles θ'' determined by (31) the constants b and φ will be positive as will be also the value of a^2 given by (29). Finally it can readily be observed that $s_1 > s_2 > s_3$ so that the relation (25) gives the correct form of the Tresca yield condition for slip bands whose inclination θ'' is determined by (31).

The entries in the last column in table 1 are found from the relation (31) and are analogous to the entries in the second and third columns of this table.

[1] Thomas, T. Y., these PROCEEDINGS, **39**, 257–265 (1953).

[2] Prepared for the Naval Research Laboratory, Washington, D. C.

[3] See Nadai, A., *The Theory of Flow and Fracture of Solids*, McGraw-Hill, New York (1950), pp. 320–327.

[4] Actual slip bands are not to be confused with the bands or markings produced by singular surfaces, e.g., characteristic surfaces, which represent a weaker form of discontinuity. See Thomas, T. Y., "Singular Surfaces and Flow Lines in the Theory of Plasticity," *J. Rational Mech. and Anal.*, April (1953).

NONLINEAR MULTIPOLES

BY L. A. ZADEH

DEPARTMENT OF ELECTRICAL ENGINEERING, COLUMBIA UNIVERSITY

Communicated by J. R. Dunning, February 25, 1953

Linear multipoles, that is, electrical networks with two or more accessible terminals, have long played a central role in network theory.[1, 2] In this note the notion of a multipole is given a much broader meaning and a system of classes of nonlinear multipoles is introduced. An indirect objective of this note is to outline a conceptual scheme which, in conjunction with the existing theories of oriented graphs[3, 4] and with the aid of machine computers, could provide an effective tool for the analysis and design of nonlinear systems.

By a multipole, or more specifically, an $m + n$-pole, we mean a device, M, which has m input terminals and n output terminals, as shown in

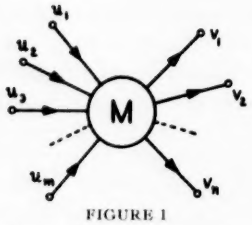

FIGURE 1
Diagrammatic representation of an $m + n$-pole.

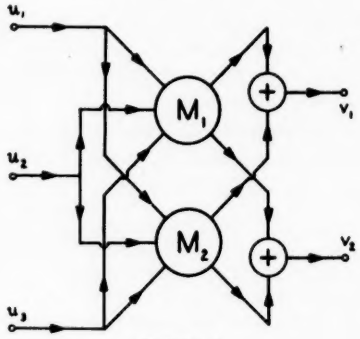

FIGURE 2
The sum of M_1 and M_2

figure 1. In the diagrammatic representation, the arrowheads serve to distinguish between the input variables, u_i, $i = 1, 2, \ldots, m$, and the output variables, v_j, $j = 1, 2, \ldots, n$. The u_i and v_j are assumed to be functions of time, but for brevity the argument t will be omitted where no ambiguity is likely to result. Furthermore, the u_i and v_j are assumed to range over specified function spaces, $U_i = \{u_i(t)\}$ and $V_j = \{v_j(t)\}$. In the sequel this assumption will often not be stated explicitly.

An $m + n$-pole is characterized by a set of n input-output relationships of the form

$$v_j = F_j(u_1, u_2, \ldots, u_m), \qquad j = 1, 2, \ldots, n, \tag{1}$$

where F_j represents an operator acting on the ordered m-tuple $(u_1, u_2, \ldots, u_m)$. In other words, F_j is an operation defined on the product space $U_1 \times U_2 \times \ldots \times U_m$ with values in V_j. In this sense, the $m + n$-pole as a whole represents an operation on $U_1 \times U_2 \times \ldots \times U_m$ to $V_1 \times V_2 \times \ldots \times V_n$. A multipole will be called *simple* if the F_j are ordinary functions of the u_i. The term *zero memory* is frequently used in the same sense in connection with nonlinear two-poles.

The problem of characterizing an $m + n$-pole in terms of explicit relations of the form (1) is of basic importance in the theory of nonlinear multipoles. One way of dealing with this problem is to consider a system of classes of nonlinear multipoles, such as that introduced in this note, and approximate a given multipole by one belonging in this system of classes. Before entering into a discussion of this approach, it is helpful to introduce the following notations and definitions.

Let M_1 and M_2 be two $m + n$-poles characterized by the input-output relationships

$$M_1: \quad v_j = F_j^{(1)}(u_1, u_2, \ldots, u_m), \qquad j = 1, 2, \ldots, n \tag{2}$$

and

$$M_2: \quad v_j = F_j^{(2)}(u_1, u_2, \ldots, u_m), \qquad j = 1, 2, \ldots, n, \tag{3}$$

respectively.

M_1 and M_2 are equivalent, $M_1 = M_2$, if the input-output relationships characterizing M_1 are identical with the corresponding relationships for M_2, that is,

$$F_j^{(1)}(u_1, u_2, \ldots, u_m) \equiv F_j^{(2)}(u_1, u_2, \ldots, u_m), \qquad j = 1, 2, \ldots, n. \tag{4}$$

The *sum* of M_1 and M_2, $M = M_1 + M_2$, is an $m + n$-pole characterized by the input-output relationships

$$M: \quad v_j = F_j^{(1)}(u_1, u_2, \ldots, u_m) + F_j^{(2)}(u_1, u_2, \ldots, u_m), \quad j = 1, 2, \ldots, n. \tag{5}$$

The diagrammatic representation for the sum multipole, M, is shown in figure 2. The $n + 1$-poles identified by the plus sign represent conventional *adders*, an adder being a multipole whose output is equal to the sum of its inputs. (Note that the validity of this and other diagrammatic representations involving two or more interconnected multipoles depends on the assumption that the external characteristics of a multipole are not affected by its connection to other multipoles. In engineering terms, this is equivalent to assuming that interconnected multipoles do not load one another.)

The *product* of a $k + n$-pole M_2 and an $m + k$-pole M_1 is an $m + n$-pole M, $M = M_2M_1$, which consists of M_1 and M_2 connected in series as indi-

cated in figure 3. From this definition it follows at once that the multipole product is associative and left-distributive, that is,

$$M_3(M_2M_1) = (M_3M_2)M_1 \tag{6}$$

and

$$(M_3 + M_2)M_1 = M_3M_1 + M_2M_1. \tag{7}$$

An $n + m$-pole, M_L^{-1}, is called a *left-inverse* of an $m + n$-pole, M, if

$$M_L^{-1}M = I \tag{8}$$

where I denotes a *unit* multipole, that is, an $m + m$-pole such that

$$v_i(t) \equiv u_i(t), \qquad i = 1, 2, \ldots, m \tag{9}$$

for all $u_i \in U_i$.

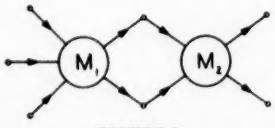

FIGURE 3
The product of M_2 and M_1.

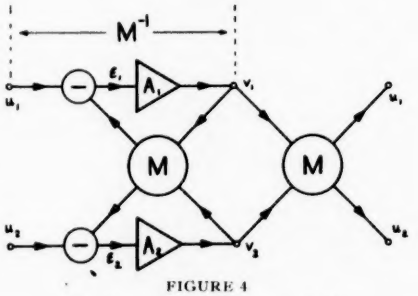

FIGURE 4
Realization of the inverse of M.

Similarly, a *right-inverse* of M, if it exists, is an $n + m$-pole, M_R^{-1}, such that

$$MM_R^{-1} = I, \tag{10}$$

where I is the unit $n + n$-pole.

The following two properties of right- and left-inverses are immediate consequences of the defining relations (8) and (10).

(i) If M_L^{-1} and M_R^{-1} both exist, then $M_L^{-1} = M_R^{-1}$.

(ii) If M_L^{-1} exists and is unique, then M_L^{-1} is also the right-inverse of M.

When M_L^{-1} and M_R^{-1} both exist, the multipole

$$M^{-1} = M_L^{-1} = M_R^{-1} \tag{11}$$

is called the *inverse* of M. The determination of the inverse of a given multipole is in general a difficult, if not intractable, mathematical problem. It is a simple matter, however, to realize approximately the inverse of a

given physical multipole with the aid of high-gain amplifiers. This can be done formally in the manner illustrated in figure 4, which shows the series connection of a 2 + 2-pole, M, and a multipole approximating its inverse, M^{-1}. The approximation to the inverse consists of M, two high-gain amplifiers A_1 and A_2, and a pair of subtractors. (A high-gain amplifier is essentially a two-pole whose output is equal to G times the input, where G, the gain of the amplifier, is a large constant.) It is seen that, as the gain approaches infinity, $\epsilon_1 = u_1 - v_1$ and $\epsilon_2 = u_2 - v_2$ approach zero, the series combination of the two multipoles approaches the unit 2 + 2-pole and, consequently, the multipole labeled M^{-1} approaches the inverse of M.

A multipole is *reducible* if it can be represented as the sum of two or more multipoles having a smaller number of poles. A reducible $m + n$-pole is *degenerate* if it can be represented as the sum of mn two-poles. The input-output relationships for a degenerate $m + n$-pole are of the form

$$v_j = \sum_{i=1}^{m} F_{ji}(u_i), \qquad j = 1, 2, \ldots, n, \tag{12}$$

where F_{ji} denotes an operator acting on u_i.

A multipole is *linear* if

$$F_j(\alpha u_1' + \beta u_1'', \alpha u_2' + \beta u_2'', \ldots, \alpha u_m' + \beta u_m'') = \alpha F_j(u_1', u_2', \ldots, u_m') + \beta F_j(u_1'', u_2'', \ldots, u_m''), \quad j = 1, 2, \ldots, n \tag{13}$$

for any real constants α and β and any time-functions u_i', $u_i'' \epsilon U_i$. A multipole is *nonlinear* if it is not linear.

An obvious but important corollary of (13) is that any linear multipole is degenerate. For in consequence of (13), we may write

$$F_j(u_1 + 0 + \ldots + 0, 0 + u_2 + \ldots + 0, \ldots, 0 + \ldots + 0 + u_m) = F_j(u_1, 0, \ldots, 0) + F_j(0, u_2, \ldots, 0) + \ldots + F_j(0, 0, \ldots, u_m) = \sum_{i=1}^{m} F_{ji}(u_i), \tag{14}$$

where

$$F_{ji}(u_i) = F_j(0, \ldots, u_i, \ldots, 0). \tag{15}$$

Because of the degeneracy of linear multipoles, any linear system may be represented as a collection of interconnected linear two-poles and adders.

We proceed now to define a certain system of classes of nonlinear $m + 1$-poles for the purpose of systematizing the characterization, realization, and optimization[5] of nonlinear multipoles. The restriction to $m + 1$-poles does not involve any loss of generality, since by virtue of (1) any $m + n$-pole may be decomposed into n $m + 1$-poles.

An $m + 1$-pole is of class $\mathfrak{M}_{1, 1, \ldots, 1}$ if its output, $v(t)$, admits a representation as an m-fold integral of the form

$$v(t) = \int_{-\infty}^{\infty}\int_{-\infty}^{\infty}\cdots\int_{-\infty}^{\infty} K[u_1(t-\tau_1), u_2(t-\tau_2), \ldots, u_m(t-\tau_m), \tau_1, \tau_2, \ldots, \tau_m, t]d\tau_1\, d\tau_2 \ldots d\tau_m, \quad (16)$$

where the $u_i(t)$ are the inputs, the τ's are the variables of integration, and K is any real function of its arguments. (K may include delta-functions of various orders.) The function $K[u_1(t-\tau_1), \ldots, u_m(t-\tau_m), \tau_1, \ldots, \tau_m, t]$ will be referred to as the *characteristic function* of the multipole with which it is associated.

It will be noted that when K does not depend explicitly on t, the $m+1$-pole which it characterizes is *time-invariant*, that is, has the property

$$v(t-t_0) = F[u_1(t-t_0), u_2(t-t_0), \ldots, u_m(t-t_0)] \quad (17)$$

for all real constants t_0. It will also be noted that in the case of any physical multipole, that is, one which operates only on the past of its inputs, the characteristic function vanishes for all negative values of the τ_i.

The class $\mathfrak{N}_{1,1,\ldots,1}$ is the lowest member of an hierarchy of classes of nonlinear $m+1$-poles, of which a general member is denoted by $\mathfrak{N}_{\alpha,\beta,\cdots,\mu}$. $\mathfrak{N}_{\alpha,\beta,\cdots,\mu}$ is defined as the class of all $m+1$-poles whose input-output relationship is expressible in the form of an $(\alpha+\beta+\ldots+\mu)$-fold integral

$$\begin{aligned} v(t) = \int_{-\infty}^{\infty}\int_{-\infty}^{\infty}\cdots\int_{-\infty}^{\infty} K[&u_1(t-\tau_{11}), u_1(t-\tau_{12}), \ldots, u_1(t-\tau_{1\alpha});\\ &u_2(t-\tau_{21}), u_2(t-\tau_{22}), \ldots, u_2(t-\tau_{2\beta}); \ldots;\\ &u_m(t-\tau_{m1}), u_m(t-\tau_{m2}), \ldots, u_m(t-\tau_{m\mu});\\ &\tau_{11}, \tau_{12}, \ldots, \tau_{1\alpha}; \tau_{21}, \tau_{22}, \ldots, \tau_{2\beta}; \ldots; \tau_{m1}, \tau_{m2}, \ldots, \tau_{m\mu}; t]\\ &d\tau_{11}\, d\tau_{12} \ldots d\tau_{1\alpha}\, d\tau_{21}\, d\tau_{22} \ldots d\tau_{2\beta} \ldots d\tau_{m1}\, d\tau_{m2} \ldots d\tau_{m\mu}. \end{aligned} \quad (18)$$

From this definition it follows at once that $\mathfrak{N}_{\alpha,\beta,\ldots,\mu} \subset \mathfrak{N}_{\alpha',\beta',\ldots,\mu'}$ if $\alpha' \geq \alpha, \beta' \geq \beta, \ldots, \mu' \geq \mu$, and that the class of linear $m+1$-poles is a subclass of every $\mathfrak{N}_{\alpha,\beta,\cdots,\mu}$.

To illustrate how an $m+1$-pole belonging in this system of classes can be characterized in terms of its responses to a family of "test" inputs, we consider for simplicity a time-invariant multipole of class $\mathfrak{N}_{1,1,\ldots,1}$. Let the inputs $u_1, u_2, \ldots, u_m$ consist of narrow rectangular pulses of width h and amplitudes $a_1, a_2, \ldots, a_m$, respectively. Furthermore, let these pulses occur at the instants $t_1, t_2, \ldots, t_m$. On substituting the expressions for the pulses in (16), we obtain the following relation between the characteristic function, K, and the response, $v(t)$, to the set of rectangular pulses:

$$K[a_1, a_2, \ldots, a_m, t-t_1, t-t_2, \ldots, t-t_m] = \frac{1}{h^m}\, v(t). \quad (19)$$

(provided $v(t) \equiv 0$ when one or more of the $u_i(t)$ are identically zero).

Thus, by varying the amplitudes $\{a_i\}$ and the instants $\{t_i\}$, one can experimentally determine the function K and thereby characterize the $m + 1$-pole under consideration via the input-output relationship (16). In other words, an $m + 1$-pole of class $\mathfrak{N}_{1,1,\ldots,1}$ is completely characterized by its responses to a family of m rectangular pulses whose amplitudes $\{a_i\}$ and times of occurrence $\{t_i\}$ range over all real values.

Once the characteristic function of an $m + 1$-pole of class $\mathfrak{N}_{\alpha,\beta,\ldots,\mu}$ has been determined, the $m + 1$-pole may be realized approximately in a canonical form such as that illustrated in figure 5. The structure shown in figure 5 represents an approximate realization of a physical, time-

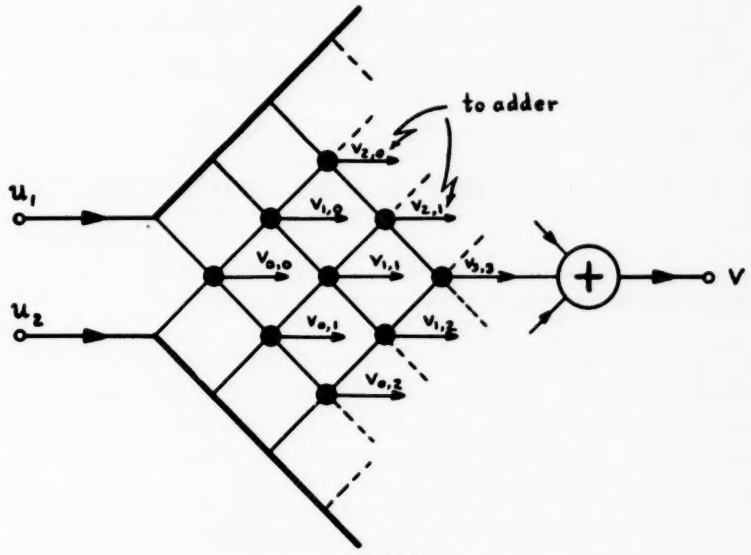

FIGURE 5
Approximate realization of a three-pole of class $\mathfrak{N}_{1,1}$.

invariant three-pole of class $\mathfrak{N}_{1,1}$ which is characterized by an input-output relationship of the form

$$v(t) = \int_0^\infty \int_0^\infty K[u_1(t - \tau_1), u_2(t - \tau_2), \tau_1, \tau_2] d\tau_1 \, d\tau_2. \qquad (20)$$

The structure consists of two tapped delay lines, an adder, and a number of simple three-poles (indicated as nodes) whose outputs are expressed by

$$v_{k,\lambda}(t) = f_{k,\lambda}[u_1(t - kT), u_2(t - \lambda T)], \qquad (21)$$

where T denotes the time-delay between two adjacent taps. The output, $v(t)$, is given by

$$v(t) = \sum_{k=0}^{\infty} \sum_{\lambda=0}^{\infty} f_{k,\lambda}[u_1(t - kT), u_2(t - \lambda T)]. \qquad (22)$$

The constant T and the $f_{k,\lambda}$ functions in (22) are chosen in such a manner that (22) constitutes an acceptable approximation to (20).

[1] Cauer, W., "Die Verwirklichung von Wechselstromswiderstanden vorgeschriebener Frequenzabhangigkeit," *Arch. f. Elektrotechnik*, **17**, 355 (1926).

[2] McMillan, B., "Introduction to Formal Realizability Theory," *Bell Syst. Tech. J.*, **31**, 217 (1952).

[3] Mason, S. J., "Signal Flow Graphs," *Proc. I.R.E.*, **39**, 297 (1951).

[4] Luce, R. D., "Two Decomposition Theorems for a Class of Finite Oriented Graphs," *Amer. J. Math.*, **74**, 701 (1952).

[5] The optimization of nonlinear two-pole filters is discussed in a paper by the writer, "Optimum Nonlinear Filters," to be published in *J. Appl. Phys.*

A STUDY OF MUTABILITY IN STREPTOMYCIN-DEPENDENT STRAINS OF ESCHERICHIA COLI

By Edgar L. Labrum

Department of Genetics, Carnegie Institution of Washington, Cold Spring Harbor, New York

Communicated by M. Demerec, January 30, 1953

Previous studies of mutability in *Escherichia coli* have dealt with specific mutational changes leading to bacteriophage resistance (Demerec,[1] Demerec and Latarjet,[2] Witkin[3]) or to streptomycin resistance (Demerec[4, 5]). More recent investigations have been concerned with "reverse" mutations from amino acid deficiency to non-deficiency in 33 auxotrophic strains representing requirements for 11 different amino acids (Demerec,[6] Demerec and Cahn[7]). These studies revealed that the various auxotrophic strains differed with regard to rates of spontaneous and induced mutation and also with respect to patterns of appearance of induced "reversions." For any one auxotrophic strain, the pattern of delayed appearance was the same regardless of the mutagenic agent used to induce the changes to non-deficiency. Since the reversions in at least some of these strains presumably involved different genetic loci, these results suggested that loci may differ with respect to rates of spontaneous and induced mutability and also with respect to patterns of appearance of induced mutations. Another finding was that although spontaneous reversions occurred readily in the 33 different auxotrophic strains studied, in 5 of them no induced mutations could be detected. Such strains were termed "mutagen stable."

The studies on mutability to be described here were concerned with mutational changes from streptomycin dependence to non-dependence in different streptomycin-dependent (*Sd*) strains of *E. coli* B/r. Crossing experiments with the K-12 strain of *E. coli*[4,8] have indicated that mutations involving streptomycin resistance and dependence occur at a single genetic locus. It is possible, therefore, that various streptomycin-dependent strains of independent mutational origin represent different alleles of a single locus. The purpose of this investigation was to compare the mutation rates and the patterns of delayed appearance of induced mutants exhibited by different *Sd* strains, and also to discover whether or not any of them showed mutagen stability.

Survey of Reversion Frequencies in 70 Sd Strains.—A series of preliminary experiments was performed in order to estimate the frequencies of spontaneous and induced reversion in a random sample of 70 strains of independ-

TABLE 1

FREQUENCIES OF SPONTANEOUS AND INDUCED MUTATION FROM STREPTOMYCIN DEPENDENCE TO NON-DEPENDENCE IN DIFFERENT *Sd* STRAINS OF *E. coli* B/r

STRAIN OF *E. coli* B/r	MUTATION FREQUENCY PER 10^9	
	SPONTANEOUS	$MnCl_2$-INDUCED
Sd-21	0	0
Sd-26	0.8	94
Sd-14	5.7	6,000
Sd-24	29	7,380
Sd-S1	54	2,800
Sd-S4	250	25,000
Sd-S5	500	15,000
Sd-S3	1,900	18,000
Sd-S9	4,000	270,000
Sd-S11	5,000	350,000
Sd-S7	16,800	206,000

ent origin. Twelve of these strains were mutants of spontaneous occurrence, isolated from independent cultures of *E. coli* B/r; ten were ultraviolet-induced mutants; and the remainder were from the stock culture collection of this laboratory.

Manganous chloride was the mutagen employed throughout the investigation. The procedure for treating bacteria with the chemical was a standard one developed at this laboratory,[9] and was the same in all experiments. *Sd* strains to be treated with $MnCl_2$ were grown in aerated cultures of nutrient broth containing streptomycin (10 μg./ml), for 24–36 hours at 37°. The cultures were then centrifuged, washed in 0.3 *M* NaCl, resuspended in 0.04% $MnCl_2$, and incubated for 1 hour at 37°. An untreated control sample was resuspended in broth instead of the chemical. The viable cell count in both treated and untreated cell suspensions was determined by plating suitable dilutions on nutrient agar containing strep-

tomycin (50 μg./ml.) and incubating 48 hours. Suitable dilutions of the treated and untreated samples were plated on plain nutrient agar and incubated for 5 days at 37°. Colonies that grew on the nutrient agar without streptomycin represented mutations from dependence to non-dependence. The mutants could be either sensitive or resistant to streptomycin.

The data shown in table 1 are representative of the results obtained in this survey of 70 strains. Most of the frequencies were calculated from colony counts of two plates, and thus are only approximations. All strains showing spontaneous-reversion frequencies of less than 10 per 10^8 were retested, and their frequencies were calculated from counts of six plates.

The results showed that none of the 70 strains was mutagen stable; that is to say, induced reversions were detected in every strain that produced spontaneous reversions. From this it was concluded that if mutagen-stable types do exist among *Sd* strains, they are certainly more rare than among the amino acid-deficient strains used by Demerec.[6]

Furthermore these data showed that apparently no two of the *Sd* strains were alike with regard to reversion frequency. This may indicate differences in mutation rate among the different strains; but there were at least two other factors that influenced the observed differences in frequency. One was the number of residual cell divisions that the *Sd* bacteria were able to undergo on plain nutrient agar. For example, in several strains tested, such as *Sd*-21 (table 1), no reversions were detected in either the treated or the untreated samples when plated on plain nutrient agar. Microscopic observation of the plates revealed that the cells had failed to divide at all, thus preventing the appearance of any spontaneous or induced mutations. This is consistent with the observations of Bertani,[10] which indicated that nearly all reversions in the *Sd*-4 strain that are detected as colonies on plain nutrient agar occur during the residual divisions undergone by the cells after plating. Spontaneous reversions that arise previously, during growth of the *Sd* cells in streptomycin broth, either are unable to survive or have a selective disadvantage. Background mutants, therefore, can be expected to represent an extremely low proportion of the reversions observed when *Sd* cells are plated on plain agar. In contrast to these strains that showed no residual growth, many strains such as *Sd*-S11 and *Sd*-7 (table 1), which underwent six or seven residual divisions on medium lacking the antibiotic, exhibited high frequencies of mutation.

Besides intrinsic differences in mutation rate and differences in extent of residual growth, there was variation in the proportion of cells surviving $MnCl_2$ treatment in different experiments. Survival varied from 10 per cent to 80 per cent, even though care was taken to perform all experiments in the same manner. Past experience with the use of $MnCl_2$ in this laboratory has indicated some correlation between survival and frequency of induced mutations.

Mutation Rates in Different Sd Strains.—Experiments were performed to determine whether or not 15 *Sd* strains did differ significantly with respect to mutation rates. Each strain was treated with $MnCl_2$ as described previously, and four plates were spread for each dilution of the control and treated samples. The number of residual divisions that each strain was able to accomplish on nutrient agar without streptomycin was determined by microscopic observations. Knowing the number of residual divisions and the number of bacteria plated, it was possible to estimate a spontaneous mutation rate per cell per generation. Rates of induced mutation were calculated on the basis of the number of bacteria plated, before any cell division occurred, and the values were corrected for spontaneous, mutations. It was probable that all the strains used in these experiments passed through a sufficiently large number of residual divisions so that all induced mutations were expressed. Each experiment was repeated on three different days.

The results, presented in table 2, show a high degree of variability among the mutation rates determined for each strain at different times. It is evident, however, that significant differences do exist among the various strains. *Sd*-U3 and *Sd*-S4, for example, were characterized by relatively low spontaneous mutation rates, whereas strain *Sd*-S12 exhibited an extremely high one. Most of the other strains had rates intermediate between these two extremes.

Pattern of Delayed Appearance of Induced Mutants.—Demerec[1] reported that cells of *E. coli* treated with either x-rays or ultra-violet radiation must pass through 10 to 12 divisions before all induced phage-resistant mutants appear. This "delayed effect" or "phenomic delay" was also observed by Davis[11] in the isolation of induced nutritionally deficient mutants of *E. coli* by the penicillin method. The phenomenon will be referred to in this paper as the "delayed appearance of induced mutants." Current views of the possible mechanisms responsible for delayed appearance have been discussed by Witkin[12] and Demerec.[6]

By plotting frequency of induced mutants against number of cell divisions elapsed since treatment, one obtains a curve representing the rate at which induced mutants appear, or the "pattern of delayed appearance." In cases where there is considerable variation among the frequencies obtained in different experiments, the percentage of the total yield of induced mutations manifested at each cell division can be plotted instead of the frequency.

From the 70 *Sd* strains used in the summary described previously, a dozen strains were chosen as being possibly suitable for these experiments. The strains selected were ones that pass through a minimal number of residual divisions on plain nutrient agar.

It was found that if the nutrient agar was "enriched" with low concentrations of streptomycin the number of residual divisions of some *Sd* strains could be increased. Thus, by plating the $MnCl_2$-treated and control sam-

TABLE 2

RATES OF SPONTANEOUS AND $MnCl_2$-INDUCED MUTATION FROM STREPTOMYCIN DEPENDENCE TO NON-DEPENDENCE IN DIFFERENT *Sd* STRAINS OF *E. coli*

STRAIN OF *E. coli* B/r	NO. OF RESIDUAL DIVISIONS	MUTATION RATES	
		SPONTANEOUS ($\times 10^{-9}$)	INDUCED ($\times 10^{-9}$)
Sd-U3	6	2.2	10
		2.7	7.9
		1.6	2.7
Sd-S4	7	5	22
		1	76
		29	25
Sd-S10	6	27	8.6
		9.1	13.7
		8	6.8
Sd-S3	5	33	66
		64	37
		17	27
Sd-S5	7	44	86
		27	155
		30	126
Sd-S8	6	63	60
		47	212
		47	72
Sd-S9	7	85	188
		37	105
		43	183
Sd-S11	6	75	228
		45	455
		53	245
Sd-U2	6	33	67
		77	179
		91	74
Sd-U7	6	66	65
		130	72
		56	70
Sd-U5	6	114	123
		82	117
		100	228
Sd-S2	6	110	168
		97	94
		124	146
Sd-U4	5	173	133
		87	81
		138	216
Sd-U1	6	278	134
		142	190
		51	198
Sd-S12	6	110	186
		149	239
		163	266

ples on a series of agar plates containing increasing concentrations of streptomycin, one could determine the reversion frequency after each successive division. The actual range of streptomycin concentrations that was effective in this respect differed for the various *Sd* strains, but in no case did it exceed 1 μg per ml.

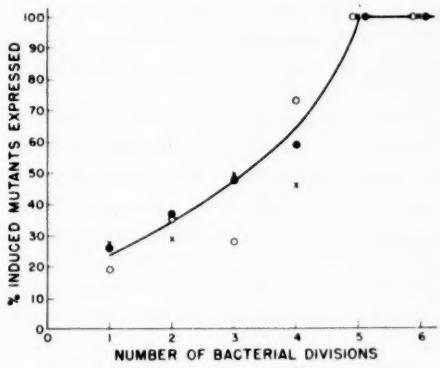

FIGURE 1↑

Fig. 1. Rate of appearance of induced reversions in the streptomycin-dependent strain B/r/-*Sd*-34 of *E. coli*. The data plotted represent the results of three independent experiments.

Fig. 2. Rate of appearance of induced reversions in the streptomycin-dependent strain B/r/-*Sd*-138 of *E. coli*. The data plotted represent the results of three independent experiments.

Fig. 3. Rate of appearance of induced reversions in the streptomycin-dependent strain B/r/-*Sd*-S1 of *E. coli*. The data plotted represent the results of three independent experiments.

FIGURE 3→

FIGURE 2↓

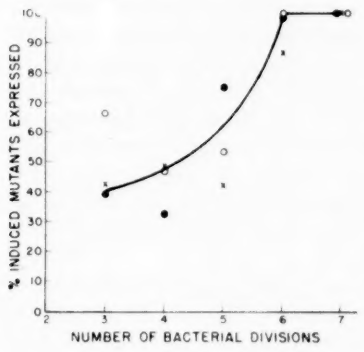

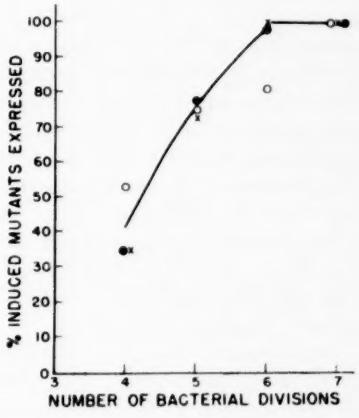

An unexpectedly large increase in number of colonies occurred when the *Sd* cells were plated on medium containing streptomycin in concentrations of 0.4 to 1 μg. per ml., and it was noted that these colonies varied greatly in size. When some of the smaller colonies were picked and streaked on both plain and streptomycin agar, it was seen that they were not true rever-

sions but apparently "semidependent" mutants, which could grow to some extent on very low concentrations of streptomycin. Since the mutation frequencies to be determined in these experiments were to represent only complete reversions, it was necessary to correct all colony counts. This was done by picking a random sample of at least 50 colonies from each set of plates that contained a different concentration of streptomycin, and streaking them out on both plain and streptomycin agar. From the results obtained it was possible to estimate what percentage of colonies represented true reversions for each concentration of streptomycin used in both control and treated series. Most of the *Sd* strains originally selected for these experiments gave rise to such a large proportion of the "semidependent" type of mutants that they could not be used.

The three strains best suited for the experimental procedures were *Sd*-S1, *Sd*-34, and *Sd*-138. In figures 1, 2, and 3 percentage of induced mutants expressed is plotted against number of divisions for each of these three strains. The curves thus obtained represent the patterns of delayed appearance. By comparing the curves it can be seen that in each case 100 per cent expression was reached at about the fifth or sixth division. Fifty per cent expression occurred at about 3 to $4^1/_2$ divisions. It was therefore concluded that the three *Sd* strains exhibited similar patterns of delayed appearance of induced mutants.

Discussion.—In a previous analysis of 163 *Sd* mutants, Demerec[4] found that practically no two strains were alike when compared on the basis of six different criteria, including spontaneous mutation rate and proportions of streptomycin-sensitive and streptomycin-resistant reversions produced. The data presented in table 2 extend these observations to include induced mutation rates. Considerable variation was encountered among separate experiments done with the same strain on different days; however, the rates for some strains were consistently low, whereas others showed consistently high or intermediate rates. Although no absolute correlation was found between spontaneous and induced rates, it was evident that there was, in general, a tendency for strains having low spontaneous rates to show relatively low induced rates, and those with high spontaneous rates to exhibit high induced rates.

Determination of the pattern of delayed appearance of induced mutants for three *Sd* strains (Figs. 1, 2, and 3) indicated that in each strain 100 per cent expression of induced mutations was reached at about the fifth or sixth division. In other respects, however, these three strains were not similar. The reversions produced by *Sd*-S1 were all streptomycin sensitive; those of *Sd*-138 were all resistant; and *Sd*-34 produced approximately 63 per cent resistant and 37 per cent sensitive reversions. They also differed with regard to the number of residual divisions they were able to undergo on plain agar.

The pattern of delayed appearance exhibited by the *Sd* strains appears to be an unusual one since 100 per cent of the total yield of induced mutations was obtained earlier than in most other mutation systems previously studied. With mutations involving resistance to coliphage T1, 100 per cent expression was not reached until the tenth or twelfth division.[1] Most of the auxotrophic mutant strains that have been analyzed[6, 7] also required more than six divisions to achieve 100 per cent expression, although in two amino acid-deficient strains all mutants had appeared by the end of the first division.

If one views the different *Sd* strains of independent origin as representing different alleles at a single locus, then it would seem likely that each different allele has its own characteristic rates of spontaneous and induced mutation. The fact that in three *Sd* strains all induced mutants had appeared by the fifth or sixth division, however, suggests that the pattern of delayed appearance is possibly determined by the genetic locus involved rather than by the particular allele.

Summary.—Frequencies of spontaneous and induced reversion from streptomycin dependence to non-dependence were estimated for 70 different *Sd* mutants of *E. coli* B/r. The results indicated that apparently no two strains were alike in this respect, and that no mutagen-stable types existed among the 70 strains.

Estimation of mutation rates from streptomycin dependence to non-dependence in 15 strains indicated wide differences among some strains.

The pattern of delayed appearance of induced mutants was determined for three different *Sd* strains. In each case, 100 per cent expression of induced mutants occurred by about the fifth or sixth division.

These results indicated that *Sd* strains of independent origin may be characterized by different rates of mutation to non-dependence, but that the pattern of delayed appearance of induced mutants is possibly similar for the different strains.

Acknowledgment.—The author wishes to express his gratitude to Dr. M. Demerec for his helpful advice and discussions during the course of this investigation.

[1] Demerec, M., PROC. NATL. ACAD. SCI., **32**, 36 (1946).

[2] Demerec, M., and Latarjet, R., *Cold Spring Harbor Symp. Quant. Biol.*, **11**, 38 (1946).

[3] Witkin, E. M., *Ibid.*, **12**, 256 (1947).

[4] Demerec, M., *Am. Nat.*, **84**, 5 (1950).

[5] Demerec, M., *Genetics*, **36**, 585 (1951).

[6] Demerec, M., *Symp. Soc. Exp. Biol.* (Cambridge); (in press).

[7] Demerec, M., and Cahn, E., *J. Bact.*; (in press).

[8] Newcombe, H. B., and Nyholm, M. H., *Genetics*, **35**, 603 (1950).

[9] Demerec, M., and Hanson, J., *Cold Spring Harbor Symp. Quant. Biol.*, **16**, 215 (1951).

[10] Bertani, G., *Genetics*, **36**, 598 (1951).
[11] Davis, B. D., *Experientia*, **6**, 41 (1950).
[12] Witkin, E. M., *Cold Spring Harbor Symp. Quant. Biol.*, **16**, 357 (1951).

*INDUCED POLLEN LETHALS FROM SEEDS OF DATURA STRAMONIUM TREATED WITH THERMAL NEUTRONS**

BY J. L. SPENCER, W. R. SINGLETON, AND A. F. BLAKESLEE

UNIVERSITY OF MASSACHUSETTS, BROOKHAVEN NATIONAL LABORATORY, AND SMITH COLLEGE GENETICS EXPERIMENT STATION

Communicated January 19, 1953

The cytogenetic effect of thermal neutrons was shown by Conger and Giles[1] to be about eleven times that of x-rays per unit dose. The difference in effectiveness is believed to be due largely to the internal origin of the protons and alpha rays which result from capture reactions.

A preliminary study of the effects of thermal neutrons on plants of *Datura stramonium* grown from treated seeds was undertaken for the purpose of discovering the induced cytogenetic aberrations, especially pollen lethals. Cartledge and Blakeslee[2] in a study of genetic changes in aged seeds have shown that pollen abortion in Datura affords a convenient and delicate index to the mutation rate. They distinguished two types of pollen abortion. In one, the chromosomal type, the pollen grains abort at an early stage resulting in small, shriveled, and empty grains. The other is marked by subnormal to very small size and usually by differences which were interpreted as degenerative changes in the character of their contents. Of ten plants listed as belonging to the gene type, Dr. Satina found all were free from obvious chromosomal abnormalities thus confirming their genic nature. Of 11 classified as chromosomal types all except three showed chromosomal abnormalities. These discrepancies may be due to securing chromosomal figures from different sectors from those from which the pollen was recorded but more likely was due to some of the lethal genes causing abortion of pollen at an early stage. In the majority of cases, however, it appears possible to distinguish pollen abortion types due to genes from those due to chromosomal abnormalities. Since further evidence in support of this distinction is given in the succeeding paper[3] we shall continue to use the terms chromosomal and gene types for the two rather distinct types with the admission that the distinction may not always be justified. In the present study the chromosomal type of aborted pollen occurs in rather definite proportions including about 25 per cent, 50 per cent, 75 per cent, or rarely 100 per cent of the grains. The gene type causes the abortion of either 25 per cent or 50 per cent of the total grains. Mutations of both

types arise naturally and are induced readily by exposure to ionizing radiations, such as x-rays. The induced mutations generally occur in limited sectors of the plant, although they often involve the entire plant. Single plants and, indeed, even single flowers, may show several types of pollen abortion due to as many mutations.

From the foregoing it is apparent that the two types of pollen abortion may be used as a rough index of the rate of both chromosomal and gene mutations. Such an index avoids the necessity of growing the large number of plants that would be required in the second generation to disclose recessive "visible" mutations. Previous work has shown that pollen abortion types are several times as frequent as recessive morphological types disclosed in the second generation.

For these experiments we employed the standard line 1 of *Datura stramonium* which has been selfed for over 40 generations and brought through a haploid generation. The seeds from three capsules that had developed from flowers having less than one per cent bad pollen were each divided into

TABLE 1

POLLEN ABORTION IN DATURA FROM THERMAL NEUTRON TREATED SEEDS

LENGTH EXPOSURE, HR.	NUMBER OF SEEDS	NUMBER OF SEEDLINGS	PLANTS MATURING	PLANTS EXAMINED	
				WITH NORMAL POLLEN	WITH ABNORMAL POLLEN
2	876	742 (85%)	647 (74%)	128 (24%)	395 (76%)
4	890	683 (76%)	321 (36%)	30 (14%)	191 (86%)
6	911	205 (22%)	32 (3.5%)	2 (11%)	17 (89%)
Control	150	139 (93%)	114 (76%)	182 (100%)	0 (0%)
Additional controls (Line 1)			82		

four lots. One lot of seed from each capsule constituted the control. The other three groups were exposed for two, four, and six hours, respectively, in a thermal column to a flux of approximately 4.6×10^8 N_{th}/cm.^{2}/sec. (The cadmium ratio was 5000:1 and the gamma contamination was about 50 r/hr.)

The pollen was examined from a single flower from each fork of the plants tested. Datura plants usually have only two forks although three or rarely four may be present. If the flower showed abnormal pollen, pollen of adjacent flowers was examined in order to delimit the sector exhibiting the pollen abnormality.

Approximately 93 per cent of the control seeds (untreated) produced seedlings, while only 85 per cent, 76 per cent, and 22 per cent of the seeds exposed for two, four, and six hours, respectively, resulted in seedlings of sufficient development to show true leaves (table 1). The 876 seeds subjected to a dosage of two hours gave rise to 647, or 74 per cent, mature plants. This percentage was slightly less than that yielded by the controls (76 per cent). The four-hour exposure of 890 seeds ultimately re-

sulted in 321, or 36 per cent, mature plants, but only 32, or 3.5 per cent, of the 911 seeds treated for six hours gave rise to mature Datura plants.

The mutation rate, based on pollen abortion, was found to be 76 per cent, 86 per cent, and 89 per cent for plants from seeds treated for two, four, and six hours, respectively. No control plants were found that yielded over four per cent bad pollen; however, previous accounts indicate that a mutation rate of about 0.5 per cent may be expected.

For the determination of the types of pollen abortion and sectoring induced by the dosage of thermal neutrons reported here, the pollen from 3517 flowers was examined (table 2). An analysis of the 2034 flowers from plants that arose from seeds exposed for two hours to thermal neutrons showed 685 which could be considered normal (less than 10 per cent bad pollen). The four-hour treatment resulted in 142 normal flowers out of the 897 examined, while the six-hour dosage yielded only seven flowers with less than 10 per cent aborted pollen out of the 84 analyzed. In other words,

TABLE 2

TYPES OF POLLEN ABORTION FOUND IN DATURA FROM THERMAL NEUTRON TREATED SEEDS

		POLLEN CONDITION				
LENGTH OF EXPOSURE, HR.	NUMBER OF FLOWERS ANALYZED	NORMAL	CHROMOSOMAL TYPE (SHRIVELED)	ABNORMAL-GENE TYPE (SMALL)	CHROMOSOMAL AND GENE TYPES (SHRIVELED AND SMALL)	TOTAL ABNORMAL
2	2034	685 (34%)	1064 (52%)	153 (8%)	132 (6%)	1349 (66%)
4	897	142 (16%)	603 (67%)	57 (7%)	95 (11%)	755 (84%)
6	84	7 (8%)	57 (68%)	3 (4%)	17 (20%)	77 (92%)
Control	502	502 (100%)				0 (0%)

only 34 per cent, 16 per cent, and 8 per cent of the flowers from plants that arose from seeds treated for two, four and six hours, respectively, were comparatively free from pollen lethals. All of the flowers from control plants were found to be normal with respect to aborted pollen.

The presence of pollen lethals resulted in flowers that contained aborted grains of either the chromosomal type, or the gene type, or a combination of both types. The latter condition, both shriveled grains and small grains in the same flower, indicated the presence of at least two mutations, one of each type. The two-hour dosage resulted in chromosomal types in 52 per cent of the flowers, gene types in 8 per cent, and both types in 6 per cent, or a total of 66 per cent (1349) abnormal flowers. The four-hour exposure yielded chromosomal types in 67 per cent of the flowers, gene types in 7 per cent, and 11 per cent with both conditions. A total of 84 per cent (755) of the flowers examined from plants from seed exposed four hours was abnormal. The six-hour dosage resulted in 92 per cent (77) of the flowers being abnormal: 68 per cent demonstrated chromosomal types of abortion, 4 per cent showed gene types, and 20 per cent both types. Of

course the number of flowers in each category would depend upon the number examined from each sector. However, the percentages stated give approximation of the severity of treatment and of the resultant induction of sectors.

The evident lethal effects on the seeds and seedlings of Datura caused by the severity of treatment at the longer exposures of four and six hours made it difficult to reach definite conclusions regarding the genetic effects of different dosages. However, if flowers with both shriveled and small grains are considered to have two types of mutations, then there have been increases in the percentages of both types with further increments of time.

If the double types, chromosomal and gene, are taken into consideration there is no significant change in the ratio of chromosomal to gene types with increased dosage.

Large pollen grains were found in some of the flowers of exposed plants, but not in the flowers on the control plants. Grains of diploid (2N) size

TABLE 3

POLLEN ABORTION SECTORS IN DATURA FROM THERMAL NEUTRON TREATED SEEDS

LENGTH OF EXPOSURE, HR.	NUMBER OF PLANTS HAVING POLLEN LETHALS		NUMBER OF PLANTS HAVING DISTINCT SECTORS BETWEEN			
	WITH SECTORS	WITHOUT SECTORS[a]	NORMAL / CHROMOSOMAL TYPE	NORMAL / GENE TYPE	CHROMOSMAL / GENE TYPE	OTHERS[b]
2	288	107 (27%)	96	19	32	141
4	132	59 (31%)	15	1	3	40
6	9	8 (47%)	2	1	1	4

[a] All flowers of plant show a single pollen abortion type.

[b] Sectors recorded, but individual flowers show both pollen abortion types.

were recorded in the following percentages: two-hour treatment, 7 per cent of the plants; four-hour treatment, 10 per cent of the plants; and six-hour treatment, 21 per cent of the plants. Pollen of larger than diploid size was rarely noted.

The number of plants that developed from treated seeds and that displayed but a single type of pollen abortion (i.e., either chromosomal or gene) in all their flowers increased from 27 per cent in the two-hour group to 47 per cent in the six-hour group (table 3). This would seem to indicate that the severity of the longer exposures induced mutations affecting pollen abortion which involved the entire plant. The pollen has its origin in the second layer of the embryo. Perhaps adjacent cells of this layer were killed by heavy dosage and only one cell which was lightly hit survived to give rise to pollen grains. With very few exceptions plants which demonstrated a single pollen abortion type throughout possessed a chromosomal type of mutation. A significant positive correlation appears to exist between pollen abortion and morphological aberrations; however, the severity of treatment at both the four- and six-hour levels tended to obscure this

pattern by making it difficult to delimit sectors clearly. Although the data at hand precluded the possibility of making rigorous comparisons between plants arising from seed subjected to thermal neutrons and plants from x-irradiated seed, no developmental or morphological disturbances or lethality patterns in Datura unique to either kind of treatment were detected. Caldecott, Frolik, and Morris[4] found that individual barley seed subjected to identical doses of x-rays were variously affected, as determined by seedling heights, but injury was much more uniform with identical doses of thermal neutrons. These investigators also reported that "differential" delayed killing was characteristic in barley exposed to 10,000 to 20,000 r units of x-radiation, but that similar lethality patterns did not occur in thermal neutron-treated material.

Further study of thermal neutron induced pollen lethals in Datura is in progress.

* Contribution from the Department of Botany, Smith College, New Series No. 48. This work has been aided by a grant from the Atomic Energy Commission.

[1] Conger, A. D., and Giles, N. H., *Genetics*, **35**, 397–419 (1950).

[2] Cartledge, J. L., and Blakeslee, A. F., PROC. NATL. ACAD. SCI., **20**, 103–110 (1934).

[3] Yost, H. T., Jr., Singleton, W. R., and Blakeslee, A. F., PROC. NATL. ACAD. SCI., **39**, 292–297 (1953).

[4] Caldecott, R. S., Frolik, E. F., and Morris, R. M., *Ibid.*, **38**, 804–809 (1952).

*THE EFFECT OF THERMAL NEUTRON RADIATION ON THE CHROMOSOMES OF DATURA**

BY HENRY T. YOST, JR., W. R. SINGLETON, AND A. F. BLAKESLEE

BIOLOGICAL LABORATORY, AMHERST COLLEGE, AMHERST, MASSACHUSETTS; BROOKHAVEN NATIONAL LABORATORY, UPTON, NEW YORK; AND GENETICS EXPERIMENT STATION, SMITH COLLEGE, NORTHAMPTON, MASSACHUSETTS

Communicated January 19, 1953

The work of Conger and Giles[1] has demonstrated the great effectiveness of thermal neutron radiation in producing chromosomal aberrations. This finding has led to the investigation of the effects of thermal neutrons on plant growth[2] and on polyploid material.[3] In the light of this work, it seems advisable to investigate the genetic effects of thermal neutron radiation and, if possible, to correlate them with chromosomal aberration. The general problem is the relationship between chromosomal aberration and the expression of genetic changes. This problem may be investigated by discerning whether increased chromosome breakage yields proportionate or disproportionate genetic change. The studies presented herewith are preliminary to the solution of this problem.

One of the great difficulties in studies correlating gene and chromosomal effects is the time which it takes for recessive mutants to appear. Indeed Tradescantia, on which the original work was done,[1] has no genetic markers; consequently there are no data available on the genetic effects of thermal neutrons. In Datura there is available an ideal test organism. A measure of the over-all mutation rate may be gained from the pollen abortion of the mature plants developing from irradiated seed. The basis for this estimate has been described elsewhere.[4, 5] In addition, there are two distinct types of aborted pollen: small, empty, shrivelled grains and very small grains with more or less degenerate contents. (For brevity these two types will be referred to as empty-shrivelled and small.) Cartledge and Blakeslee[6] have indicated that there is a correlation between these two types of abortion and the gene and chromosomal types of mutation. They have suggested that the small grains are associated with point gene mutation, and the empty-shrivelled type with chromosomal mutation. This distinction was confirmed cytologically by Dr. Satina from study of a limited number of cases of each type. It was deemed important to test this hypothesis with the neutron radiation, since, if it were true, it would provide a rapid survey method for a much larger number of plants than could be investigated cytologically. The work reported here bears specifically on this problem.

Experimental Procedures and Results.—Seeds of Datura stramonium, Line 1, were exposed to radiation in the thermal column of the nuclear reactor at the Brookhaven National Laboratory for a period of two hours. The flux was approximately 4.6×10^8 $N_{th}/cm.^2/sec.$ The cadmium ratio was about 5000:1 and the gamma contamination was about 50 r/hr. The control seeds and the radiated seeds came from the same parents. All seeds were germinated in the greenhouse and subsequently transferred to the field. The mature plants were studied for pollen abnormalities and sector of good and bad pollen delimited for each plant.[5] Buds were then obtained from both the good and bad sectors, and aceto-carmine smear preparations of the anthers were made. The metaphase and anaphase of the first meiotic division were scored for abnormalities.

Segmental interchanges are the most easily detected chromosomal aberrations in Datura. In this case, there is the formation of a circle or chain of 4, 6, 8, etc., depending upon the number of chromosomes involved. Translocations involving the satellites are also scored readily. In general they give rise to a configuration similar to a bow-tie, with the translocated parts joined at the center. Large deficiencies can be scored as well as deficiencies or duplications of whole chromosomes. No attempt was made to determine the frequency of inversions, and it is probable that small deficiencies would be missed unless the fragment remained in the cell. It is evident from these studies and from others[6, 7] that segmental interchanges

give a reliable measure of the rate of breakage. Wherever there was any doubt about the nature of a configuration, several determinations of the same sector were made. In a large majority of the cases the configurations were confirmed by Dr. Satina, to whom we are greatly indebted.

The results of the comparison of pollen abortion types are summarized in table 1. It is immediately evident that there is a correlation between the

TABLE 1

CYTOLOGICAL CHECK ON POLLEN ABORTION TYPES FROM NEUTRON-IRRADIATED SEEDS (2 HOURS—4.6×10^8 N_{TH}/CM.^{2}/SEC.)

POLLEN ABORTION, CHROMOSOMAL TYPES			POLLEN ABORTION, GENE TYPE		
PLANT NO.	POLLEN, %	CHROMOSOMES	PLANT NO.	POLLEN, %	CHROMOSOME
510175-18	50	④ + 11 bvts.;[a] 12 bvts.	510175-2	50	12 bvts.
510175-33	50	12 bvts.	510175-18	50	12 bvts.
510175-40	25	④	510175-63	50	④
510175-52	50	12 bvts.	510175-93	50	12 bvts.
510175-55	50	④ + 11 bvts. + frag.;[a] 12 bvts.	510175-111	25	12 bvts.
510175-56	50	④	510176-32	50	12 bvts.
510175-63	50	④	510176-97	25	12 bvts.
510175-92	50	Chain of 6	510176-118	50	12 bvts.
510175-111	25	④	510175-20	25	12 bvts.
510176-1	50	Sat. trans.	510176-69	25	④
510176-14	25	④	510176-64	50	12 bvts.
510176-25	50	④	510176-70	50	12 bvts.
510176-30	50	④			
510176-32	50	④			
510176-38	25	④			
510176-52	50	Sat. trans.			
510176-63	25	④			
510176-67	25	12 bvts.			
510176-83	50	Sat. trans.			
510176-86	50	12 bvts.			
510176-97	25	④			
510176-5	50	⑥			
510176-26	50	④			
510176-139	50	Sat. trans.			
510176-118	50	④			

[a] Retested.

types of pollen abortion and the types of mutation. Chi-square tests indicate that there is a highly significant difference between the two types of abortion with regard to the proportion of chromosomal aberration present in each case. The P value determined for this comparison is 0.0005. There can be little doubt that the two types of pollen abortion show different chromosomal patterns. Table 2 shows the results of studies made on good sectors and plants; that is, on plants showing less than 10% pollen

abortion of any type. It is evident that there is little indication of chromosomal aberration in this group. It is interesting to note that one of the normal sectors showing a segmental interchange is from the same plant (510175-63) which showed a segmental interchange in the small pollen group of table 1. This is an indication that there is reason to doubt that the small pollen is associated in any way with the segmental interchange. Taking both tables together, it is evident that there are some cases in which segmental interchanges do not give rise to pollen abnormalities. However, since in all cases in which empty-shrivelled sectors showed segmental interchanges the good sectors on that same plant showed no segmental interchanges, there is good evidence that the two effects are related. There is good reason to believe, on the other hand, that in cases of small pollen showing segmental interchanges there is no relation between the two other than one of chance association.

Plants number 510175-18 and 510175-55 are worthy of separate consideration. In each of these an extra pair of chromosomes was apparent on the first determination. Subsequent determinations, however, failed to show this extra pair. In both cases, the extent of the damage to the chromosomes was apparently limited to one bud, or at least to a very small sector.

TABLE 2

CYTOLOGICAL CHECK ON PLANTS SHOWING NORMAL POLLEN

POLLEN ABORTION, %	NUMBER OF PLANTS	CHROMOSOMES
0–1	30	12 bvts.
0–1	2*	④
2–5	17	12 bvts.
5–10	6	12 bvts.

* 510176-69; 510176-49.

Discussion.—The data just cited indicate that it is permissible to group the aborted pollen into two distinct types. These two types are different morphologically and genetically. Grains which are empty and shrivelled are due to an early abortion and seem to be positively correlated with chromosomal aberrations. There are several cases in which no chromosomal aberration was observed; nevertheless, the only types of aberration observed were of the translocation type, and it is evident that inversions and small deficiencies could go undetected. Therefore, it seems quite safe to term the empty-shrivelled pollen a chromosomal type. On the other hand, the small pollen group showed very few chromosomal abnormalities. It is true that small deficiencies would be easily missed in this case, and there is no basis for a distinction being made on the old question of point gene mutation versus the infinitesimal deficiency. Still, the lack of segmental interchanges makes a broad distinction permissible, and the small pollen may be classed

as gene type. Such a distinction makes it possible to set up a rapid survey method for the whole field of plants, classing them for number of mutants and mutant type simultaneously from the morphology of the pollen. This should be of great aid in the investigation of future radiation problems in Datura. The question of deficiencies in general deserves further attention in the near future. There is little evidence into which group small deficiencies would fall.

Considering the general problem of the relation of the gene and chromosome mutant types developing from neutron radiation in the light of these data, it is evident that the gene type are few in number compared to the chromosomal type. In fact almost 70% of the plants showed chromosomal-type pollen. At low doses it would be expected that the gene type would far outnumber the chromosomal type of mutation, especially since the aberrations scored were of the "two-hit" type. At higher doses, however, the reverse relationship might hold. That is, more of the treated cells would tend to have chromosomal aberrations, and the gene type would be obscured. There is some indication of this given in table 1. It will be noted that the great proportion of the types showing segmental interchanges have 50% bad pollen. In previous studies, it has been demonstrated that segmental interchanges in Datura may give rise to 25% bad pollen, but generally have good pollen.[7] There is a striking difference between the data collected with thermal neutron radiation and those from x-rays, heat, aged seed, etc. This difference may be explained on the basis that the dose of neutrons was great enough to give a large number of cells with both chromosomal aberrations and gene mutations, and these cells give rise to flowers with 50% bad pollen as a result of the two types of aberration. On the other hand, the possibility still remains that the segmental interchanges induced by thermal neutron radiation are different in extent from those induced by other agents. It is quite likely that the aberrations scored consist of complexes of breaks rather than simple segmental interchanges resulting from two breaks. These data clearly support the findings of Conger and Giles[1] that the thermal neutron radiation is extremely effective in producing chromosome breaks. The earlier work of Frolik and Morris[8] indicated that there was little difference in the effectiveness of x-rays and neutrons in the induction of sectors in corn. Our data seem to indicate that the neutrons are far more effective. The solution of the general problem, however, must await further studies at lower doses of neutron radiation.

Final consideration must be given to the two cases which showed extra chromosomes. These plants were numbers 510175-18 and 510175-55 (table 1). The original preparations derived from these plants showed cells in which extremely complex aberrations had been induced. In plant 55 particularly there was evidence of very extreme damage and only the mini-

mum found is reported here. The cells were aberrant to the extent that it was hard to find metaphase figures showing clear configurations, although the slide was good.

An extra chromosome, at least in the second layer,[4] is generally marked by some easily detectable morphological abnormality. One would expect that the presence of an extra bivalent should have produced very clear morphological differences. Nevertheless, when the plant was examined there was no morphological abnormality seen. For this reason more slides were made of this particular sector. Upon examination there was no evidence found of chromosomal abnormalities. There are two possibilities to explain this occurrence. One is that a single cell was affected and survived to give rise to the only bud examined in each plant at a much later date. If this be the case, it is reasonable to suppose that the cell never became involved with more than a limited portion of the plant, since there was no morphological abnormality detected. This is scarcely a plausible explanation, since innumerable cell divisions must have taken place after the induction of the aberrations. On the other hand, it is possible that these two buds represent cases of delayed effects of the neutron radiation. It is possible that activated molecules were induced by the neutron capture and that later decay might result in the release of energy sufficient to cause chromosomal abnormalities. The major difficulty with such an hypothesis is that one must assume a relatively stable condition, since it is of very long duration, and since the "active state" must pass through several cell generations. On the whole, however, the latter of the two possibilities seems the more plausible. Certainly this suggestion is worth further study in the near future.

Summary.—Data have been presented which indicate that pollen abortion types in Datura may be classed in two distinct groups with respect to the type of mutation involved. Those showing empty-shrivelled grains result from chromosomal aberration, and those showing small grains result from gene mutation. With thermal neutron radiation there is a high preponderance of the chromosomal type of aborted pollen. The data suggest the possibility of extremely delayed effects induced in the chromosomes of Datura after thermal neutron radiation.

* Contributions from the Department of Botany, Smith College, New Series, No. 49. This work was supported by contract with the U. S. Atomic Energy Commission.

[1] Conger, A. D., and Giles, N. H., *Genetics*, **35**, 397–419 (1950).

[2] Caldecott, R. S., Frolik, S. F., and Morris, R. M., *Rec. Gen. Soc.*, **21**, 15–16 (1952).

[3] Konzak, C. F., and Singleton, W. R., *Ibid.*, **21**, 40–41 (1952).

[4] Satina, S., and Blakeslee, A. F., *Am. J. Bot.*, **28**, 862–871 (1941).

[5] Spencer, J. L., Singleton, W. R., and Blakeslee, A. F., PROC. NATL. ACAD. SCI., **39**, 288–292 (1953).

[6] Cartledge, J. L., and Blakeslee, A. F., *Ibid.*, **20**, 103–110 (1934).

[7] Bergner, A. D., Satina, S., and Blakeslee, A. F., *Ibid.*, **19**, 103–115 (1933).

[8] Frolik, E. F., and Morris, R., *Agron. J.*, **42**, 293–303 (1950).

ON SOME VARIATIONAL PROBLEMS OCCURRING IN THE THEORY OF DYNAMIC PROGRAMMING

BY RICHARD BELLMAN, IRVING GLICKSBERG, AND OLIVER GROSS

THE RAND CORPORATION, SANTA MONICA, CALIFORNIA

Communicated by J. von Neumann, February 5, 1953

1. Introduction.—The purpose of this note is to present some results of our investigation of a class of interesting and important variational problems arising in connection with problems involving the control of a system over a time interval. We may, on one hand, desire to maintain a dynamic system of mechanical, economic, or other origin, in or near a specified state at minimum cost, where the cost is compounded of two parts, the first part measured in terms of the deviation of the system from the desired state, and the second part measured by the cost of the resources used for control. Alternatively, we may, given a fixed quantity of resources, wish to maximize or minimize the output of a system.

The mathematical difficulties encountered in treating problems of this type depend upon the mathematical model used to represent the system, the functionals employed to measure the cost of deviation and the cost of control, and the constraints imposed upon the permissible type of control.

We shall present here only some results we have obtained for systems whose state at any time t is described by a column vector $x(t)$ satisfying a linear vector-matrix equation

$$\frac{dx}{dt} = Ax + f(t), \qquad x(0) = c, \tag{1.1}$$

where A is constant.

An equation of this type enters in connection with problems of continuous control. If we take account of time-lags, in place of (1.1) we obtain differential-difference equations, the simplest type of functional equation allowing for hereditary effects. If in place of continuous control, intermittent control is used, (1.1) will be replaced by a difference equation.

With reference to (1.1), let $y(t)$ be the desired state of system at time t, and let $F(x - y)$ be the functional measuring the total cost of deviation over an interval $[0, T]$, $G(f)$ be the functional measuring the cost of control as exercised through the forcing term $f(t)$, and $H(c)$ be a function measuring the cost of control as exercised through starting the system in state c.

We may then minimize the total cost $J(f, c) = F(x - y) + G(f) + H(c)$, or minimize $F(x - y)$ subject to $G(f) \leq a_1$, $H(c) \leq a_2$. There is an equivalence between these two types of problems, the second of which leads directly, via Lagrange multiplier techniques, to Sturm-Liouville problems of non-classical type. If time-lags are permitted, we are led to consider

Sturm-Liouville problems for differential-difference equations. These topics will be discussed in subsequent publications.

We shall present here some results we have obtained for the cases where F and G are linear or quadratic functionals and the constraints upon f are of simple type such as $0 \leq f_i \leq m_i$. For simplicity we shall assume that c is fixed.

2. Linear and Quadratic Functionals.—The methods used to obtain the following results are interesting mixtures of abstract and analytic techniques reinforcing each other at critical points. What constitutes the difficulty of the problem, of course, is that free variations are only occasionally permissible.

THEOREM 1. *Let the scalar quantity u satisfy the first order equation, $du/dt = -u + f(t)$, $u(0) = 1$. Then the minimum of $\int^T (1-u)^2\,dt$ over all f subject to $0 \leq f \leq a_1 > 1$, $\int_0^T f\,dt \leq a_2 < T$, is furnished by*

$$\begin{aligned} f(t) &= 0, && 0 \leq t \leq a_3 \\ &= a_4, && a_3 \leq t < a_5 \\ &= 0, && a_5 \leq t \leq T, \end{aligned} \tag{2.1}$$

where a_3, a_4, a_5 are known constants determined by complicated transcendental equations.

The function, f, which under the same conditions yields the minimum of $\int_0^T (du/dt)^2$ is

$$\begin{aligned} f(t) &= a_6(t-a_8)^2 + a_7(t-a_8), && 0 \leq t < a_8 \\ &= 0, && a_8 \leq t \leq T, \end{aligned} \tag{2.2}$$

where again a_6, a_7, and a_8 are constants determined by T.

THEOREM 2. *If u satisfies the above equation, the minimum of $\int_0^T f^2\,dt$ subject to the constraint $-a_9 \leq 1 - u \leq a_9$, $0 < a_9 < 1$, for $0 \leq t \leq T$, is furnished by,*

$$\textit{for} \quad 0 \leq T \leq \log b, \ (b = 1 - a_9), \quad f = 0, \quad 0 \leq t \leq T \tag{2.3}$$

$$\textit{for} \quad \log b < T \leq \log c, \ (c = b/(1 - \sqrt{1-b^2})), \quad f = 2(b - e^{-T})\,e^t/(e^T - e^{-T}), \ 0 \leq t \leq T;$$

$$\textit{for} \quad \log c < T, \quad \begin{aligned} f &= (1 - \sqrt{1-b^2})e^t, && 0 \leq t \leq \log c, \\ &= b, && \log c \leq t \leq T \end{aligned}$$

3. Linear Functionals.—The problems arising in connection with maximizing or minimizing $\int_0^T (x(t), dG(t))$ subject to constraints of the form $\int_0^T (f, c_i)\,dt = a_i$, $0 \leq f_i \leq m_i$, where (y, z) denotes the inner product, may readily be converted into Neyman-Pearson type and do not possess any new features of interest.

A more interesting problem is one of the following sort:

THEOREM 3. *Consider the equation*

$$\frac{dx_i}{dt} = \sum_{j=0}^{N} a_{ij}y_j,\ i = 1, 2, \ldots, N,\ x_i(0) = c_i \qquad (3.1)$$

where the a_{ij} are non-negative. The choice of the functions y_i which maximizes $J = \int_0^T \left[\sum_{i=1}^{N} (x_i - y_i)\right] dt$, subject to the constraints $0 \leq y_i \leq x_i$ is given by $y_i = x_i$, $0 \leq t \leq T_i$, where the T_i are determined by the c_i, a_{ij} and T, and $y_i = 0$, $T_i < t < T$.

This problem arises in economics in connection with maximization of profit, as was pointed out to us by H. Markowitz. Many other interesting problems arise if we replace the functional $\int_0^T (x, dG)$ by the functional $\int_0^T \operatorname{Min}_i (x_i(t))\, dt$. We shall discuss these "bottleneck" problems subsequently.

4. *Quadratic Functionals.*—If we choose all the functionals occurring to be quadratic, measuring the cost, referring to (1.1), by $J(f) = \int_0^T (x - y, x - y)\, dt + a_1 \int_0^T (f, f)\, dt$, the problem of minimizing $J(f)$ over all $f \in L^2(0, T)$ is one which may be solved completely by standard variational techniques. Using the known representation theorems expressing the solutions of linear inhomogeneous differential and differential-difference equations in terms of the solutions of the homogeneous equations,[1, 2] the problem reduces to that of minimizing, in the scalar case,

$$J(f) = \int_0^T \left(a(t) + \int_0^t k(t, t_1)f(t_1)\, dt_1\right)^2 dt + a_1 \int_0^T f^2\, dt_1, \qquad (4.1)$$

over all $f \in L^2(0, T)$.

The corresponding problem for difference equations may be included in the above by a judicious use of Stieltjes integrals.

It is now easy to establish

THEOREM 4. *If $a(t) \in L^2(0, T)$, and $\int_0^t k^2(t, t_1)\, dt_1$ is uniformly bounded for $0 \leq t \leq T$, there is a unique function $f \in L^2(0, T)$ which furnishes the minimum to $J(f)$. It satisfies the integral equation*

$$\int_0^T k(t_1, t)\left[a(t_1) + \int_0^{t_1} k(t_1, t_2)f(t_2)\, dt_2\right] dt_1 + a_1 f = 0. \qquad (4.2)$$

If as in the case of differential equations,

$$a(t) = \int_0^t k(t, t_1)b(t_1)\, dt_1$$

for $b \in L^2(0, T)$, the value of $J(f)$ for the minimizing f is $a_1 \int_0^T f(t)b(t)\, dt$.

A similar result holds for the discrete analog. For those problems arising from differential equations, the integral equation may be converted into a differential equation of twice the original order, with a two-point boundary condition. A similar but more complicated result is obtained in the case of the differential-difference equations. Since the integral equa-

tions which occur are of Fredholm type, it is important to establish an *a priori* existence and uniqueness theorem.

The related problem of minimizing $\int_0^T (a(t) + \int_0^t k(t, t_1)f(t_1)\,dt_1)^2\,dt$ subject to $\int_0^T f^2\,dt \leq a_2$, may be made to depend upon the above problem, under certain assumptions concerning $k(t, t_1)$. In passing, let us note the following interesting result, which admits of considerable generalization,

THEOREM 5. *Let* $g(r) = \text{Min} \int_0^T (c - x, c - x)\,dt$, *subject to* $\int_0^T (f, f)\,dt = r < r^* = T(c, c)$, *and let*

$$\int_0^T (e^{A(t-t_1)}f(t_1), c - x)\,dt_1 = \lambda(r)f(t) \tag{4.3}$$

be the equation satisfied by the minimizing function $f(t)$, *where* $\lambda(r)$ *is a Lagrange multiplier. Then* $dg(r)/dr = \lambda(r)$.

5. *Further Problems.*—We have in what has preceded considered only some of the simplest representatives of the problems encountered in planning over time. Frequently, in applications, there are forcing terms g, arising from exogenous causes beyond our control, so that the equation takes the form

$$\frac{dx}{dt} = Ax + f + g, \qquad x(0) = c. \tag{5.1}$$

There are now two points of view that we may take. We may consider g to be a random function, with known expected value and auto-correlation function, and seek to minimize $\underset{g}{\text{Exp}}\ J(f, g) = J(f)$. In some applications this is a reasonable procedure.

In connection with other applications, it is better to introduce the concepts of game theory. In this way, arise the problems of determining

$$\underset{f}{\text{Min}}\ \underset{g}{\text{Max}} \int_0^T (x - y, x - y)\,dt, \quad \underset{g}{\text{Max}}\ \underset{f}{\text{Min}} \int_0^T (x - y, x - y)\,dt, \tag{5.1}$$

subject to $\int_0^T (f, f)\,dt \leq a_1$, $\int_0^T (g, g)\,dt \leq a_2$, and many interesting and difficult questions concerning games over function space.

[1] Bellman, R., "On the Boundedness of Solutions of Non-linear Differential and Difference Equations, *Trans. Am. Math. Soc.*, **62**, 357–386 (1947).

[2] Bellman, R., "On the Boundedness of Solutions of Non-linear Differential-Difference Equations," *Ann. Math.*, **50**, 347–355 (1949). See also, "On the Theory of Dynamic Programming," PROC. NATL. ACAD. SCI., **38**, 716–719 (1952).

FOURIER TRANSFORMS OF TIME SERIES

BY S. BOCHNER

PRINCETON UNIVERSITY

Communicated January 19, 1953

We take all *bounded* intervals $\Delta \equiv \Delta_{\alpha\beta}$: $(\alpha \leq x < \beta)$ on the open line $(-\infty, \infty)$ and we consider complex-valued finitely-additive random interval functions $F(\Delta)$ for which always

$$E\{|F(\Delta)|^2\} < \infty. \tag{1}$$

We call $F(\Delta)$ a *Khintchine function* if for any two intervals Δ_1: (α_1, β_1), Δ_2: (α_2, β_2) and any real t we have

$$E\{F(\Delta_1)\ \overline{F(\Delta_2)}\} = E\{F(\Delta_1')\ \overline{F(\Delta_2')}\}$$

where Δ_m' is the translated interval $(\alpha_m + t, \beta_m + t)$, $m = 1, 2$. We call it *orthogonal* if

$$E\{F(\Delta_1)\ \overline{F(\Delta_2)}\} = 0 \text{ for } \Delta_1 \cdot \Delta_2 = 0,$$

and *orthonormal* if furthermore

$$E\{|F(\Delta)|^2\} = c|\Delta| = c(\beta - \alpha)$$

for all $\Delta = \Delta_{\alpha\beta}$, and we then usually put $c = 1$. It follows easily that $F(\Delta)$ is orthonormal if and only if it is an orthogonal Khintchine function.

THEOREM 1. *(i) Heuristically, that is, subject to criteria, with "any" Khintchine function $F(\Delta)$ there is associable an orthogonal function $G(\Delta)$, its Fourier transform, such that*

$$F(\Delta_{\alpha\beta}) = \int_{-\infty}^{\infty} \frac{e^{2\pi i\beta y} - e^{2\pi i\alpha y}}{2\pi i y}\, dG(y) \tag{2}$$

where "$dG(y)$" symbolizes Stieltjes integration with respect to the interval function $G(\Delta)$.

(ii) Conversely, with "any" orthogonal function $G(\Delta)$ there is associable a Khintchine function $F(\Delta)$ such that

$$G(\Delta_{\gamma\delta}) = \int_{-\infty}^{\infty} \frac{e^{-2\pi i\delta x} - e^{-2\pi i\gamma x}}{-2\pi i x}\, dF(x), \tag{3}$$

and the two transformations (2), (3) are inverses of one another.

(iii) Furthermore, if $\varphi(x)$, $\psi(y)$ are numerical functions sufficiently small at $\pm\infty$ such that

$$\varphi(x) = \int_{-\infty}^{\infty} e^{2\pi i x y}\, \psi(y)\, dy \tag{4}$$

then (2) implies

$$\int_{-\infty}^{\infty} \varphi(x - \xi)\, dF(\xi) = \int_{-\infty}^{\infty} e^{2\pi i x\eta}\, \psi(\eta)\, dG(\eta)$$

In particular we have

$$\int_{-\infty}^{\infty} \varphi(-\xi) dF(\xi) = \int_{-\infty}^{\infty} \psi(\eta)\, dG(\eta) \tag{5}$$

and, formally, the validity of this relation for sufficiently many pairs $\{\varphi, \psi\}$ *is equivalent with the formula (2) for all intervals* (α, β).

(*iv*) *Finally, for the random point function*

$$f_\varphi(x) = \int_{-\infty}^{\infty} \varphi(x - \xi)\, dF(\xi)$$

we formally have

$$E\{f_\varphi(x + t)\, \overline{f_\varphi(x)}\} = \int_{-\infty}^{\infty} e^{2\pi i t\eta}\, |\psi(\eta)|^2\, d\Gamma(\eta)$$

where

$$\Gamma(\Delta) = E\{|G(\Delta)|^2\} \tag{6}$$

is a non-negative finitely additive interval function which is of bounded variation in every finite interval (only).

Perhaps the best known "rigorous" case of this "heuristic" theorem arises if we take a random point function $f(x)$ which has finite second moment and is L_2-continuous and then put

$$F(\Delta_{\alpha\beta}) = \int_\alpha^\beta f(x)\, dx.$$

This set function is a Khintchine function if and only if the correlation

$$E\{f(x + t)\, \overline{f(x)}\} = R(t)$$

is independent of x (and is continuous in t), and the known theorem is in part as follows.

THEOREM 2.[3, 6] *A random function* $f(x)$ *is such a Khintchine point function if and only if we have*

$$f(x) = \int_{-\infty}^{\infty} e^{2\pi i x y}\, dG(y)$$

where $G(\Delta)$ *is an orthogonal function whose second moment is bounded,*

$$\Gamma(\Delta) = E\{|G(\Delta)|^2\} \leq R(0).$$

We then also have

$$R(t) = \int_{-\infty}^{\infty} e^{2\pi i t\eta}\, d\Gamma(\eta)$$

and $G(\Delta)$ *is uniquely determined if it is* L_2*-continuous from the left, say.*

Another rigorous case, a seemingly different one, is as follows.

THEOREM 3.[4] *An orthonormal function* $F(\Delta)$ *has an orthonormal Fourier transform* $G(\Delta)$, *and relation (5) can then be validated for pairs of functions* $\{\varphi, \psi\}$ *both in* $L_2(-\infty, \infty)$.

There are other classes of functions $\{F(\Delta)\}$ which are invariant under Fourier transformations, as for instance the class of functions which are Gaussian in the sense that for any disjoint intervals $\Delta_1, \ldots, \Delta_k$ the joint distribution function of the k random variables

$$F(\Delta_1), \ldots, F(\Delta_k) \tag{7}$$

is a Gaussian one.

Such an $F(\Delta)$ need not be a Khintchine function, but if the characteristic function of the joint distribution of (7) has the special form

$$\exp\left[-u(|\Delta_1|\alpha_1^2 + \ldots + (\Delta_k|\ \alpha_k^2)\right] \tag{8}$$

for some fixed $u > 0$ then $F(\Delta)$ is even orthonormal, and it is, in fact, a so-called Wiener-process. Now, the family of such $\{F(\Delta)\}$ is again invariant under Fourier transformation. As a matter of fact if we take a fixed averaging weight $d\rho(u) \geq 0$ in $0 \leq u < \infty$ with $\int_0^\infty d\rho\,(u) = 1$ and if we replace (8) by

$$\int_0^\infty \exp\left[-u(|\Delta_1|\ \alpha_1^2 + \ldots + (|\Delta_k|\ \alpha_k^2)\right] d\rho(u)$$

then such a class $\{F(\Delta)\}$ is invariant likewise.[1]

We are now going to bring Theorems 2 and 3 together by means of a statement which is the main remark of the present paper.

THEOREM 4. *If $\{f_\epsilon(x)\}$, $0 < \epsilon < \infty$ is a family of Khintchine point functions which is such that for any $\epsilon > 0$, $\epsilon' > 0$ we have*

$$f^{\epsilon+\epsilon'}(x) = \int_{-\infty}^{\infty} \frac{1}{\sqrt{\epsilon}}\, e^{-\pi/\epsilon(x-\xi)^2} f^{\epsilon'}(\xi)\, d\xi \tag{9}$$

then there exists an orthogonal function $G(\Delta)$ such that

$$f^{\epsilon}(x) = \int_{-\infty}^{\infty} e^{2\pi i x y}\, e^{-\epsilon\pi y^2}\ dG(y) \tag{10}$$

and

$$E\{f^{\epsilon}(x+t)\,\overline{f^{\epsilon}(x)}\} = \int_{-\infty}^{\infty} e^{2\pi i t y}\, e^{-2\epsilon\pi y^2} d\Gamma(y); \tag{11}$$

meaning for instance that if we put

$$G^{\epsilon}(\Delta_{\gamma\delta}) = \int_{\gamma}^{\delta} e^{-\epsilon\pi y^2}\, dG(y),$$

then we have

$$f^{\epsilon}(x) = \int_{-\infty}^{\infty} e^{2\pi i x y}\, dG^{\epsilon}(y)$$

in the sense of Theorem 2.

Now, if we take a Khintchine function $f(x)$ to which Theorem 2 applies and form

$$f^{\epsilon}(x) = \int_{-\infty}^{\infty} \frac{1}{\sqrt{\epsilon}}\, e^{-\pi/\epsilon(x-\xi)^2} f(\xi)\, d\xi \tag{12}$$

then we obtain a family to which Theorem 4 applies, and the spectral functions $G(\Delta)$, $\Gamma(\Delta)$ in Theorem 4 are the same as those in Theorem 2.

On the other hand if we take an orthonormal $F(\Delta)$ to which Theorem 3 applies then the family

$$f^{\epsilon}(x) = \int_{-\infty}^{\infty} \frac{1}{\sqrt{\epsilon}} e^{-\pi/\epsilon (x-\xi)^2} dF(\xi)$$

falls under Theorem 4, and the spectral functions $G(\Delta)$, $\Gamma(\Delta)$ of Theorem 4 are now those of Theorem 3, and thus Theorems 2 and 3 have been brought together rather closely.

Notwithstanding this, if we take an arbitrary family $\{f^{\epsilon}(x)\}$ to which Theorem 4 applies, then it can be represented as an integral (12) by means of a Khintchine point function $f(x)$ if and only if $\Gamma(\Delta)$ has bounded variation in $(-\infty, \infty)$,

$$\int_{-\infty}^{\infty} d\Gamma(y) \leq R(0).$$

Now, for $\Gamma(\Delta) = c|\Delta|$, $c > 0$, this variation is always unbounded, and thus, in their proper versions, Theorems 2 and 3 appear to be very different indeed, nevertheless.

The distance between Theorems 2 and 3 can also be stated in certain quantitative terms. If $\{\varphi, \psi\}$ are connected by (4) then for the function

$$f_{\varphi}^{\epsilon}(x) = \int_{-\infty}^{\infty} \varphi(x-\xi) f^{\epsilon}(\xi)\, d\xi,$$

we obtain from (10), (11) the relations

$$f_{\varphi}^{\epsilon}(x) = \int_{-\infty}^{\infty} e^{2\pi i x y - \epsilon \pi y^2} \psi(y)\, dG(y)$$

$$E\{f_{\varphi}^{\epsilon}(x+t)\,\overline{f_{\varphi}^{\epsilon}(x)}\} = \int_{-\infty}^{\infty} e^{-2\epsilon\pi y^2} |x(y)|^2\, d\Gamma(y),$$

and if $G(\Delta)$ and $\psi(y)$ are such that

$$\int_{-\infty}^{\infty} |\psi(y)|^2\, d\Gamma(y) < \infty \tag{13}$$

then the limit

$$\lim_{\epsilon \to 0} f_{\varphi}^{\epsilon}(x) \tag{14}$$

exists in an appropriate sense. Now, if $\Gamma(\Delta)$ has bounded total variation, then (13) holds for $\psi(y) = 1$ and this being the Fourier transform of the Dirac function, the limit (14) is then a point function $f(x)$ as in Theorem 2. However for $\Gamma(\Delta) = c|\Delta|$ we have, say

$$\int_{-\infty}^{-1} + \int_{1}^{\infty} \frac{1}{y^2} d\Gamma(y) < \infty, \tag{15}$$

and thus (13) holds for $\psi(y) = 1/\pi y \sin 2\pi a y$, this being the transform of the function $\varphi(x)$ which is $= 1$ in $|x| \leq a$, and 0 outside, and this then leads

to a boundary set function $F(\Delta)$ as in Theorem 3. In general, if for a given family $f^\epsilon(x)$ there exists an exponent k for which

$$\int_{-\infty}^{-1} + \int_{1}^{\infty} \frac{1}{y^{2k}}\, d\Gamma(y) < \infty,$$

then the limit (14) exists as a kth order set function as was introduced by this author in the theory of generalized Fourier integrals[2] (and later carried further in the work of Laurent Schwartz). But this kind of generalization would be worth undertaking only if requirements of stationarity and orthogonality would not be introduced from the very beginning as we have done for the present, and problems of smoothing and inversion of smoothing would be approached as well, as we will do on another occasion.

Returning to Theorem 4 we note that the semigroup-requirement (9) could be replaced by other ones, as for instance by

$$f^{\epsilon+\epsilon'}(x) = \frac{1}{\pi} \int_{-\infty}^{\infty} \frac{f^{\epsilon'}(\xi)\, d\xi}{\epsilon^2 + (x-\xi)^2}$$

in which case we have

$$f^\epsilon(x) = \int_{-\infty}^{\infty} e^{2\pi i x y - 2\epsilon\pi|y|}\, dG(y)$$

instead of (10). The two-variable function $f^\epsilon(x)$ is then harmonic in the complex variable $x + i\,\epsilon$ in the half-plane $\epsilon > 0$, with $f(x)$, if existing, being then its boundary value, and this set-up certainly has its attractions for further studies. But the function $f^\epsilon(x)$ of Theorem 4 is a random-valued solution of the diffusion equation

$$\frac{\partial^2 f^\epsilon(x)}{\partial x^2} = 4\pi \frac{\partial f^\epsilon(x)}{\partial \epsilon}$$

and stochastically this kind of approximation might be more appealing perhaps.

Finally, to complete the picture, we will state the integral-time-counterpart to Theorem 1 and we note that to a large extent it will be "rigorous" from the very beginning.

THEOREM 5.[1, 4] *A (two-way) sequence $\{f_n\}$ of random variables is a Khintchine sequence if and only if there exists an orthogonal function $G(\Delta)$ on the closed circle*

$$\Delta_0 : 0 \leq x < 1 \tag{16}$$

such that

$$f_n = \int_{\Delta_0} e^{2\pi i n y}\, dG(y) \tag{17}$$

Dually, if $G(\Delta)$ is a Khintchine function on (16) then (17) defines an orthogonal sequence and we have

$$E\{|f_n|^2\} = \int_{\Delta_0} e^{2\pi int}\, dR(t),$$

where

$$R(t) = E\{G(\Delta_0 + t)\,\overline{G(\Delta_0)}\}.$$

Conversely if an orthogonal sequence $\{f_n\}$ *is such that for every interval in* (16) *the series*

$$G(\Delta_{\gamma\delta}) = \sum_{-\infty}^{\infty} \frac{e^{-2\pi i\delta n} - e^{-2\pi i\gamma n}}{-2\pi in} f_n$$

converges suitably, then this $G(\Delta)$ *is a Khintchine set function for which* (17) *holds.*

[1] "Stochastic Processes," *Annals Math.*, **48,** 1014–1061 (1947).

[2] Bochner, S., *Fouriersche Integrale*, Leipzig, 1932.

[3] Cramer, H., "On Harmonic Analysis in Certain Functional Spaces," *Arkiv Mat., Astr. och Fysik*, **28B,** No. 12, 1942.

[4] Doob, J. L., "Time Series and Harmonic Analysis," *Proc. Berkeley Symp. Math. Statistics and Probability*, Berkeley, **1949,** 303–343.

[5] Karhunen, K., "Uber lineare Methoden in der Wahrscheinlichkeitsrechung," *Ann. Acad. Sci. Fennicae, Ser. A. I.*, **37** (1947).

[6] Khintchine, A., "Korrelationstheorie der stationaren Stochastischen Prozesse," *Math. Annalen*, **190,** 604–615 (1934).

[7] Loeve, M., Appendix to: Levy, P., *Processus Stochastiques*, Paris (1948).

*ON THE BASIS THEOREM FOR FINITE ABELIAN GROUPS: IV**

BY JESSE DOUGLAS

COLUMBIA UNIVERSITY, NEW YORK

Communicated February 1, 1953

1. The existence of a basis for any finitely generated vector space is immediate; one has only to select a minimal subset of generators. The brief proof depends essentially on the fact that the domain of scalars is a *field;* this permits solution of any linear relation among vectors for any one of these vectors whose coefficient $\neq 0$.

Why is more required to establish a basis for any finite abelian group G? Fundamentally, it is because the corresponding module $M = (G, A)$ is, in general, only that and not a vector space. Here the "external" operation is $\theta \to a\theta$ (additive notation), and the operator domain A consists of the integers a considered modulo m, where m denotes the maximum period[1] of the elements θ of G.

Thus A is, in general, only a *ring*, not a field. However, in the particular

case where m is a prime p, A is indeed a *field*, the abelian group becomes a finite vector space, and the proof of the basis theorem runs very simply as follows.

By hypothesis, $p\theta = 0$ for every element θ of G. Let $S = (\theta_1, \theta_2, \ldots, \theta_r)$ be a *minimal* set of generators of G. Then (we assert) this set must be *independent*, and so constitutes, according to definition, a *basis* of G. "Independent" means that in any linear relation

$$a_1\theta_1 + a_2\theta_2 + \ldots + a_r\theta_r = 0$$

each term $a_i\theta_i = 0$; in the present case this is equivalent to $a_i \equiv 0 \pmod{p}$ for $i = 1, 2, \ldots, r$. Otherwise, x exists such that $xa_i \equiv 1 \pmod{p}$ for some a_i (use of the field property, existence of a reciprocal); then, by multiplication with x,

$$xa_1\theta_1 + \ldots + xa_{i-1}\theta_{i-1} + \theta_i + xa_{i+1}\theta_{i+1} + \ldots + xa_r\theta_r = 0;$$

thus θ_i is a linear combination of the other θ's, and the proper subset $S - \theta_i$ of S is still a system of generators—but this is contrary to the supposed minimality of S.

The proof offered in the present note consists in a slight adaptation of this argument for the *prime period* case so as to afford an inductive procedure applying to the *prime-power period* case, which is essentially the general case.

2. Let p denote any prime and λ any positive integer. We shall say that a finite abelian group G is "of p^λ-type" or is a "p^λ-group" if every element θ of G obeys the equation

$$p^\lambda\theta = 0. \tag{1}$$

A *primary* abelian group is one which is of p^λ-type for some p and λ. Because of the standard fact that every finite abelian group is a direct product of primary groups, we may restrict the proof of the basis theorem to primary groups.

3. THEOREM. *Every primary abelian group has a basis.*

The proof is by induction on λ. For $\lambda = 1$, the theorem has been proved in the introductory section.

Assuming, then, that the theorem is true for all groups of $p^{\lambda-1}$-type ($\lambda > 1$), we shall infer its truth for the p^λ-type.

Let G_λ denote any p^λ-group. Consider the subgroup $G_{\lambda-1}$ of elements $p\theta$ where θ ranges over G_λ. Then by definition (1) we have $p^{\lambda-1}(p\theta) = 0$; hence $G_{\lambda-1}$ is a $p^{\lambda-1}$-group. By hypothesis, therefore, $G_{\lambda-1}$ has a basis

$$B = (p\theta_1, p\theta_2, \ldots, p\theta_m).$$

To the set of elements θ_i whose p-multiples form B adjoin all elements ω of G_λ which obey the equation

$$p\omega = 0. \tag{2}$$

In this way we form the set[2]

$$S = (\theta_1, \theta_2, \ldots, \theta_m, \omega_1, \omega_2, \ldots, \omega_n).$$

We assert that *S is a system of generators for G_λ*. To see this, let ϕ denote any element of G_λ; then $p\phi$ belongs to $G_{\lambda-1}$ and is therefore expressible in the form

$$p\phi = a_1 p\theta_1 + a_2 p\theta_2 + \ldots + a_m p\theta_m.$$

Hence

$$p(\phi - a_1\theta_1 - a_2\theta_2 - \ldots - a_m\theta_m) = 0;$$

thus the element represented by the parentheses obeys (2) and is accordingly one of the ω's:

$$\phi - a_1\theta_1 - a_2\theta_2 - \ldots - a_m\theta_m = \omega_t,$$

so that

$$\phi = a_1\theta_1 + a_2\theta_2 + \ldots + a_m\theta_m + \omega_t,$$

which establishes our assertion.

4. Now, the set S, being finite, must contain a *minimal* subset S_0 of generators of G_λ; by rearranging notation we may suppose

$$S_0 = (\theta_1, \theta_2, \ldots, \theta_r, \omega_1, \omega_2, \ldots, \omega_s).$$

We assert that this set is *independent*, and therefore constitutes a *basis* of G_λ.

Indeed, let

$$a_1\theta_1 + \ldots + a_r\theta_r + b_1\omega_1 + \ldots + b_s\omega_s = 0 \tag{3}$$

be any linear relation among the elements of S_0.

Then *each coefficient a_i, b_j must be divisible by p*. For suppose, e.g., a_i non-divisible by p. Then an integer x exists such that $xa_i \equiv 1 \pmod{p^\lambda}$. Multiplying (3) by x and taking account of (1), we get

$$xa_1\theta_1 + \ldots xa_{i-1}\theta_{i-1} + \theta_i + xa_{i+1}\theta_{i+1} \ldots + xa_r\theta_r + xb_1\omega_1 + \ldots + xb_s\theta_s = 0.$$

Hence θ_i, expressible as a linear combination of other elements of S_0, may be omitted without loss of the generative character of the set—but this is contrary to the *minimal* assumption regarding S_0.

Each coefficient in (3) being therefore divisible by p, this relation takes the form

$$c_1 p\theta_1 + \ldots + c_r p\theta_r + d_1 p\omega_1 + \ldots + d_s p\omega_s = 0.$$

Here each ω-term $= 0$ because of (2), and then each θ-term $= 0$ because of the independence of the elements $p\theta_1, \ldots, p\theta_r$, which are part of the basis B of $G_{\lambda-1}$. The proof of our main theorem is now complete.

* Work on this paper supported in part by contract with the Office of Ordnance Research, U. S. Army. Previously published papers by the author on the same topic: these PROCEEDINGS, **37**, 359–362, 525–528, 611–614 (1951).

[1] Equal to the l.c.m. of the periods, since, in an abelian group, the period of any element is a divisor of the maximum period.

[2] The basis B may be assumed not to contain the identity, i.e., $p\theta_i \neq 0$ for all i; hence no θ is equal to an ω, and the elements of S are all different.

---

*GAMES WITH EQUILIBRIUM POINTS**

BY RICHARD OTTER AND JOHN DUNNE

DEPARTMENT OF MATHEMATICS, UNIVERSITY OF NOTRE DAME

Communicated by J. von Neumann, February 5, 1953

This paper deals with the combinatorial aspects of games of strategy, in particular with the relation between the information partition and the set of strategies. In his book J. von Neumann[1] has shown that a zero-sum two-person game is strictly determined (s.d.) provided there is perfect information. Utilizing the notion of equilibrium point introduced by Nash,[2] Kuhn[3] has generalized this theorem to the general finite game. On the other hand, it is easy to see that there are less restrictive conditions on the information partition which allow a game to be s.d. regardless what the pay-off functions are. In this paper we state a theorem which characterizes these games structurally. Only the proof of sufficiency is given; that of necessity, being a good deal simpler and less informative, is omitted.

A *rooted tree* is a finite, non-empty, partially ordered set T in which (i) there is an element r satisfying $r \leq v$ for every $v \in T$ and (ii) for every $v \in T - \{r\}$ there is only one descending chain $v = v_n > v_{n-1} > \ldots > v_0 = r$ such that v_i and v_{i-1} are adjacent in T for $i = 1, 2, \ldots, n$. We call the elements of T *vertices*, the element r mentioned in (i) the *root* of T and read the relation $u < v$ as "u is lower than v." For each $v \in T$, let $A(v)$ denote the set of elements in T adjacent to and higher than v, and let $\beta(v)$ denote the number of elements in $A(v)$. The family $\mathfrak{B} = (\overset{i}{\beta}(i) i \geq 0)$, is a partition of the set T. We put $E = \overset{1}{\beta}(0)$ and call its elements *end-points* and put $B = T - E$ and call its elements *branch-points*.

Suppose now that for each $v \in B$ we select a fixed enumeration of the set $A(v)$, i.e., $A(v) = \{u_1, u_2, \ldots, u_{\beta(v)}\}$. We express the fact that u_i is the ith vertex attached to v by writing $u_i = \langle v, i \rangle$. If we now express v in the

same way in terms of the vertex immediately below it and proceed in this way down to the root r to which we assign the symbol $\langle 0 \rangle$, we get that each vertex u may be expressed in the form $u = \langle 0, i_1, i_2, \ldots, i_n \rangle$ and we say we have a *coordinate system* in T.

In order to define a game we follow McKinsey[4] in requiring that there be given (*i*) a rooted tree T with a coordinate system (*ii*) the player partition $\mathcal{P} = (P_k)_{k \geq 0}$ of the set B, (*iii*) the information partition $\mathfrak{D}$ of the set B, (*iv*) a probability measure μ_0 on Σ_0, the set of strategies for chance, and (*v*) a family $\gamma = (g_k)_{k \geq 1}$ of real valued functions defined on E. We call the quadruple $\Gamma = (T, \mathcal{P}, \mathfrak{D}, \mu_0)$ a *game structure* and the pair (Γ, γ) we call a *game*.

We consider the indices $k = 0, 1, 2, \ldots$ in 1–1 correspondence with a set of *players*, the player corresponding to index 0 is called *chance*, the rest *personal* players.

The information partition $\mathfrak{D}$ is required to be a refinement of the partition $\mathcal{P}$ and of the trace of $\mathfrak{B}$ on B. We also require of $\mathfrak{D}$ that if $u < v$ then u and v are not in the same set from $\mathfrak{D}$. The equivalence relation that exists between two vertices u, v when they belong to the same information set $D \in \mathfrak{D}$ is written as $u \equiv v$, and sometimes as $u \equiv v\ (k)$, provided $D \subset P_k$.

In order to explain what is meant by Σ_0 mentioned above we let Σ consist of all those mappings σ of B into T such that

(*a*) $\sigma(v) \in A(v)$

(*b*) if $\sigma(u) = \langle u, i \rangle$, $\sigma(v) = \langle v, j \rangle$ and $u \equiv v$ then $i = j$. We consider Σ as subset of $\prod_{v \in B} A(v)$ and observe that it is determined when T, $\mathcal{P}$, $\mathfrak{D}$ are given. Its elements we term *strategies*. The set $\Sigma_k = pr_{P_k}(\Sigma)$ is called the set of *strategies for player k* and we evidently have $\Sigma = \prod_{k \geq 0} \Sigma_k$.[5] We may write for $\sigma \in \Sigma$, $\sigma = (\sigma_0, \sigma_1, \sigma_2, \ldots) = (\sigma_k)_{k \geq 0}$ where $\sigma_k = pr_{P_k}(\sigma)$. It should be pointed out that the previously given definitions of a game have suffered from an inadequate description of the probabilities involved. All that has been supposed given is $\mu_0(\sigma_0 \mid \sigma_0(v) = \langle v, i \rangle)$ for each $v \in P_0$ and $i = 1, 2, \ldots \beta(v)$. This data alone does not suffice to determine μ_0 which one needs to know in order to compute the expected pay-off.

For each $\sigma \in \Sigma$ the last term of the sequence r, $\sigma(r)$, $\sigma(\sigma(r))$, $\ldots$ which is meaningful is an end-point $\pi(\sigma)$. The correspondence $\sigma \to \pi(\sigma)$ determines the mapping π of Σ *on* E. We then put

$$f_k(\sigma_1, \sigma_2, \ldots) = \int_{\Sigma_0} g_k(\pi(\sigma_0, \sigma_1, \sigma_2, \ldots))\, d\mu_0(\sigma_0) \qquad k = 1, 2, \ldots$$

and call these the *expected pay-off functions*. We put for $v \in T$

$$S(v) = \{\sigma \in \Sigma \mid v \leq \pi(\sigma)\}$$

$$S_k(v) = pr_{P_k}(S(v)) \qquad k = 0, 1, 2, \ldots$$

The following lemmas are very useful in the theory. Their proofs are simple and we omit them.

LEMMA 1. *(a) We have $\sigma \in S(v)$ if and only if $u < v$ implies $\sigma(u) \leq v$. (b) We have $\sigma_k \in S_k(v)$ if and only if $u < v$ and $u \in P_k$ implies $\sigma_k(u) \leq v$.*

LEMMA 2. $S(v) = \prod_{k \geq 0} S_k(v)$.

LEMMA 3. *(a) $S_k(u) \cap S_k(v) = \phi$ if and only if for some $u_1, v_1 \in P_k$ with $u_1 \equiv v_1$ we have $\langle u_1, i \rangle \leq u$ and $\langle v_1, j \rangle \leq v$ where $i \neq j$. (b) $S_k(u) \subset S_k(v)$ if and only if for each $v_1 \in P_k$ with $v_1 < v$ there is a $u_1 \in P_k$ with $u_1 \equiv v_1$ and such that both $\langle u_1, i \rangle \leq u$ and $\langle v_1, i \rangle \leq v$ for some i.*

For $\sigma_k \in \Sigma_k$ let us define the "track of σ_k" by $\mathrm{tr}(\sigma_k) = \{v \in T \mid \sigma_k \in S_k(v)\}$ then the previously given definitions of equivalent strategies amount to this: σ_k equivalent to σ_k' if and only if $\mathrm{tr}(\sigma_k) = \mathrm{tr}(\sigma_k')$. We may also call two information patterns $\mathfrak{D}$, $\mathfrak{D}'$ (for the same T, $\mathfrak{P}$) *equivalent* whenever $\mathrm{tr}(\Sigma_k) = \mathrm{tr}(\Sigma_k')$ for $k = 0, 1, 2, \ldots$ where Σ_k, Σ_k' are determined by $(T, \mathfrak{P}, \mathfrak{D})$ and $(T, \mathfrak{P}, \mathfrak{D}')$ respectively.

We call a set $C \subset P_k \cup P_0$, $k \neq 0$, *connected* for player k if any two of its vertices may be *connected;* that is, if $u, v \in C$ then there is a sequence $u = u_0, u_1, \ldots, u_n = v$ such that $u_i \in C$ and either u_1 adjacent u_{i-1} or $u_i \equiv u_{i-1}$ (k) and $S_k(u_i) \cap S_k(u_{i-1}) \neq \phi$ for $i = 1, 2, \ldots, n$.

A set $K \subset P_k \cup P_0$, $(k \neq 0)$, is an *info component* for player k means that (i) K is connected, (ii) its minimal vertices belong to P_k and (iii) K is maximal, i.e., if $K' \supset K$ and satisfies conditions (i) and (ii) then $K' = K$.

LEMMA 4. *For any game structure $\Gamma = (T, \mathfrak{P}, \mathfrak{D}, \mu_0)$ there is an information partition $\mathfrak{D}'$ equivalent to $\mathfrak{D}$ all of whose sets are connected for the player to whom they belong.*

Proof: We put $u \equiv' v$ (k) if and only if $u \equiv v$ (k) and u and v may be connected. Evidently the partition $\mathfrak{D}'$ defined thereby is a refinement of $\mathfrak{D}$, hence $\mathrm{tr}(\Sigma_k) \subset \mathrm{tr}(\Sigma_k')$. Suppose that $\mathrm{tr}(\sigma_k')$ is not an element of $\mathrm{tr}(\Sigma_k)$ then there exist u, v with $u \equiv v$ (k) and with $\langle u, i \rangle, \langle v, j \rangle \in \mathrm{tr}(\sigma_k')$ but $i \neq j$, hence $u \equiv' v$ is not true. If $S_k(u) \cap S_k(v) = \phi$ we may replace u, v by the u_1, v_1 of Lemma (3*a*). By working down toward the root in this way we see we may suppose $S_k(u) \cap S_k(v) \neq \phi$ but this means $u \equiv' v$ which is a contradiction. Thus $\mathfrak{D}'$ is equivalent to $\mathfrak{D}$ and it is clear that its sets are connected.

THEOREM. *Let $\Gamma = (T, \mathfrak{P}, \mathfrak{D}, \mu_0)$ be a game structure where $B_1 = \phi$ and $\mu_0(S_0(v)) > 0$ for every $v \in T$. In order that the game (Γ, γ) possess an equilibrium point for every family γ of payoff functions, it is necessary and sufficient that whenever for some $k > 0$ we have $u \equiv v$ (k) and $S_k(u) \cap S_k(v) \neq \phi$ we also have $S_j(u) = S_j(v)$ for any $j \neq 0, k$.*

Before proceeding to the proof of the sufficiency we shall establish a lemma:

LEMMA 5. *Under the condition of the theorem the info components have the following properties:*

(*a*) *If J, K are distinct info components belonging to personal players j, k, respectively, and if there is a vertex $v \in J$ higher than some vertex $v_1 \in K \cap P_k$ then there is an integer i such that for every vertex $u \in J$ we have $u \geq \langle u_1, i \rangle$ for some $u_1 \equiv v_1(k)$.*

(*b*) *If $u < v$ and both lie in some info component J of player j then so do all vertices between u and v.*

(*c*) *If M is the set of minimal vertices of an info component then $M \cap \bigcap_{k \geq 1} tr(\sigma_k)$ is either empty or it is M and $M \cap tr(\sigma_0)$ is either empty or it is a single element of M.*

Proof: (*a*) We first suppose that $j \neq k$. Now the two vertices $u, v \in J$ may be connected in J. $u = w_0, w_1, \ldots, w_n = v$. If $w_i \equiv w_{i-1}(j)$ and $S_j(w_i) \cap S_j(w_{i-1}) \neq \phi$ then by the condition of the theorem $S_k(w_i) = S_k(w_{i-1})$. If w_i is adjacent to w_{i-1} we have $S_k(w_i) = S_k(w_{i-1})$ because w_i, w_{i-1} are not elements of P_k. Now since $v_1 \in P_k$, and $v_1 < v$ say $\langle v_1, i \rangle \leq v$ then by Lemma (*3b*) there is a $u_1 \equiv v_1(k)$ such that $\langle u_1, i \rangle \leq u$. The case $j = k$ follows from this and part (*b*) by similar arguments.

(*b*) Put $W = \{w \in T \mid u < w < v\}$ then $W \subset P_j \cap P_0$. For suppose $v_1 \in W \cap P_k$, $k \neq 0$, j, and let K be the info component in which v_1 lies. Then J, K satisfy the hypotheses of part (*a*) so we find there is a u_1 such that $v > v_1 > u > u_1$ and $v_1 \equiv u_1(k)$. This contradicts the definition of an information pattern, so $W \subset P_j \cup P_0$. Since J is a maximal connected set we have $W \subset J$.

(*c*) This follows directly from part (*a*) and Lemma 1.

Proof of Theorem (*Sufficiency*): Since the question of whether or not $(\sigma_1, \sigma_2, \ldots)$ is an equilibrium point may be settled by looking at $\mathrm{tr}(\sigma_1)$, $\mathrm{tr}(\sigma_2)$, $\ldots$, we may suppose by Lemma 4 that the info sets for each player are connected for him. We proceed by induction on the number of info components in the game. If there is just one info component belonging, say, to player 1, then for $k > 1$, $P_k = \phi$ so Σ_k consists of a single element $\dot{\sigma}_k$. So if $\dot{\sigma}_1$ maximizes $f_1(\sigma_1, \dot{\sigma}_2, \ldots)$ then $(\dot{\sigma}_1, \dot{\sigma}_2, \ldots)$ is an equilibrium point. The case of no info components is even simpler.

Suppose now there are $N > 1$ info components and that the theorem is true for games with less than N info components. Using Lemma (*5a*) we easily construct an info component K' such that the set $E' = \{u \in T - K' \mid u > v \text{ for some } v \in K'\}$ is subset of E. Let M denote the set of vertices minimal in K', then r is not an element of M. For indeed any other vertex is higher than r and so if $r \in M \subset K'$ then $T = K' \cup E'$ which contradicts $N > 1$. If we now construct $T' = K' \cup E' \cup \{r\}$ then T' is a tree whose root is r (Lemma (*5b*)) with E' for its set of end-points. We construct a game $(\Gamma', \gamma') = (T', \mathcal{P}', \mathfrak{D}', \mu_0', \gamma')$ by relativizing the original game to T' and by assigning r to chance. Thus $\mathcal{P}'$ is the trace of $\mathcal{P}$ on K' except that P_0' contains r, $\mathfrak{D}'$ is the trace of $\mathfrak{D}$ on K' together with $\{r\}$.

We put $\Theta_0 = pr_{P_0 \cap K'}(\Sigma_0)$ then $\Sigma_0' = \Theta_0 \times M$ is the set of strategies for chance in Γ'. We put for $\sigma_0' \in \Sigma_0'$,

$$\mu_0'(\sigma_0') = \mu_0'(\theta_0, u) = \frac{\mu_0(\overset{-1}{p'} r_{P_0 \cap K'}(\theta_0) \cap S_0(u))}{\mu_0(S_0(M))}$$

This is a probability measure on Σ_0' because by Lemma (5c) $(S_0(\mu))_{u \in M}$ is a partition of $S_0(M)$. And finally we put $\gamma' = (g_k')_{k \geq 1}$ where g_k' is the restriction of g_k to E'. Evidently, the game (Γ', γ') has just one info component, namely K'. Let $(\dot{\sigma}_1', \dot{\sigma}_2', \ldots)$ be an equilibrium point.

Now put $E'' = (E - E') \cup M$, $K'' = B - K'$ and finally $T'' = K'' \cup E''$, then T'' is a tree with r as root and E'' as its end-points. We construct a game (Γ'', γ'') by letting $\mathcal{P}''$, $\mathfrak{D}''$ be the trace of $\mathcal{P}$, $\mathfrak{D}$, respectively, on K''. Then $\Sigma_0'' = pr_{P_0''}(\Sigma_0)$ is the set of strategies for chance in Γ'' and we put $\mu_0''(\sigma_0'') = \mu_0(\overset{-1}{pr'})_{P_0'' \sigma_0''})$. Finally, we put $\gamma'' = (g_k'')_{k \geq 1}$ where

$$g_k''(e'') = \begin{cases} g_k(e'') & \text{if } e'' \in E - E' \\ f_k'(\dot{\sigma}_1', \dot{\sigma}_2', \ldots) & \text{if } e'' \in M \end{cases}$$

The game $(\Gamma,'' \gamma'')$ satisfies the hypothesis of the theorem and has N-1 info components so there is an equilibrium point $(\dot{\sigma}_1'', \dot{\sigma}_2'', \ldots)$.

We identify the pair $(\dot{\sigma}_k', \dot{\sigma}_k'')$ with a strategy $\dot{\sigma}_k \in \Sigma_k$ by putting $\dot{\sigma}_k = \dot{\sigma}_k''$ for $k \geq 2$ and

$$\dot{\sigma}_1(v) = \begin{cases} \dot{\sigma}_1'(v) & \text{for } v \in P_1' = K' \cap P_1 \\ \dot{\sigma}_1''(v) & \text{for } v \in P'' = (B - K') \cap P_1 \end{cases}$$

That $\dot{\sigma}_k \in \Sigma_k$ for $k \geq 2$ is obvious. For $k = 1$, we observe that if $\dot{\sigma}_1(u) = \langle u, i \rangle$ and $\dot{\sigma}_1(v) = \langle v, j \rangle$ where $u \equiv v$ (1) then because of the connectedness of the information sets either u, v are both in K' or both in K'' so $i = j$.

It is now an elementary computation to show that $(\dot{\sigma}_1, \dot{\sigma}_2, \ldots)$ is an equilibrium point for (Γ, γ).

COROLLARY. *If in addition $P_0 = \phi$ then in order that (Γ, γ) possess an equilibrium point for every family γ it is necessary and sufficient that $u \neq v$ and $u \equiv v$ (k) imply $S_k(u) \cap S_k(v) = \phi$. Hence the information partition is equivalent to one with 1-element sets, i.e., perfect information.*

* This work was supported in part by the Office of Naval Research, in part by the National Bureau of Standards.

[1] von Neumann, J., and Morgenstern, O., *Theory of Games and Economic Behavior*, Princeton University Press, 1944, pp. 112–128.

[2] Nash, J. F., these PROCEEDINGS, **36**, 48–49 (1950).

[3] Kuhn, H. W., *Ibid.*, **36**, 570–576 (1950).

[4] McKinsey, J., *Introduction to the Theory of Games*, McGraw-Hill, 1952, pp. 119–120.

[5] We are following the customary conventions for product sets, e.g., if $P_k = \phi$ then Σ_k is taken as some 1-element set. The notation is for the most part that of Bourbaki, N., *Theorie des Ensembles*, Hermann, Paris, 1939.

ON THE NUMBER OF HUSIMI TREES, I

BY FRANK HARARY AND GEORGE E. UHLENBECK

DEPARTMENTS OF MATHEMATICS AND PHYSICS, UNIVERSITY OF MICHIGAN

Communicated by J. von Neumann, December 31, 1952

1. Introduction.—It was pointed out by one of us[1] that the theory of the so-called virial development of the equation of state of a non-ideal gas, leads to combinatorial problems for certain types of linear graphs, which can be considered as direct generalizations of the well-known "trees" of Cayley. We have called the simplest such types of graphs *Husimi trees* since they were first introduced in a paper by Husimi.[2] A Husimi tree is a connected graph in which no line lies on more than one cycle. It is characterized by the numbers $n_2, n_3, n_4 \ldots$ of lines, triangles, quadrilaterals, etc., out of which it is built up. A *pure* Husimi tree is one which consists of only one type of figure. Otherwise we speak of *mixed* Husimi trees. A pure Husimi tree consisting only of lines is a *Cayley tree*. If it consists only of triangles we will call it a *cactus*.

There are two kinds of combinatorial problems connected with each type of graph. The first and simplest kind of problem is to find the number of topologically different graphs if *all* points are distinguished from each other. For Cayley trees of p points the answer[3] is simply p^{p-2}. For Husimi trees of p points and of type $n_2, n_3, \ldots, n_p$ the answer[2] is:

$$\frac{p!}{\prod_{i=2}^{p} [(i-1)!]^{n_i} n_i!} \, p^{\sum_{i=2}^{p} n_i - 2}$$

which clearly specializes to p^{p-2} for Cayley trees. The second and more difficult kind of problem is to find the number of topologically different graphs if the points are not distinguishable.[4] For Cayley trees the problem has been solved[5] in all details. The method has always been to start with finding the number of "rooted" trees, in which one point is preferred, and then to enumerate the different types of "free" trees in terms of the different rooted trees. We have generalized this procedure to Husimi trees, and the main purpose of this note is to present an outline of the method and some particular results.

2. The Number of Rooted Husimi Trees.—To simplify the writing we will exemplify the method for the case of cacti. Let $\Delta(x) = \sum_{0}^{\infty} \Delta_n x^n$ be the counting series (generating function) for the number Δ_n of rooted cacti consisting of n triangles ($\Delta_0 = 1$). Starting from the root we can classify the different cacti according to the number r of principal leaves, which are

the triangles having the root point in common. Let $\Delta^{(r)}(x)$ be the counting series of the cacti with r main leaves then obviously:

$$\Delta(x) = 1 + \sum_{r=1}^{\infty} \Delta^{(r)}(x).$$

To obtain $\Delta^{(1)}(x)$ one has to find in terms of $\Delta(x)$ the counting series $\xi(x)$ of an unordered pair of rooted cacti since from the two remaining points of the single triangle, which starts out from the root, any combination of two rooted cacti can emerge. Although $\xi(x)$ can be found very simply, it is useful to already apply here the notation and results of the Hauptsatz of Pólya's paper (Ref. 5, p. 163). Let $\mathfrak{P}$ be a permutation group; then we denote by $Z(\mathfrak{P})$ the so-called cycle index,[6] and by $Z(\mathfrak{P}, f(x))$ the function which results if one replaces f_k by $f(x^k)$. Let $\mathfrak{S}_n$ denote the symmetric group of degree n. By an immediate application of the Hauptsatz, we obtain:

$$\Delta^{(1)}(x) = x\xi(x) = xZ(\mathfrak{S}_2, \Delta(x)) = \frac{x}{2}[\Delta(x^2) + \Delta^2(x)]. \qquad (1)$$

The extra factor x in (1) takes account of the single main leaf triangle.

A second application of Pólya's Hauptsatz then gives $\Delta^{(r)}(x)$. One has to choose at each of r places a pair of rooted cacti, and therefore:

$$\Delta^{(r)}(x) = x^r Z(\mathfrak{S}_r, \xi(x)). \qquad (2)$$

The factor x^r takes account of the r main leaves. Clearly (1) is a special case of (2). By a simple calculation, one finally obtains:

$$\Delta(x) = 1 + \sum_{r=1}^{\infty} x^r Z(\mathfrak{S}_r, \xi(x))$$

$$= \exp\left[\sum_{s=1}^{\infty} \frac{x^s}{2s}\{\Delta(x^{2s}) + \Delta^2(x^s)\}\right] \qquad (3)$$

as the functional equation for $\Delta(x)$.

The generalization to rooted pure Husimi trees consisting of m-gons is accomplished by redefining the function $\xi(x)$ in equation (3) appropriately. If $T^{(m)}(x)$ is their counting series, then the functional equation is

$$T^{(m)}(x) = \exp\left[\sum_{s=1}^{\infty} \frac{x^s}{s} \xi_{m-1}(x^s)\right], \text{ where}$$

$$\xi_{m-1}(x) = \frac{1}{2}\left[(T^{(m)}(x))^{m-1} + (T^{(m)}(x^2))^{\left[\frac{m-1}{2}\right]} (T^{(m)}(x))^{\frac{1+(-1)^m}{2}}\right]. \qquad (4)$$

The extension to mixed Husimi trees is very simple. It is necessary to introduce counting series with as many variables as there are kinds of polygons in the tree. For instance, let $T(n_2, n_3)$ be the number of rooted trees consisting of n_2 lines and n_3 triangles; one then has for the counting series:

$$T(x, y) = \sum_{n_2,\, n_3 = 0}^{\infty} T(n_2, n_3) x^{n_2} y^{n_3}$$

and the functional equation:

$$T(x, y) = \exp \sum_{r=1}^{\infty} \left[\frac{x^r}{r} T(x^r, y^r) + \frac{y^r}{2r} \left\{ T(x^{2r}, y^{2r}) + T^2(x^r, y^r) \right\} \right]. \quad (5)$$

3. The Dissimilarity Characteristic.—To count the number of free Husimi trees we will generalize the method which Otter[5] developed for the case of Cayley trees, and which makes use of the notion of the dissimilarity characteristic. Consider a Husimi tree H with points belonging to different sets, say of different color.[7] The notion of similarity for points, lines or cycles, will be defined in terms of those automorphisms of the tree H, which also preserve the color of the points. Call p^*, l^*, c^* the number of dissimilar points, lines and cycles in H. Let a be the number of symmetry axes of H, which do not pass through a cycle. Clearly a can only be zero or one. By a symmetry of a cycle we will always mean a symmetry of the whole tree with respect to the cycle. Let c^*_{pp} and c^*_{ll} be the number of dissimilar cycles, which have at least one point to point, respectively line to line symmetry axis. Then one can show:[8]

$$1 = p^* - (l^* - a) + (c^* - c^*_{pp} + c^*_{ll}). \quad (6)$$

For Cayley trees this reduces to Otter's theorem $1 = p^* - (l^* - a)$, which can also be expressed in the form

$$1 = p^* - l^*_1, \quad (6a)$$

where l^*_1 is the number of dissimilar lines having no symmetry. Analogously for pure Husimi trees consisting of m-gons one can express the dissimilarity characteristic in terms of the numbers of dissimilar m-gons which have a certain type of symmetry. For instance for cacti there are the three symmetry types:

FIG. 1

where the letters refer to rooted cacti. Let c^*_1, c^*_2, c^*_3 be the number of dissimilar triangles of the three respective types of symmetry occurring in a given cactus H. Then clearly

$$\begin{aligned} l^* &= 3c^*_1 + 2c^*_2 + c^*_3 \\ c^* &= c^*_1 + c^*_2 + c^*_3 \end{aligned}$$

and since $a = 0$ and $c^*_{pp} = c^*_{ll} = 0$ (as is the case for all pure Husimi trees, consisting of odd polygons) one obtains from (6):

$$1 = p^* - 2c^*_1 - c^*_2. \tag{6b}$$

For a pure Husimi tree consisting of quadrilaterals one has five types of symmetry, illustrated by:

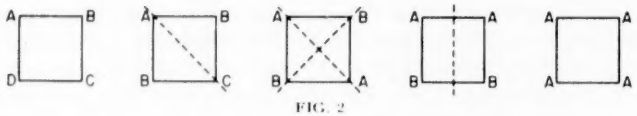

FIG. 2

If $c^*_1, \ldots, c^*_5$ denote again the number of dissimilar quadrilaterals of these symmetry types occurring in a given tree, then one has

$$\begin{aligned} l^* &= 4c^*_1 + 2c^*_2 + c^*_3 + 3c^*_4 + c^*_5 \\ c^* &= c^*_1 + c^*_2 + c^*_3 + c^*_4 + c^*_5 \\ c^*_{pp} &= c^*_2 + c^*_3 + c^*_5 \\ c^*_{ll} &= c^*_4 + c^*_5. \end{aligned}$$

Thus one gets from (6), since a is of course again zero:

$$1 = p^* - 3c^*_1 - 2c^*_2 - c^*_3 - c^*_4. \tag{6c}$$

In this way one can go on and we have obtained for every pure Husimi tree consisting of m-gons a formula of the form:

$$1 = p^* - \sum_{i=1}^{s(m)} \alpha_i c^*_i \tag{6d}$$

where $s(m)$ is the number of symmetries of an m-gon and the α_i are integers expressible as simple number-theoretic functions of m.

4. *Functional Equations for the Number of Free Husimi Trees.*—Let

$$t^{(m)}(x) = \sum_{n=0}^{\infty} t^{(m)}_n x^n$$

be the counting series for the number $t^{(m)}_n$ of free Husimi trees consisting of n m-gons. The problem is to find a functional equation for $t^{(m)}(x)$ in terms of the counting series $T^{(m)}(x)$ for the rooted trees. Now it is clear that by summing the dissimilarity characteristic, written in the form (6d), over all pure Husimi trees of n m-gons, one gets:

$$t^{(m)}_n = T^{(m)}_n - \sum_{i=1}^{s(m)} \alpha_i Y^{(m)}_{i,n} \tag{7}$$

where the $Y^{(m)}_{i,n}$ is the total number of dissimilar m-gons of the ith symmetry type in the collection of Husimi trees of n m-gons. From (7) one then gets:

$$t^{(m)}(x) = T^{(m)}(x) - \sum_{i=1}^{s(m)} \alpha_i Y_i^{(m)}(x) \tag{8}$$

where the $Y_i^{(m)}(x)$ are the counting series for the $Y_{i,n}^{(m)}$.

By using the methods of Pólya[9] one can find in any specific case the counting series $Y_i^{(m)}(x)$ in terms of $T^{(m)}(x)$ by inspection. For instance, since in a Cayley tree one gets a line with no symmetry by hanging on its two end-points two different rooted Cayley trees, one gets for Cayley trees ($t^{(2)}(x) \equiv t(x)$; $T^{(2)}(x) \equiv T(x)$) from (6a):

$$t(x) = T(x) - Y_1(x)$$

with:[10]

$$\begin{aligned} Y_1(x) &= x\,[Z(\mathfrak{A}_2, T(x)) - Z(\mathfrak{S}_2, T(x))] \\ &= \frac{x}{2}\,[T^2(x) - T(x^2)], \end{aligned}$$

which leads to the result of Otter:

$$t(x) = T(x) - \frac{x}{2}\,[T^2(x) - T(x^2)]. \tag{9a}$$

Analogously for cacti, the counting series for triangles with no symmetry is given by:

$$\begin{aligned} Y_1^{(3)}(x) &= x\,[Z(\mathfrak{A}_3, T^{(3)}(x)) - Z(\mathfrak{S}_3, T^{(3)}(x))] \\ &= \frac{x}{6}\,[\Delta^3(x) - 3\Delta(x)\Delta(x^2) + 2\Delta(x^3)] \end{aligned}$$

where we have written $\Delta(x)$ for $T^{(3)}(x)$. Since triangles of the second symmetry type must have two isomorphic rooted trees on two end-points which are different from the tree on the third end-point, one sees easily that:

$$Y_2^{(3)}(x) = x[\Delta(x)\Delta(x^2) - \Delta(x^3)].$$

Writing $\delta(x)$ for $t^{(3)}(x)$, one gets therefore from (6b):

$$\delta(x) = \Delta(x) - \frac{x}{3}\,[\Delta^3(x) - \Delta(x^3)]. \tag{9b}$$

Turning now to pure Husimi trees consisting of quadrilaterals, we have to consider the symmetry types shown in Fig. 2. Clearly, any two different pairs AA and BB of rooted trees will lead to a quadrilateral of the third and fourth symmetry type. Therefore:

$$\begin{aligned} Y_3^{(4)}(x) &= Y_4^{(4)}(x) = x[Z(\mathfrak{A}_2, Q(x^2)) - Z(\mathfrak{S}_2, Q(x^2))] \\ &= \frac{x}{2}\,[Q^2(x^2) - Q(x^4)] \end{aligned}$$

where again we have replaced for simplicity $T^{(4)}(x)$ by $Q(x)$. For the second symmetry type, one has to count the number of arrangements of two different trees A and C together with a pair B, B, where B is "independent"[9] of A and C. Therefore:

$$\begin{aligned} Y_2^{(4)}(x) &= xQ(x^2)[Z(\mathfrak{A}_2, Q(x)) - Z(\mathfrak{S}_2, Q(x))] \\ &= \frac{x}{2}[Q^2(x)Q(x^2) - Q^2(x^2)]. \end{aligned}$$

Finally for the first symmetry type one has to begin with the number of different quadruples of rooted trees A, B, C, D. This is counted by $Z(\mathfrak{A}_4, Q(x)) - Z(\mathfrak{S}_4, Q(x))$. This last expression must then be multiplied by 3 since the four different rooted trees can be arranged in three non-equivalent ways at the four vertices of a quadrilateral. However this is not enough. If two of the rooted trees are identical one can still arrange them in a completely unsymmetric fashion on the corners of a quadrilateral. We therefore have to add the number of arrangements of two different trees (say B, C) together with a pair (say A, A) of identical trees. This is counted just as for the second symmetry type by

$$Q(x^2)[Z(\mathfrak{A}_2, Q(x)) - Z(\mathfrak{S}_2, Q(x))].$$

But now we have too much, because A can *not* be equal to B or C, since otherwise the quadrilateral would have a symmetry. So we must subtract the number of arrangements A, A, A, C where A is different from C. This is clearly counted by $Q(x^3)Q(x) - Q(x^4)$, and so we get altogether:

$$Y_1^{(4)}(x) = \frac{x}{8}[Q^4(x) - 2Q^2(x)Q(x^2) - Q^2(x^2) + 2Q(x^4)].$$

From equation (6c) one then gets the final formula ($t^{(4)}(x) = q(x)$):

$$q(x) = Q(x) - \frac{x}{8}[3Q^4(x) + 2Q^2(x)Q(x^2) - 3Q^2(x^2) - 2Q(x^4)] \quad (9c)$$

In this way one can go on, but the details become very involved. Using the same method we have also derived the equations for pure Husimi trees consisting of pentagons and hexagons, and the results (after correcting an error pointed out by R. Z. Norman) are:

$$p(x) = P(x) - \frac{2}{5}x[P^5(x) - P(x^5)] \quad (9d)$$

$$h(x) = H(x) - \frac{x}{12}[5H^6(x) + 3H^2(x)H^2(x^2) - 4H^3(x^2) - 2H^2(x^3) - 2H(x^6) \quad (9e)$$

From these results one can further easily obtain a formula for the counting of mixed Husimi trees. In this case, one easily sees that the dissimilarity characteristic (6) can be written in the form:

$$1 = p^* - \sum_k \sum_i c^*_{i,k} \tag{10}$$

where $c^*_{i,k}$ is the number of dissimilar cycles of k points and the ith symmetry type (for $k = 2$, this refers to lines not contained in a cycle). Therefore one can combine the formula (9) in an additive fashion except that now one has to use counting series with more variables. For instance, for free Husimi trees consisting of lines and triangles one finds for the counting series $t(x, y)$ the functional equation:

$$t(x, y) = T(x, y) - \frac{x}{2}[T^2(x, y) - T(x^2, y^2)] - \frac{y}{3}[T^3(x, y) - T(x^3, y^3)]$$

where $T(x, y)$ is determined by (5).

In a subsequent paper we hope to present a more systematic treatment of the general case of pure trees consisting of m-gons, and an asymptotic evaluation of their numbers.

1. Uhlenbeck, G. E., "Some Basic Problems of Statistical Mechanics," Gibbs Lecture, Am. Math. Soc. (1950); (in process of publication). Compare also Riddell, R. J., "Contributions to the Theory of Condensation," Doctoral thesis, University of Michigan (1951); (in process of publication).

2. Husimi, K., "Note on Mayer's Theory of Cluster Integrals," *J. Chem. Phys.*, **18,** 682–684 (1950).

3. Cayley, A., "Collected Mathematical Papers," **13,** 26–28, Cambridge (1889–1898). Other proofs are given by Pólya, reference 5, p. 201, and by Bol. G., *Abhandl. Math. Seminar Hansischen Univ.*, **12,** 242 (1938).

4. The two problems mentioned are clearly two extreme cases of the general problem of finding the number of topologically different graphs in which the points are undistinguishable in sets. For instance "multiply rooted" Cayley trees belong to the more general case. Compare Harary and Uhlenbeck, "On Some Generalizations of Rooted Trees," Abstract 131, *Bull. Am. Math. Soc.*, **58,** 168 (1952).

5. Cayley, A., "Collected Mathematical Papers," **3,** 242–246 and **11,** 365–367. Pólya, G., "Kombinatorische Anzahlbestimmungen für Gruppen, Graphen und Chemische Verbindungen," *Acta Math.*, **68,** 145–254 (1937). Otter, R., "The Number of Trees," *Annals of Math.*, **49,** 583–599 (1948).

6. The cycle index of a permutation group is defined (see Pólya, reference 5, p. 159) as follows:

$$Z(\mathfrak{P}) = \frac{1}{h} \sum_{(j_t)} h_{j_1, j_2, \ldots, j_s} f_1^{j_1} f_2^{j_2} \ldots f_s^{j_s}$$

where h is the order and s the degree of $\mathfrak{P}$; $f_1, f_2, \ldots, f_s$ are s variables; $h_{j_1, \ldots, j_s}$ is the number of permutations of $\mathfrak{P}$ containing j_1 cycles of length 1, j_2 of length 2, etc. The round summation sign is over all s-tuples (j_t) such that $1j_1 + 2j_2 + \ldots + sj_s = s$. We will be primarily interested in the symmetric group, for which

$$h_{j_1,\ldots,j_s} = \frac{s!}{1^{j_1}j_1!\,2^{j_2}j_2!\,\ldots\,s^{j_s}j_s!}$$

7. For free Husimi trees all points belong to the same set. The dissimilarity characteristic relation (equation (6)) is however also valid in the more general case.

8. Harary, F., and Norman, R. Z., "The Dissimilarity Characteristic of Husimi Trees," *Annals Math.*; (in process of publication).

9. We will make special use of the result (Pólya, Ref. 5, pp. 161 and 172) that the number of ways in which *n different* figures, from the figure collection counted by $f(x)$, may be distributed on n points is counted by

$$Z(\mathfrak{A}_n, f(x)) - Z(\mathfrak{S}_n, f(x)),$$

where $\mathfrak{A}_n$ is the alternating group of degree n.

We also make frequent use of Pólya's result, p. 164, that for two independent figure collections, the corresponding counting series is the product of the individual ones.

10. In this and all subsequent formulas for the $Y_i(x)$, the extra factor x is needed to account for the cycle to which all the rooted trees, A, B, ... are connected.

STUDIES IN THE CONFORMAL MAPPING OF RIEMANN SURFACES, I

By Maurice Heins*

Brown University and University of Paris

Communicated by Marston Morse, February 20, 1953

1. We are concerned with an analysis of the exact form of the Lindelöf inequality for directly conformal maps of one Riemann surface with positive boundary into another. Let F and G denote Riemann surfaces with positive boundary, let $\mathcal{G}_F$ and $\mathcal{G}_G$ denote their respective Green's functions, let f denote a directly conformal map of F into G (not necessarily univalent onto), and let $n(p)$ denote the multiplicity of f at $p \in F$. The exact form of the Lindelöf inequality may be taken as the assertion that for such F, G, f for each $q \in G$, the residual term u_q in

$$\mathcal{G}_G[f(p), q] = \sum_{f(r)=q} n(r)\mathcal{G}_F(p, r) + u_q(p) \qquad (1.1)$$

is non-negative harmonic on F. We observe that u_q is the greatest harmonic minorant of $\mathcal{G}_G[f(p),q]$.

We shall use the following terminology.[2] A non-negative harmonic function on a Riemann surface will be termed *quasi-bounded* provided that it may be represented as the limit of a monotone non-decreasing sequence of non-negative bounded harmonic functions all having the given surface as their domain; a non-negative harmonic function on a Riemann surface will be termed *singular* provided that the only bounded non-negative harmonic function on the surface dominated by it is identically zero. Par-

reau[2] has shown that a non-negative harmonic function on a Riemann surface admits a unique representation as the sum of a quasi-bounded harmonic function and a singular harmonic function having the given surface as their domain. Our first result is:

THEOREM A: (1) *$(p, q) \to u_q(p)$ is upper semi-continuous on $F \times G$. Let v_q denote the quasi-bounded component of u_q. Then $(p, q) \to v_q(p)$ is lower semi-continuous on $F \times G$.* (2) *Either $v_q = 0$ for all $q \in G$ or else for no q.* (3) *The set of q for which $u_q - v_q > 0$ is an F_σ of capacity zero.*

Part (3) generalizes in several respects a corresponding result proved by Frostman[1] for Blaschke products. The proof of (1) depends upon the upper semicontinuity of $q \to u_q(p)$ for each p and the lower semicontinuity of $q \to v_q(p)$ as well as uniformity properties of non-negative harmonic functions that are assured by the Harnack inequality. (2) depends upon known properties of the Green's function. The proof of (3) lies deeper as might be expected. The key idea of the proof lies in showing that for a Green's potential P on G, where

$$P(q) = \int \mathcal{G}_G(q, s) d\mu(s), \tag{1.2}$$

μ being a non-negative mass distribution on G, with compact kernel, the greatest harmonic minorant of $P \circ f$ is

$$\int u_q d\mu(q) \tag{1.3}$$

and the quasi-bounded component of (1.3) is

$$\int v_q d\mu(q) \tag{1.4}$$

2. *Maps of Type-Bl.* We term f of *type*-Bl provided that v_q vanishes (for all q). In case $F = G = (|z| < 1)$, this is tantamount to saying that for $|\alpha| < 1$,

$$\frac{f - \alpha}{1 - \bar{\alpha} f}$$

is a Blaschke product save for a set of α of capacity zero.

We say that f is of *type-Bl at $q (\in G)$* provided that there exists a relatively compact Jordan region Ω, $q \in \Omega \subset G$ such that (1) $f^{-1}(\Omega)$ is not empty, (2) the restriction of f to a component of $f^{-1}(\Omega)$ is of type-Bl relative to Ω for *each* component of $f^{-1}(\Omega)$. We say that f is *locally of type- Bl* provided that f is of type-Bl at each point of G. It is to be remarked that in these latter definitions the hypothesis that F and G have positive ideal boundaries may be dropped. We have:

THEOREM B: (1) *If G has (as previously) positive ideal boundary and f is of type-Bl, then for each region $\Omega \subset G$, the restriction of f to a component of $f^{-1}(\Omega)$ is of type Bl relative to Ω for each component of $f^{-1}(\Omega)$.* (2) *If G has positive ideal boundary and f is locally of type-Bl, then f is of type-Bl.*

An essential component of the proof is the following lemma.

LEMMA C. *Given u subharmonic on F and f locally of type-Bl, let U be defined on G as the upper function of* $\sup_{f(p)=q} u(p)$. *If $U < +\infty$, then U is subharmonic on G.*

A consequence of theorem B is that the classical theorem of Iversen may be extended to maps which are locally of type-Bl. Lemma C admits a number of applications to other problems. By way of illustration we cite:

THEOREM D: *Let G have positive ideal boundary and let u be singular positive harmonic on G. If $f:F \to G$ is of type-Bl, then $u \circ f$ is singular on F.*

Theorem D leads to the following consequence for convergent infinite Blaschke products: the set of Fatou boundary values of modulus one of a convergent infinite Blaschke product is the unit circumference and each such Fatou boundary value of modulus one is attained at infinitely many points of the unit circumference.

* The author is a Fulbright Research Fellow and President's Fellow of Brown University for the academic year 1952–1953.

[1] Frostman, O., Potentiel d'équilibre et capacité des ensembles avec quelques applications à la théorie des fonctions. Lund Thesis (1935).

[2] Parreau, M., Sur les moyennes des fonctions harmoniques et analytiques et la classification des surfaces de Riemann. Paris Thesis (1952).

THE PARAMETRISATION AND ELEMENT OF VOLUME OF THE UNITARY SYMPLECTIC GROUP

BY F. D. MURNAGHAN

INSTITUTO TECNOLÓGICO DE AERONÁUTICA, SÃO JOSÉ DOS CAMPOS, BRASIL

Communicated January 21, 1953

We have given previously in these PROCEEDINGS[1] a system of parameters for, and the complete element of volume (including the in-class factor as well as the well-known class factor) of, the n-dimensional rotation and unitary groups and we complete, in the present note, this problem for the classical groups by giving a system of parameters for, and the complete element of volume of, the $2k$-dimensional unitary symplectic group.

The $2k$-dimensional symplectic group, over the field of complex numbers, may be presented as the collection of $2k \times 2k$ matrices, X, with complex elements, which are such that $X'I_{2k}X = I_{2k}$ where $I_{2k} = \begin{pmatrix} 0 & -E_k \\ E_k & 0 \end{pmatrix}$. Writing X as a 2×2 block matrix $\begin{pmatrix} A & C \\ B & D \end{pmatrix}$, whose elements are $k \times k$ ma-

trices, X is symplectic if, and only if, $B'A$ and $D'C$ are symmetric and $D'A - C'B = E_k$. Thus a 2×2 matrix is symplectic if, and only if, it is unimodular. It is known that all symplectic matrices, for any value of k, are unimodular but the proofs we have seen of this fundamental fact are unnecessarily complicated. In fact $\begin{pmatrix} D' & -C' \\ 0 & E_k \end{pmatrix} \begin{pmatrix} A & C \\ B & D \end{pmatrix} = \begin{pmatrix} E_k 0 \\ BD \end{pmatrix}$ so that $(\det D')(\det X) = \det D$. If, then, D is non-singular $\det X = 1$. If D is singular we observe that $\begin{pmatrix} E_k & 0 \\ \epsilon E_k & E_k \end{pmatrix}$ is symplectic and unimodular, no matter what is the complex number ϵ, and we form the product $\begin{pmatrix} E_k & 0 \\ \epsilon E_k & E_k \end{pmatrix} \begin{pmatrix} A & C \\ B & D \end{pmatrix} = \begin{pmatrix} A & C \\ \epsilon A + B & \epsilon C + D \end{pmatrix}$ which is symplectic (being the product of two symplectic matrices). Since $\epsilon C + D$ is singular for at most k values of ϵ there exists an ϵ for which $\begin{pmatrix} A & C \\ \epsilon A + B & \epsilon C + D \end{pmatrix}$ is unimodular and this implies that $\begin{pmatrix} A & C \\ B & D \end{pmatrix}$ is unimodular.

The unitary symplectic group of dimension $2k$ is the collection of $2k \times 2k$ matrices which are at once symplectic and unitary. Its typical matrix is of the form $\begin{pmatrix} A & -\bar{B} \\ B & \bar{A} \end{pmatrix}$ where $B'A$ is symmetric and $A^*A + B^*B = E_k$. It is a $k(2k + 1)$-parameter group, k of the parameters being class parameters and $2k^2$ in-class parameters. Thus when $k = 1$, in which case the group is the unimodular unitary 2-dimensional group, we have 1 class and 2 in-class parameters; when $k = 2$, we have 2 class and 8 in-class parameters; when $k = 3$, we have 3 class and 18 in-class parameters and so on. It is natural, then, that the problem of determining the in-class factor of the element of volume of the group is a more serious one than the already solved problem of determining the class factor. Any unitary symplectic matrix $X = \begin{pmatrix} A & -\bar{B} \\ B & \bar{A} \end{pmatrix}$ may be transformed, by means of a unitary symplectic matrix V, into diagonal form: $V^* X V = \begin{pmatrix} D & 0 \\ 0 & \bar{D} \end{pmatrix}$. If the diagonal elements of D are $e^{i\alpha_1}, \ldots, e^{i\alpha_k}$ the k angles $\alpha_1, \ldots, \alpha_k$ (each of which may be taken to lie in the interval $0 \leq \alpha \leq \pi$) may be taken as the class parameters of the group and the class factor of the element of volume of the group is well known to be

$$\sin^2 \alpha_1 \ldots \sin^2 \alpha_k \prod_{\substack{p \leq q \\ 1}}^{k} \{1 - \cos(\alpha_p - \alpha_q)\} \{1 - \cos(\alpha_p + \alpha_q)\} d\alpha_1 \ldots d\alpha_k$$

or the product of this by any positive constant.

In order to obtain a convenient system of in-class parameters we con-

sider the particular unitary symplectic $2k \times 2k$ matrices $(\overset{*}{pq})$, each of which involves two parameters β and τ, p and $q > p$ being any pair of distinct numbers from the set $1, \ldots, k$ or, else, p being any number of this set and q being $p + k$. The notation will be clear from the following examples for the case $k = 3$:

$$(23) = \begin{pmatrix} 1 & 0 & 0 & 0 & 0 & 0 \\ 0 & ce^{i\tau} & -s & 0 & 0 & 0 \\ 0 & s & ce^{-i\tau} & 0 & 0 & 0 \\ 0 & 0 & 0 & 1 & 0 & 0 \\ 0 & 0 & 0 & 0 & ce^{-i\tau} & -s \\ 0 & 0 & 0 & 0 & s & ce^{i\tau} \end{pmatrix}; \qquad (14) = \begin{pmatrix} ce^{i\tau} & 0 & 0 & -s & 0 & 0 \\ 0 & 1 & 0 & 0 & 0 & 0 \\ 0 & 0 & 1 & 0 & 0 & 0 \\ s & 0 & 0 & ce^{-i\tau} & 0 & 0 \\ 0 & 0 & 0 & 0 & 1 & 0 \\ 0 & 0 & 0 & 0 & 0 & 1 \end{pmatrix}$$

where $c = \cos\beta$ and $s = \sin\beta$. We place a subscript under the parentheses (pq) when we have to distinguish different pairs (β,τ); thus we obtain $\underset{1}{(23)}$ by replacing β and τ by β_1, τ_1 in the formula above, and so on. Then any 2×2 unitary symplectic matrix X can be written as $(12)\,\delta$ where δ is a diagonal unitary symplectic 2×2 matrix; any 4×4 unitary symplectic matrix may be written as $\underset{4}{(12)}\ \underset{3}{(24)}\ \underset{2}{(12)}\ \underset{1}{(13)}\delta$, where δ is a diagonal unitary symplectic 4×4 matrix; any 6×6 unitary symplectic matrix may be written $\underset{9}{(12)}\ \underset{8}{(23)}\ \underset{7}{(36)}\ \underset{6}{(12)}\ \underset{5}{(23)}\ \underset{4}{(12)}\ \underset{3}{(25)}\ \underset{2}{(12)}\ \underset{1}{(14)}\delta$, where δ is a diagonal unitary symplectic 6×6 matrix and so on. The factors preceding δ may be conveniently separated into sets of $1, 3, 5, \ldots, (2k-1)$ each (counting from the right); thus, when $2k = 4$, we write $\{\underset{4}{(12)}\ \underset{3}{(24)}\ \underset{2}{(12)}\}\ \{\underset{1}{(13)}\}\delta$; when $2k = 6$ we write $\{\underset{9}{(12)}\ \underset{8}{(23)}\ \underset{7}{(36)}\ \underset{6}{(12)}\ \underset{5}{(23)}\}\ \{\underset{4}{(12)}\ \underset{3}{(25)}\ \underset{2}{(12)}\}\ \{\underset{1}{(14)}\}\delta$ and so on. Each of the angles β lies in the interval $0 \leq \beta \leq \pi/2$ while each of the angles τ may lie in any one of the 4 quadrants. Turning to the formula $X = V\begin{pmatrix} D & 0 \\ 0 & \bar{D} \end{pmatrix}V^*$ we suppose V factored in the manner described and observe that since δ commutes with $\begin{pmatrix} D & 0 \\ 0 & \bar{D} \end{pmatrix}$ it may be omitted. Thus V is the product of $1 + 3 + \ldots + (2k-1) = k^2$ factors, each involving 2 parameters β, τ, and we take these $2k^2$ parameters as the in-class parameters of the group.

The in-class factor of the element of volume of the group possesses the cumulative property (with respect to the dimension of the group) that the element of volume of the $(2k+2)$-dimensional group contains as a factor the element of volume of the $2k$-dimensional group. The coefficient of $(d\beta)\ (d\tau)$, i. e., of the product of the differentials of the k^2 β's and k^2 τ's, is a function of the β's only and always contains $\sin 2\beta_1 \sin 2\beta_2 \ldots \sin 2\beta_{k^2}$, which we shall denote simply by $\Pi(\sin 2\beta)$, as a factor. For $k = 1$ the in-class factor of the element of volume is

$$dV_2 = (\sin 2\beta)d\beta\, d\tau$$

(it being always understood that the element of volume may be multiplied by any convenient positive constant). For $k = 2$ it is

$$dV_4 = (\cos^4 \beta_2)\ (\sin^2 \beta_3)\ \Pi\ (\sin 2\beta)\ (d\beta)\ (d\tau)$$

there being 4 β's and 4 τ's. For $k = 3$ it is

$$dV_6 = (\cos^6 \beta_5)\ (\cos^4 \beta_2)\ (\sin^2 \beta_8 \sin^4 \beta_7 \sin^2 \beta_5)\ (\sin^2 \beta_3)\ \Pi\ (\sin 2\beta)\ (d\beta)\ (d\tau)$$

there being 9 β's and 9 τ's. For $k = 4$ it is

$$dV_8 = (\cos^8 \beta_{10})\ (\cos\ \beta_5)\ (\cos^4 \beta_2)\ (\sin^2 \beta_{15} \sin^4 \beta_{14} \sin^6 \beta_{13} \sin^2 \beta_{11} \sin^4 \beta_{10}) \times (\sin^2 \beta_8 \sin^4 \beta_7 \sin^2 \beta_5)\ (\sin^2 \beta_3)\ \Pi\ (\sin 2\beta)\ (d\beta)\ (d\tau)$$

there being 16 β's and 16 τ's; and so on. In dV_{2l} the part involving the cosines starts out with $\cos^{2k}\ \beta_{(k-1)^2+1}$, each factor of this part being $\cos^{2j} \beta_{(j-1)^2+1}$, $j = k, k-1, \ldots, 2$. The part involving the even powers of the sines starts out with $\sin^2 \beta_{k^2-1}$, and consists of various factors corresponding to the described grouping of the factors of V. For example, when $k = 5$, in which case we have 50 in-class parameters, the first (and largest) of these groups of factors is $\underset{25}{(12)}\ \underset{24}{(23)}\ \underset{23}{(34)}\ \underset{22}{(45)}\ \underset{21}{(5.10)}\ \underset{20}{(12)}\ \underset{19}{(23)}\ \underset{18}{(34)}\ \underset{17}{(45)}$ and the corresponding part of the factor which involves the even powers of the sines is

$$\sin^2 \beta_{24} \sin^4 \beta_{23} \sin^6 \beta_{22} \sin^8 \beta_{21} \sin^2 \beta_{19} \sin^4 \beta_{18} \sin^6 \beta_{17}.$$

[1] Murnaghan, F. D., these PROCEEDINGS, **38**, 69–73, 127–129 (1952).

HEAT CONDUCTION ON ARBITRARY RIEMANNIAN MANIFOLDS

BY D. C. SPENCER

DEPARTMENT OF MATHEMATICS, PRINCETON UNIVERSITY

Communicated by S. Lefschetz, January 12, 1953

Let $M = M^n$ be an arbitrary orientable Riemannian manifold of class C^∞ and of dimension n. We consider the exterior differential forms on M, and we use the notation of de Rham[2] in which the Laplace-Beltrami operator is the negative of the usual one. The scalar product of two p-forms φ, ψ is

$$(\varphi, \psi) = \int_M \varphi \wedge *\psi = (\psi, \varphi)$$

while the Dirichlet scalar product is

$$D(\varphi, \psi) = (d\varphi, d\psi) + (\delta\varphi, \delta\psi)$$

where d is the operator of exterior differentiation and δ (applied to p-forms) is equal to $(-1)^{np+n+1}*d*$. We define the norm $\|\varphi\|$ by the usual formula $\|\varphi\|^2 = (\varphi, \varphi)$, and we write $D(\varphi) = D(\varphi, \varphi)$. We say that the p-form φ is in the domain of the operator d if φ is of class C^1 and $\|\varphi\| < \infty$, $\|d\varphi\| < \infty$. We define the domain of δ in a similar way, and we say that φ is the domain of Δ if φ is of class C^2 with $\|\varphi\| < \infty$, $\|\Delta\varphi\| < \infty$. The closures of these domains are defined in the usual Hilbert space sense.

We introduce the following spaces where the superscript p refers to the degree of the forms:

$$\begin{aligned}
A^p &= \{\varphi \mid \|\varphi\| < \infty\},\ B^p = \{\varphi \mid \varphi \text{ in the closures of } d, \delta\}.\\
C^p &= \{\varphi \mid \varphi \in C^\infty,\ \varphi \text{ with compact carrier}\},\\
D^p &= \{\varphi \mid \varphi \text{ in the closures of } d, \delta, \Delta\},\\
G^p &= \{\varphi \mid \varphi \in D^p,\ D(\varphi, \psi) = (\varphi, \Delta\psi) \text{ for every } \psi \in D^p\},\\
N^p &= \{\varphi \mid \psi \in D^p,\ D(\varphi, \psi) = (\Delta\varphi, \psi) \text{ for every } \psi \in D^p\}.
\end{aligned}$$

If B_c^p is the subspace of B^p formed by taking the closure, in the norm $D(\varphi) + \|\varphi\|^2$, of the space C^p, it turns out that $G^p \subset B_c^p$.

Let s be a positive number, and write

$$D_s(\varphi, \psi) = D(\varphi, \psi) + s(\varphi, \psi),\ \Delta_s = \Delta + s.$$

The Green's operator $\mathbf{G}_s$ is the one-one linear mapping of A^p onto $\mathbf{G}^p$ whose inverse is Δ_s, while the Neumann's operator $\mathbf{N}_s$ is the one-one linear mapping of A^p onto N^p whose inverse is Δ_s.

THEOREM. *For each positive* s *the Green's and Neumann's operators exist. They are symmetric operators and they satisfy* $D_s(\mathbf{G}_s\varphi) \leq \|\varphi\|^2/s$, $D_s(\mathbf{N}_s\varphi) \leq \|\varphi\|^2/s$.

Let

$$F_s^p(\lambda) = \{\varphi \mid \varphi \in A^p,\ (\mathbf{N}_s - \lambda)\varphi = 0\}$$

be the space of eigenforms belonging to the eigenvalue λ. Since $\mathbf{N}_s$ is bounded, therefore continuous, $F_s^p(\lambda)$ is a closed space and, moreover, we have

$$F_s^p(\lambda) = \{\varphi \mid \varphi \in N^p,\ \Delta_s\varphi = \varphi/\lambda\}.$$

In fact, if $\psi \in N^p$, $\Delta_s\psi = 0$, then $0 = (\Delta_s\psi, \psi) = D_s(\psi)$ so ψ vanishes identically if $s > 0$. If $\varphi \in F_s^p(\lambda)$, then $\|\varphi\|^2/\lambda = (\Delta_s\varphi, \varphi) = D_s(\varphi) \geq s\|\varphi\|^2$, and it follows that $\lambda \geq 1/s$ with equality if, and only if, $D(\varphi) = 0$. Hence

$$F^p = F_s^p(s) = \{\varphi \mid \varphi \in A^p,\ d\varphi = \delta\varphi = 0\}.$$

Since the Neumann's operator $\mathbf{N}_s$ is bounded and symmetric, therefore self-adjoint, we have by the spectral theorem

$$\mathbf{N}_s = \int_0^{1/s} \lambda\, d\mathbf{E}_s(\lambda)$$

where $E_s(\lambda)$ is the canonical spectral field associated with $\mathbf{N}_s$.

Finally, let $t > 0$ and define

$$\mathbf{W}_t = \int_0^{1/s} \exp[(\lambda s - 1)t/\lambda]\, d\mathbf{E}_s(\lambda)$$

For each fixed $t > 0$, $\mathbf{W}_t$ is a symmetric operator which is bounded by 1. Moreover, since $\mathbf{W}_{t_1} \cdot \mathbf{W}_{t_2} = \mathbf{W}_{t_1 + t_2}$, these operators form a semigroup. We see that $\mathbf{W}_0$ is the identity operator, $\mathbf{W}_\infty = \lim \mathbf{W}_t (t \to \infty)$ is the operator $\mathbf{F} = \mathbf{F}^p$ which projects orthogonally onto the space F^p, and that $(\Delta + \partial/\partial t)\mathbf{W}_t = 0$. Given $\alpha \in A^p$, $\|\mathbf{W}_t\alpha\|$ is a non-increasing function of t and $\mathbf{W}_t\alpha$ is a solution of the heat equation with initial distribution α.

Analogous considerations apply to the Green's operator, but the space F^p is replaced by the subspace

$$F_c^p = \{\varphi \mid \varphi \in B_c^p,\ d\varphi = \delta\varphi = 0\}.$$

The heat operator in this case, call it $\mathbf{V}_t$, differs in general from $\mathbf{W}_t$ in that it tends, as $t \to \infty$, to the operator $\mathbf{F}_c = \mathbf{F}_c^p$ which projects orthogonally onto the space F_c^p.

We say that M is a totally bounded manifold (shortly, a b-manifold) if M is a compact subdomain of some larger Riemannian manifold R. If M is a b-manifold, there exists a Green's operator $\mathbf{G}_0$ which is a completely continuous linear mapping of A^p onto $G^p = F_c^p$ whose kernel is F_c^p and whose inverse mapping is Δ. Moreover, in this case, F_c^p is the subspace of harmonic p-forms on R which vanish identically outside M.

The opposite of a b-manifold is a u-manifold (totally unbounded manifold) which is characterized by the property that, for each p, $0 \leq p \leq n$, every p-form in the closure of the operator Δ belongs to N^p. If M is a u-manifold, the spaces G^p and N^p coincide, so $\mathbf{G}_s = \mathbf{N}_s$ for $s > 0$ and $\mathbf{W}_t = \mathbf{V}_t$. Let

$$H_s^p = \{\varphi \mid \varphi \in A^p,\ \Delta_s\varphi = 0\}.$$

On a u-manifold the space H_s^{p-}, $s > 0$, contains only the form 0, and $H^p = H_0^p = F^p = F_c^p$. Furthermore, the operators d, δ and Δ commute with $\mathbf{N}_s$ and $\mathbf{W}_t$. It follows, in particular, that the period

$$P(\alpha, C^p) = \int_{C^p} \mathbf{W}_t\alpha$$

of any given closed form $\alpha \in A^p$ on a finite (differentiable) p-cycle is independent of t, and therefore

$$P(\alpha, C^p) = \int_{C^p} \mathbf{F}\alpha = P(\mathbf{F}\alpha, C^p).$$

Finally, we observe that, on a u-manifold, the closure under the norm of the space of forms $d\varphi$, $\varphi \in A^{p-1}$, is the same as the closure of the space of forms $d\varphi$, $\varphi \in C^{p-1}$, and similarly for the operators δ, Δ. A u-manifold therefore has negligible boundary in the sense of Gaffney,[1] that is $(d\alpha, \beta) =$

$(\alpha, \delta\beta)$ for every α in the domain of d and every β in the domain of δ. In fact, a u-manifold is one which has negligible boundary in Gaffney's sense and satisfies the further condition that any form φ in the domain of Δ satisfies $\|d\varphi\| < \infty$, $\|\delta\varphi\| < \infty$, $\|\delta d\varphi\| < \infty$, $\|d\delta\varphi\| < \infty$ and hence $\Delta\varphi = d\delta\varphi + \delta d\varphi$. Compact (closed) manifolds are a subclass of u-manifolds; the heat equation on compact manifolds was considered by Milgram and Rosenbloom.[3]

There are manifolds which have negligible boundary but are not u-manifolds. For example, let R be a compact Riemannian surface and let φ be the potential function on R which has a (logarithmic) source at one point, a sink at another point, and is regular harmonic everywhere else. If we remove from R the source and the sink points, we obtain a manifold M which has negligible boundary, but M is not a u-manifold since φ lies in the domain of $\Delta(\Delta\varphi = 0)$ but not in the domain of d.

[1] Gaffney, M. P., "The Harmonic Operator for Exterior Differential Forms," PROC. NATL. ACAD. SCI., **37**, 48–50 (1951).

[2] de Rham, G., and Kodaira, K., "Harmonic Integrals," mimeographed notes, Institute for Advanced Study, Princeton, N. J. (1950).

[3] Milgram, A. N., and Rosenbloom, P. C., "Heat Conduction on Riemannian Manifolds I, II," PROC. NATL. ACAD. SCI., **37**, 180–184 (1951), and **37**, 435–438 (1951).

*ABSOLUTE VALUED ALGEBRAS**

BY FRED B. WRIGHT

UNIVERSITY OF CHICAGO

Communicated by A. A. Albert, February 26, 1953

Let A be a not necessarily associative algebra over the real field R, which is a normed linear space under a norm satisfying, in addition to the usual requirements, the equation $|xy| = |x| \cdot |y|$, for every x, y of A. Such an algebra is called absolute-valued. A. A. Albert has shown[1] that a finite dimensional absolute-valued algebra with a unit element is isomorphic to one of the following: (1) the real field R; (2) the complex field C; (3) the quaternion algebra Q; (4) the Cayley-Dickson algebra D. He has further shown[2] that an absolute-valued algebraic algebra is finite dimensional; hence the preceding result applies. Taken with the Gelfand-Mazur theorem this latter result implies that the same theorem holds for power-associative absolute-valued algebras with unit element. This suggests the possibility of extending the result to arbitrary absolute-valued algebras. The theorem of §2 shows that the theorem indeed holds for absolute-valued division algebras.

§1. *Preliminary Considerations.*—For the reader's convenience, the

relevant definitions and results of the above cited papers will be set forth in this section, but no proofs are given here.

An algebra A over a field R is a vector space over R closed with respect to an operation called multiplication, denoted by xy, which satisfies identically the following for all x, y, z of A and a of R: $(x + y)z = xz + yz$; $z(x + y) = zx + zy$; $(ax)y = a(xy) = x(ay)$. The algebra is said to have a unit element e if there is an element e of A such that $ex = xe = x$ for every x of A. The unit element will always be denoted by the same symbol as the number 1. We may then identify R with the subalgebra of A generated by 1.

The linear transformations R_a and L_a on the vector space of A are defined for each a of A by $x \to xa = xR_a$ and $x \to ax = xL_a$. The algebra A is called a division algebra if both R_a and L_a have inverses as linear transformations for every $a \neq 0$ in A.

Throughout this paper, R is taken to be the real field. Then an algebra over R is called absolute-valued if there is a mapping $x \to |x|$ of A into R satisfying: $|x| \geq 0$; $|x| = 0$ if and only if $x = 0$; $|xy| = |x| \cdot |y|$; $|x + y| \leq |x| + |y|$; $|ax| = |a| \cdot |x|$ for every x, y of A and a of R.

Two algebras A and B over R are isotopes of each other if they have the same underlying vector space and if multiplication $x \circ y$ in A is defined in terms of the multiplication xy in B by the relation $x \circ y = (xP)(yQ)$, where P, Q are fixed invertible linear transformations on the common underlying vector space.

Every element x of A generates a subalgebra $A[x]$ of A. A is called algebraic if $A[x]$ is finite dimensional for every x of A.

The principal results of Albert are stated here as lemmas 1–3.

LEMMA 1: *An absolute valued division algebra is an isotope of an absolute valued algebra with a unit.*

LEMMA 2: *An absolute valued algebraic algebra with a unit element is finite dimensional.*

LEMMA 3: *A finite dimensional absolute valued algebra with a unit element is isomorphic to one of the following: (1) the real field R; (2) the complex field C; (3) the quaternion algebra Q; (4) the Cayley-Dickson algebra D.*

§2. *Absolute Valued Division Algebras.*—

LEMMA 4: *An absolute valued division algebra with a unit is an inner product space.*

Proof: It is sufficient[4] to show that for every x, y of A with $|x| = |y| = 1$ the inequality $|x + y|^2 + |x - y|^2 \geq 4$ holds. In the identity $(1 + x)^2 - (1 - x)^2 = 4x$, let $|x| = 1$; since $|1| = 1$, it follows that

$$|1 + x|^2 + |1 - x|^2 \geq 4 \tag{1}$$

Now if a, b are any two elements of A with $|a| = |b| = 1$, let $x = aR_b^{-1}$; then $|x| = 1$. Furthermore, $(1 + x)R_b = b + a$ and $(1 - x)R_b = b - a$.

It is clear that $|1 + x| = |b + a|$ and $|1 - x| = |b - a|$. Substitution in (1) gives

$$|b + a|^2 + |b - a|^2 \geq 4. \tag{2}$$

THEOREM: *Every absolute valued division algebra with a unit is algebraic.*

Proof: There is now an inner product (x, y) defined on A with $(x, x) = |x|^2$. By standard procedures this inner product space may be completed to be a real Hilbert space H, in which A is contained as a dense linear subspace, and in which the inner product on H agrees with the inner product on A, for elements of A. Let M be the algebra generated by 1 in A; M is a one-dimensional subspace of H and is hence closed. We write $H = M \oplus M'$, where M' is the orthogonal complement of M in H. Every element x of A has a unique expression as $x = a + by$, where a, b are in R and y is an element of A contained in M', $|y| = 1$. Since $(1, y) = 0$ and $(y, y) = 1$, it results that $(1 + y, 1 + y) = 2$ and $(1 - y, 1 - y) = 2$. But if u, v are any two elements of A, $(u, u)(v, v) = |u|^2|v|^2 = |uv|^2 = (uv, uv)$. Then it results that $(1 - y^2, 1 - y^2) = 4$, or $(1, y^2) = -1$. But y^2 can be written $y^2 = c + dz$, where c, d are in R and $|z| = 1$, z is in both A and M'. Then $c = -1$, $d = 0$; or $y^2 = -1$.

For arbitrary x of A, with $x = a + by$ as above, define $x^* = a - by$; then $x + x^* = 2a$, $x^*x = a^2 - b^2$. But $x^2 - (x + x^*)x + x^*x = 0$ is an identity, so that $x^2 - 2ax + (a^2 - b^2) = 0$, which shows that A is algebraic.

Then the use of lemmas 1–3 above gives a complete description of all absolute valued division algebras, even without unit element.

§3 *Remarks.*—In the proof of the theorem, use is made of the assumption that A is a division algebra only in passing from (1) to (2). It is natural to suppose that (2) can be proved independently of (1). The ptolemaic inequality[4] seems made to order for this.

The connection of this result with the Gelfand-Mazur[3] theorem seems worth noting. This result says that an associative normed (the weaker condition $|xy| \leq |x| \cdot |y|$ is assumed) algebra over the reals, without topological divisors of zero, is either the reals, complexes, or quaternions. The difficulty in extending this result to algebras which are not assumed to be associative is the lack of an adequate definition in such algebras of the spectrum. It is also to be noted that there exist normed division algebras over the reals which are not absolute valued. All known examples are finite dimensional; it may be conjectured that every normed division algebra over the reals is finite dimensional.

* This paper was prepared under contract with the Office of Naval Research.

[1] Albert A. A. *Annals of Math.* **48,** 495–501 (1947).

[2] Albert, A. A., *Bull. Amer. Math. Soc.*, **55,** 763–768 (1949).

[3] Kaplansky, I., *Duke Math. J.*, **16,** 399–418 (1949).

[4] Schoenberg, I. J., *Proc. Amer. Math. Soc.*, **3,** 961–964 (1952).

AN ANALYSIS OF THE SYNTHESIS AND DISTRIBUTION OF THE CONTRACTILE PROTEIN, MYOSIN, IN THE DEVELOPMENT OF THE HEART

BY JAMES D. EBERT

INDIANA UNIVERSITY*

Communicated by B. H. Willier, February 10, 1953

The development of the heart presents a series of problems in morphogenesis and differentiation which afford an unexcelled opportunity for the analysis of the interrelationships of specific structural and functional properties during ontogeny. As the heart is formed, so it begins to beat. In the chick embryo of 7 somites the paired primordia of the heart have already begun to fuse; local contractions have been recorded in the heart of the 9-somite embryo.[1, 2] The onset of contractility has been correlated with the time at which significant histogenic changes have been recorded, e.g., the first appearance of cross-striations at the 10-somite stage[3] and the first detectable glycogen in the embryo of "about 28 hours."[4] The early contractions have been described as of a fundamental myogenic nature since they occur well in advance of the time at which the first nerve fibers approach the heart.

The early morphogenesis and onset of contractility of the heart are foreshadowed by a precocious restriction of the heart-forming cells to relatively well-defined areas of the blastoderm. Willier and Rawles[5] and Rawles[6] have described two large bilaterally situated areas of the head-process blastoderm endowed with heart-forming potency. No critical information has been presented concerning the location of the heart-forming areas earlier than the head-fold stage. Rudnick[7] has concluded from a review of the pertinent data that the heart mesoderm must be very early in a highly organized state, and is early invaginated to migrate laterally to its definitive position. A similar conclusion was reached by Bacon[8] in his analysis of the development of the heart in *Amblystoma*.

In contrast to the fund of information from the field of experimental morphogenesis, information concerning the chemistry and cellular physiology of the development of the heart is almost completely lacking. The void may be due, at least in part, to the difficulties encountered in studying the contractile proteins in minute quantities, as illustrated by the experiences of Herrmann and his coworkers,[9, 10] who have not been able to make determinations of actomyosin in skeletal muscle of the chick embryo prior to the ninth day of incubation, although fibrillations and cross-striations have been observed in the 7-day embryo, a time at which muscular response to mechanical stimulation and histological differentiation of motor centers in the central nervous system also have been described. In the

present investigation the difficulty in detecting minute quantities of cardiac contractile proteins is largely overcome through the application of the precise techniques of immunochemistry.

In earlier reports[11, 12] it was shown, by absorption and precipitin tests, that antisera produced in rabbits against extracts of adult chicken heart will react with extracts of the early chick embryo prior to the morphogenesis of the heart. The early blastoderm must therefore contain antigens identical, or closely related, to those of adult heart. This conclusion is supported by the finding that when early blastoderms are cultured in media containing antiheart sera, the development of the heart is differentially suppressed.

It becomes of interest to determine next the relationship of the specific antigenic components of cardiac muscle present in the early blastoderm to the contractile proteins, actin and myosin. We ask the following questions: (1) Do actin and myosin develop simultaneously? Is the development of each protein an independent event or does the development of one precede that of the second and have a causal role in its synthesis?

(2) Are there differences in the contractile proteins of cardiac and skeletal muscle which play a significant role in the precocious restriction of cardiac contractile proteins to the heart-forming areas of the blastoderm, and in the early onset of contractility? Only after the facts relative to the time of synthesis and distribution of the cardiac contractile proteins are available will it be possible to attack the basic problem of the factors controlling their synthesis. The specific objective of this report is to present findings relative to the time of synthesis and progressive localization of cardiac myosin in the early chick embryo.

METHODS AND RESULTS

1. Preparation of Myosin.—Cardiac and skeletal myosins were extracted from heart and hind limb muscle, respectively, of adult New Hampshire Red chickens of both sexes, following the method described by Mommaerts and Parrish,[13] in which myosin and actomyosin are simultaneously precipitated from the muscle extract by dialysis, most of the actomyosin being irreversibly insoluble. The remaining actomyosin is precipitated from the redissolved myosin by adjusting the ionic strength and pH. Actin-free myosin is then crystallized by dilution with glass-distilled water. Twelve to 36 fresh adult chicken hearts were used in each extraction (100 to 350 g. of fresh cardiac muscle). Two minor deviations from the technique described by Mommaerts and Parrish should be noted: (1) following dialysis for 18 hours, the ionic concentration of the muscle extracts is frequently not reduced sufficiently to permit maximal precipitation; therefore, 200 ml. of glass-distilled water per 100 g. of muscle is added directly to the extract following dialysis. (2) Mommaerts and Parrish

describe an average yield of 1.2 g. of myosin from 100 g. of muscle. Our yields have been consistently lower: from chicken cardiac muscle, 750 mg. of myosin per 100 g., and from chicken skeletal muscle, 410 mg. of myosin per 100 g. of muscle extracted.

It must be emphasized at the outset of the discussion that although the extraction technique employed yields actin-free myosin which approaches purity, the final product is not monodisperse. Mommaerts and Parrish state that the purity of their preparations is of the order of 85–90 per cent. Preliminary studies of cardiac myosin indicate that the degree of purity of the preparation is only slightly lower than that described by Mommaerts and Parrish.

2. *Production of Antisera.*—Despite the brief positive report by Keszтyus, Nikodemusz, and Szilagyi[14] that myosin is antigenic, our early attempts to produce potent antisera in rabbits against cardiac myosin from adult chickens were unrewarding.[12] Hence it seems advisable to record here, briefly, the more important details of the immunization procedure which has proved to be reliable in our laboratory during the past year. First, it is essential that the myosin used for injections be either freshly prepared or stored for less than one week at −20°C. In the latter case, it should be thawed only once. The use of freshly extracted myosin for each injection is prohibitively expensive of both time and materials, hence we have made extractions weekly. The myosin should be a bluish-translucent gel; no shreds are desired. The myosin is stored and injected in the phosphate-KCl solution described by Mommaerts and Parrish, at pH 6.8, ionic strength 0.5.

Individual rabbits vary greatly in their antibody response to injected myosin. To date, of 22 rabbits injected with cardiac myosin, only 12 have produced antisera of sufficient potency to be of value. In general, the immunization schedules are so arranged that each adult male rabbit receives a series of intravenous injections on alternate days over a two-week period, totaling 18–20 mg. of protein, is rested for 4–6 days and bled. After 20–25 days further rest, a second series of injections is started, in which a first injection of 4–6 mg. of protein is given intraperitoneally, followed by a total of 48–60 mg., intravenously, on alternate days over a two-week period. Once again the rabbits are bled following 4–6 days rest. Our rabbits have consistently built up circulating antibodies against myosin rapidly, and lost them rapidly. Hence the rabbits are bled 4–6 days rather than the more general 7–10 days after the last injection of a series. Sera are sterilized by passage through a Seitz filter and stored at −20°C. No preservative is added.

3. *Specificity of Antisera.*—The titer and specificity of each serum was determined by the precipitin technique, employing homologous or heterologous antigen. A preliminary titration was made with a constant

volume of full-strength serum and progressively decreasing quantities of homologous antigen. The end-point of the antigen dilution series was then titrated with serial dilutions of serum. In this manner, inhibition due to excess antigen is avoided, the serum end-point being greatest with the last active dilution of antigen.[15-17] A total of 54 antisera from 22 rabbits has been assayed. Appropriate controls have been carried out with sera of uninjected rabbits. The effective serum dilution titers of the antisera tested ranged from 1:64 to 1:8192. Only those sera with titers of at least 1:512 with homologous antigen were retained (31 antisera). Potent sera were then tested for reactivity with heterologous antigen (skeletal myosin). The results clearly show that the antisera against cardiac myosin are highly tissue-specific, i.e., that cardiac and skeletal myosins differ markedly in antigenic constitution. The highest titer obtained in tests of 27 antisera against cardiac myosin with nine separate fresh preparations of the heterologous antigen, skeletal myosin, is 1:256. There is a consistent difference of 4–5 tubes in the reactivity of each serum with homologous and heterologous antigen. In further tests, antisera were first completely absorbed with adult skeletal myosin, and then tested with homologous antigen. Much of the specific reactivity of the sera was retained. The reduction in reactivity due to elimination of antibodies to reactive groups in the heterologous antigen ranged from 1 to 4 tubes. Therefore, due to the marked difference in antigenic constitution of cardiac and skeletal myosins, it is possible to prepare, by absorption procedures, antisera highly specific for adult cardiac myosin. In the sections to follow, all references to antisera against adult cardiac myosin refer to these highly specific, absorbed antisera.

4. Myosin in the Developing Heart.—It will be of interest to examine next the evidence pertaining to the antigenic specificity of cardiac myosin during development, as determined by an analysis of the reactivity of antisera against adult cardiac myosin with cardiac extracts from embryos of 36 hours to 18 days incubation. All embryos used in these experiments were of the New Hampshire Red breed, from eggs incubated at 37.5°C. After removing the embryos from the eggs as quickly as possible, the hearts were removed (in an iced Petri dish), freed from excess blood with filter paper, weighed rapidly on a micro-torsion balance and minced finely with scissors on chilled waxed paper. The mince was homogenized in a Ten Brock glass tissue grinder in buffered KCl solution. At 18 days, 60 hearts, and at 13 days, 144 hearts were extracted by the technique described for adult cardiac muscle, with a workable yield of purified myosin. At the earlier stages, however, it was necessary to employ a crude extract of cardiac muscle (containing both myosin and actomyosin), since a measurable yield of purified myosin could not be obtained from the small quantities of material available. Hearts of embryos of from 36 hours to 12 days in-

cubation were homogenized in the buffered KCl solution. The homogenate was clarified by filtration through cheesecloth followed by centrifugation at 3600 r. p. m. for 30 minutes at 1°C. Both the purified cardiac myosin from older embryos and the clarified cardiac extract from younger embryos were tested for reactivity with antisera against adult cardiac myosin employing several modifications of the precipitin technique, including (1) the ring test, (2) the Hanks technique,[15, 18] and (3) the micro (capillary) method of Ten Cate and Van Doorenmaalen,[19] kindly demonstrated to me by the authors in their laboratory. All preparations from cardiac muscle, both the purified myosin and the clarified extract from younger embryos, reacted positively with all antisera tested. Cardiac extracts and purified cardiac myosin from embryos at the following stages have been tested: 36, 48, and 72 hours, 5, 7, 9, 12, 13, 15, and 18 days. At least three separate fresh extracts have been tested at each stage, each extract being reacted with at least three potent anticardiac myosin sera. Further, by the absorption technique, employing repeated absorptions with em-

TABLE 1

CARDIAC MYOSIN IN THE EARLY EMBRYO

HAMBURGER AND HAMILTON STAGE	TOTAL NUMBER OF EMBRYOS EXTRACTED	NUMBER OF FRESH EXTRACTS TESTED	NUMBER OF ANTISERA USED WITH EACH EXTRACT	TOTAL NUMBER OF TEST SERIES	NUMBER OF POSITIVE REACTIONS	HIGHEST TITER
1	264	5	3	15	0	—
2	248	5	3 or 4	18	1	4
3	236	5	3	15	15	256
4	381	7	2 or 3	17	17	256
5	140	3	2 or 3	8	8	512

bryonic cardiac antigens of any of the stages tested, it has been clearly demonstrated that all activity of the antisera for adult cardiac myosin can be removed. It is concluded, therefore, that the embryonic heart, from 36 hours through 18 days incubation, contains antigens or reactive groups identical, or closely related to those found in adult cardiac myosin.

5. Cardiac Myosin in the Embryo Prior to Morphogenesis of the Heart.—The question next arises as to the time at which the reactive groups of cardiac myosin first can be detected in the early embryo. In this series of experiments, embryos in stages 1 to 5 of the Hamburger-Hamilton series (pre-streak through head-process stages) were extracted following the method described for the extraction of cardiac tissue of embryos from 36 hours to 12 days incubation. Three dozen or more embryos at each stage were rapidly removed from the yolk, trimmed and washed to remove adhering yolk, and homogenized in ice-cold KCl-phosphate solution in the Ten Brock grinder. The homogenate was allowed to stand for 1 hour at 2°C., with constant stirring, and then clarified by filtration through cheesecloth, followed by centrifugation. The resultant clear extract was

used as the test antigen in precipitin tests with antisera against adult cardiac myosin, chiefly by the Hanks' and capillary methods. The results, which are summarized in table 1, are based on 73 separate serum-dilution series of reactions, for which a total of 1269 embryos has been extracted. It is clear that reactive groups identical with or closely related to cardiac myosin first can be detected in the embryo by the methods employed at stage 3, the mid-streak blastoderm. All tests of pre-streak, and 17 out of 18 tests of initial streak embryos were negative. At the latter stage one exception was noted—a trace reaction in the first 2 tubes of 1 series. The experiment was repeated with 3 additional fresh extracts of embryos at the same stage; all were completely negative with the same antiserum; therefore the trace reaction is not regarded as significant, likely being due to an error in staging one or more embryos in the extract in question.

6. Distribution of Cardiac Myosin in the Early Embryo.—Rawles[6] has

TABLE 2

ANTERO-POSTERIOR DISTRIBUTION OF CARDIAC MYOSIN

HAMBURGER AND HAMILTON STAGE	TOTAL NUMBER OF EMBRYOS EXTRACTED	NUMBER OF FRESH EXTRACTS TESTED	NUMBER OF ANTISERA USED WITH EACH EXTRACT	TOTAL NUMBER OF TEST SERIES	SECTION OF EMBRYO TESTED	NUMBER OF POSITIVE REACTIONS	HIGHEST TITER
4	601	11	2–4	29	Ant.	29	64
					Mid (node)	29	256
					Post.	29	256
5	664	12	2–4	31	Ant.	0	...
					Mid (node)	31	256
					Post.	2	4

mapped rather precisely the shape, average dimensions and position of the heart-forming areas in the chick blastoderm at the head process stage. Her cogent analysis has provided the experimental target for the present investigation. Attention was directed first to a study of the distribution of cardiac myosin in the antero-posterior axis of the embryo at stages 4 and 5. The blastoderm at stage 4 or 5 was divided into 3 segments, designated anterior, mid (containing the node), and posterior, by 2 transverse cuts made with glass or freshly sharpened steel needles across the blastoderm at the levels defined by Rawles as the anterior and posterior limits of the heart-forming areas, 0.6 mm. in front of, and 0.45 mm. behind, the node, respectively. Anterior, mid, and posterior segments, respectively, were pooled in cold buffered KCl solution and extracted following the procedure described for whole embryos. The clarified extracts were tested for the presence of reactive groups of cardiac myosin by the capillary method. The results are summarized in table 2. It is clear that in the

embryo at stage 4, cardiac myosin is found in all 3 sections of the embryo in the antero-posterior axis. The data further suggest, but do not prove, that the amount of cardiac myosin in the mid and posterior segments is greater than in the anteriormost region of the stage 4 embryo. In order to establish the observed difference as a significant one it will be necessary to so modify the present micro-techniques that strictly quantitative data can be obtained. Efforts in this direction are being continued. In the embryo at stage 5, cardiac myosin is confined to the mid segment in the antero-posterior axis, being absent from the anterior and posterior segments. Cardiac myosin is limited in its distribution in the antero-posterior axis, therefore, to a region slightly over one millimeter in length. The possible mechanism of the progressive localization of cardiac myosin will be discussed in a later section, but it should be emphasized at this point that the

TABLE 3

MEDIO-LATERAL DISTRIBUTION OF CARDIAC MYOSIN

HAMBURGER AND HAMILTON STAGE	TOTAL NUMBER OF EMBRYOS EXTRACTED	NUMBER OF FRESH EXTRACTS TESTED	NUMBER OF ANTISERA USED WITH EACH EXTRACT	TOTAL NUMBER OF TEST SERIES	SECTION OF EMBRYO TESTED	NUMBER OF POSITIVE REACTIONS	HIGHEST TITER
4	271	6	2 or 3	13	Left lat.	13	64
					Median (streak)	13	64
					Right lat.	13	64
5	339	7	2 or 3	16	Left lat.	16	64
					Median (streak)	14	8
					Right lat.	16	64
6–7	273	5	2 or 3	11	Left lat.	11	128
					Median (streak)	0	...
					Right lat.	11	128

demonstrated localization is of a specific contractile protein and not merely of prospective cardiac cells destined for the synthesis of that protein.

Next let us consider the distribution of cardiac myosin in the medio-lateral axis. Again the data of Rawles provide the morphological basis for our experiments. Groups of embryos at stages 4 and 5 were transected as previously described, 0.6 mm. before, and 0.45 mm. behind, the node. The mid-piece, however, was further subdivided into 3 sections, by 2 cuts perpendicular to its cut surfaces, 0.2 mm. on either side of (and roughly paral'el to) the node. The resultant sections, designated left lateral, median, and right lateral, respectively, were pooled and extracted, and tested for the presence of the reactive groups of cardiac myosin as previously described. The data are are summarized in table 3.

In the embryo at stage 4, cardiac myosin is approximately equally

distributed in the 3 sections tested in the medio-lateral axis, and has not been localized to the heart-forming areas. In the embryo at stage 5, although cardiac myosin is largely localized in the lateral areas, traces of the reactive groups are found in the median section (0.4 mm. wide) containing the streak. Thus the data are not in complete agreement with the finding by Rawles that the median area does not produce heart when grafted to the chorio-allantoic membrane. Although the reaction is weak, it is consistently found and is believed to be significant. It appeared likely that cardiac cells are being invaginated even as the streak regressed. In order to determine whether the localization of cardiac myosin to the prospective heart-forming areas is complete at a later stage, the experiments were extended to include stages 6–7 (stage 6 is the transitional head-fold stage, difficult to "schedule"; hence stages 6 and 7 are pooled). The results, shown in table 3, demonstrate that in the embryo at stages 6–7 the median (streak) region does not contain cardiac myosin detectable by the immunochemical methods employed.

Discussion

The labile protein which has been characterized from the physicochemical point of view (at least within reasonable limits), and designated "myosin" by most workers in the field of muscle chemistry has been the myosin extracted from rabbit skeletal muscle. The further questions as to whether myosin is species- and organ-specific have received little attention. A recent study[20] of skeletal myosins prepared from tissues of the rabbit, rat, and mouse has led to the conclusion that the myosins from these species are practically indistinguishable on the basis of a comparison of electrophoretic properties, sedimentation rates, yields, viscosities, and specific refractive increments. On the other hand, the very fact that myosins have been shown to be antigenic argues for species differences of sufficient magnitude to account for their observed ability to stimulate antibody production. Kesztyus, Nikodemusz, and Szilagyi[14] report that rabbit skeletal myosin is antigenic in dogs, but that it is not isoantigenic. Our own findings show that chicken cardiac myosin is antigenic in the rabbit.

With respect to the problem of the organ-specificity of myosin, Snellman and Gelotte[21] have reported that cardiac and skeletal myosins of the rabbit show several differences, e.g., in solubility and in the sedimentation constant, and in the firmness with which actin and myosin are bound (less in cardiac than in skeletal actomyosin). The results of the present study clearly show that cardiac and skeletal myosins are markedly different in antigenic constitution, a difference which has been of importance in establishing the specificity of the antisera employed in detecting cardiac myosin in the early embryo. The question remains unanswered, however, as to whether antigenic differences reflect important physical differences in

the proteins, and is currently the objective of a comparative physical study in this laboratory.

Next let us consider the question as to whether embryonic cardiac myosin is qualitatively the same as that in the adult. On the basis of differences in behavior of actomyosins from newborn and adult animals (guinea pigs, rats, mice) upon the addition of adenosinetriphosphate, Ivanov and Kasinova[22] concluded that actomyosin in the newborn animal differs qualitatively from that in the adult. Csapo and Herrmann[10] do not support this conclusion, arguing that, at least in their comparison of chick embryonic and adult actomyosins, only quantitative changes occur. Our findings support the latter view, inasmuch as the reactive groups of cardiac myosin capable of combining with specific antisera to adult cardiac myosin do not change qualitatively from the embryo of 36 hours to the embryo of 18 days or, in fact, to the adult fowl.

It will be of interest to consider next the questions of the time of synthesis and localization of cardiac myosin in the early embryo, with particular reference to the concept of organ-forming areas. It is necessary to recognize at the outset of the discussion that while the data clearly demonstrate that a major synthesis of cardiac myosin is initiated only after the prospective mesodermal cells of the epiblast have invaginated, the evidence does not permit a discussion of the problem of mechanism of synthesis. It is clearly possible that "traces" of cardiac myosin may be present in the earlier embryo-quantities which cannot be detected even by the highly sensitive methods employed. The present findings do present a sound chemical basis for further experiments designed to test the related hypotheses of the regulation of the growth and differentiation of an organ by its own products[15, 23] and of pattern formation involving the specific suppression of embryonic differentiation by metabolites of differentiated tissues.[24] We ask, for example, whether the reported failure of cardiac tissues to differentiate in the presence of extracts or products of fully differentiated heart muscle[23, 24] results from a suppression of the synthetic activities of the tissue (e.g., in the synthesis of contractile proteins), or from a failure in morphogenesis of synthesized products.

Tests of developmental potencies of small pieces of the chick blastoderm through transplantation to the chorio-allantoic membrane clearly show that each of the isolated pieces possesses a relatively restricted developmental capacity. Particular structures develop only from rather definite areas of the blastoderm; in short, the organ-forming areas are localized to a remarkable extent. Recently, the nature and significance of the concept of the organ-forming areas has been the object of sharp criticism.[25] Yet most of the investigators who have employed this approach have been acutely aware of its major limitation, namely that each of the isolated pieces is triploblastic, and have, in fact, emphasized the importance of

tissue interactions. Moreover, it has been recognized that the degree of specificity of localization of the several organ-forming areas differs. In fact, on the basis of his recent investigation of the localization of prospective neural plate in the early chick blastoderm, in which the results obtained by transplantation and explantation are shown to be in close agreement with those obtained by marking methods, Spratt[26] has concluded that both types of methods reveal primarily the prospective fates of different regions of the blastoderm. In the case of the heart-forming areas, however, as Rudnick has emphasized,[7] the areas are amazingly large, exceeding in size the actual myocardial anlagen. Thus it appears that the heart-forming areas are areas of prospective potency and not of prospective fate.

Implicit in our definition of an organ-forming area, e.g., the heart-forming area, has been the assumption that the cells of that area of the embryo are destined to become specialized for the synthesis of the specific proteins characteristic of the definitive organ, and that the progressive localization of the heart-forming area is a localization of prospective myosin (and other cardiac protein) synthesizing cells. Yet the present findings demonstrate the progressive localization of the specific reactive groups of cardiac myosin, and not merely of prospective cardiac cells. Cardiac myosin is synthesized in the early embryo and can be detected in stage 3; in the embryo at stage 4, the protein is detected in all sections of the embryo analyzed (presumably in the mesoderm, although the present experiments do not prove this), being more concentrated in the mid and posterior, than in the anteriormost, regions. This finding is not in complete agreement with the results of explantation experiments. Spratt[27] studied the development of pulsating heart masses from anterior and posterior pieces of early blastoderms cultivated *in vitro*, and concluded that although heart-forming potency is wide-spread in pre-streak embryos (see also ref. 28), it later becomes localized in the median portion of the posterior half of the streak at stage 4. Rudnick[29, 30] likewise found that prior to its definitive localization at stage 5, the center of the heart-forming region lies posterior in the streak. The present findings do suggest that the synthesis of myosin is greater in the posterior than in the anterior part of the blastoderm; nevertheless some cardiac myosin is synthesized in the anterior part of the embryo. It is interesting to note that both Spratt and Rudnick used the classical plasma-embryo extract medium in their explantation studies, a medium which according to the reports cited above[23, 24] might suppress cardiac differentiation, since in the absence of a statement to the contrary, the embryo extract is assumed to be an extract of the whole embryo, including the heart.

In the embryo at stage 5, and even more clearly at stages 6–7, the localization of cardiac myosin is in good agreement with the data of Rawles. Cardiac myosin is progressively restricted in distribution; at stage 5 the protein is limited at least to the region bounded by the anterior and pos-

terior borders of the heart-forming areas defined by Rawles, viz., 0.6 mm. forward of, and 0.45 mm. behind, the node. The localization of cardiac myosin in the medio-lateral axis is not completed until stages 6–7, although the protein is largely confined to the lateral heart-forming areas at stage 5.

It is probable that the bulk synthesis of cardiac myosin is initiated only following the invagination of the prospective cardiac cells through the patent streak. The first condition being fulfilled, myosin is synthesized in all areas of the embryo tested.

Emphasis has already been placed on the fact that it is those cells already activately synthesizing cardiac myosin, as defined by its combining groups which are localized, and not merely those cells destined to synthesize the protein. Obviously the present findings do not fall readily into any category with respect to current theories of differentiation. In fact, no single interpretation is offered here. If it is postulated either that myosin synthesis is a self-limiting reaction or that other factors are limiting (e.g., availability of substrate, to cite one of the arguments frequently advanced), it then becomes necessary to explain the disappearance of myosin from the noncardiac areas of the blastoderm. At first thought it appears unlikely that the specificity of the protein might be altered and the protein redirected into other channels. Yet Daly and Mirsky[31] have offered evidence of the synthesis of a protein "pool" in the exocrine pancreas, a pool from which highly specific proteins are rapidly synthesized as the secretory activity of the gland demands that the supply of specific enzymes be replenished. The degree of change of specificity in these transformations is not known. It is possible that the localization of the protein is merely a sorting-out or segregation phenomenon, the result of cellular movements within the mesoderm. Our present knowledge of morphogenetic movements within the mesoderm does not permit a critical evaluation of this possibility.

The question is posed as to whether it will be possible to characterize other organ-forming areas by immunochemical or biochemical methods. Obviously an organ or tissue must fulfill two criteria for successful experimentation in this direction, both of which are admirably fulfilled in the heart-forming areas: it must be an organ which attains early morphological or functional status and for which a sound chemical basis of function has been established. Several of the organ-forming areas which fulfill the second criterion, e.g., the thyroid-forming area, fail when the first criterion is considered. In our laboratory at present one possibility is being investigated (in addition to the analysis of the synthesis of cardiac actin as related to the present study), viz., an immunochemical study of the "pigment-forming area" of the blastoderm. Further discussion and interpretation of the findings and their bearing on the significance of the concept of "organ-forming areas" is reserved pending the outcome of these experiments.

* Contribution number 521 from the Zoological Laboratories. The investigation is supported by grants from the National Science Foundation (NSF-G15) and Indiana University, and by an Indiana University Graduate School Research Fellowship. I wish to acknowledge the intellectual and material aid of the staff of the Department of Biology, Massachusetts Institute of Technology, where the investigation was initiated, and the technical assistance of Alton M. Mun and Louise A. Ross.

[1] Hamburger, V., and Hamilton, H. L., *J. Morph.*, **88**, 49–92 (1951).

[2] Patten, B. M., and Kramer, T. C., *Am. J. Anat.*, **53**, 349–375 (1933).

[3] Lewis, M. R., *Johns Hopkins Hosp. Bull.*, **30**, 176–181 (1919).

[4] Allen, H. J., *Biol. Bull.*, **36**, 63–70 (1919).

[5] Willier, B. H., and Rawles, M. E., *Proc. Soc. Exptl. Biol. Med.*, **32**, 1293–1296 (1935).

[6] Rawles, M. E., *Physiol. Zool.*, **16**, 22–42 (1943).

[7] Rudnick, D., *Quart. Rev. Biol.*, **19**, 187–212 (1944).

[8] Bacon, R. L., *J. Exptl. Zool.*, **98**, 87–125 (1945).

[9] Herrmann, H., *Ann. N. Y. Acad. Sci.*, **55**, 99–108 (1952).

[10] Csapo, A., and Herrmann, H., *Am. J. Physiol.*, **165**, 701–710 (1951).

[11] Ebert, J. D., *J. Exptl. Zool.*, **115**, 351–377 (1950).

[12] Ebert, J. D., *Ann. N. Y. Acad. Sci.*, **55**, 67–84 (1952).

[13] Mommaerts, W. F. H. M., and Parrish, R. G., *J. Biol. Chem.*, **188**, 545–552 (1951).

[14] Kesztyus, L., Nikodemusz, S., and Szilagyi, T., *Nature*, **163**, 136 (1949).

[15] Ebert, J. D., *Physiol. Zool.*, **24**, 20–41 (1951).

[16] Martin, D. S., *J. Lab. Clin. Med.*, **28**, 1477–1482 (1943).

[17] Kabat, E., and Mayer, M., *Experimental Immunochemistry*, Charles C Thomas, Springfield, Ill., 1948.

[18] Hanks, J. H., *J. Immunol.*, **28**, 95–104 (1935).

[19] Ten Cate, G., and Van Doorenmaalen, W. J., *Koninkl. Ned. Akad. Wetenschap., Proc.*, **53**, 3–18 (1950).

[20] Miller, G., Golder, R. H., Eitelman, E., and Miller, E., *Arch. Biochem. and Biophys.*, **41**, 125–137 (1952).

[21] Snellman, O., and Gelotte, B., *Exp. Cell Res.*, **1**, 234–252 (1950).

[22] Ivanov, I. I., and Kasinova, B. S., *Doklady Akad. Nauk. S. S. R.*, **60**, 417 (1948).

[23] Weiss, P., *Science*, **115**, 487–488 (1952).

[24] Rose, S. M., *Anat. Rec.*, **113**, 527 (suppl.) (1952).

[25] Waddington, C. H., *The Epigenetics of Birds*, Cambridge University Press, 1952.

[26] Spratt, N. T., Jr., *J. Exptl. Zool.*, **120**, 109–130 (1952).

[27] Spratt, N. T., Jr., *Ibid.*, **89**, 69–101 (1942).

[28] Olivo, O. M., *Compt. rend. assoc. anat.*, **23**, 357 (1928).

[29] Rudnick, D., *Anat. Rec.*, **70**, 351–368 (1938).

[30] Rudnick, D., *J. Exptl. Zool.*, **79**, 399–427 (1938).

[31] Daly, M. M., and Mirsky, A. E., *J. Gen. Physiol.*, **36**, 243–255 (1952).

THE STRUCTURE OF THE MACRONUCLEUS OF PARAMECIUM AURELIA*

BY R. F. KIMBALL

BIOLOGY DIVISION, OAK RIDGE NATIONAL LABORATORY, OAK RIDGE, TENNESSEE

Communicated by T. M. Sonneborn, February 2, 1953

Two types of bodies can be seen in the macronucleus of living *Paramecium aurelia* by phase-microscope observations.[1] One consists of spherical granules, about 1 μ in diameter, scattered more or less at random. The other type is seen only when the macronucleus is broken by compression. It consists of what appear to be many fine filaments, almost completely filling the nucleus. However, the filaments are so near the limits of resolution that their form cannot be determined with certainty.

Paramecia exposed to lethal doses of ultraviolet radiation show a typical series of changes in the larger granules over the course of the several hours before death.[2] The granules clump together and fuse into one or a few large vacuolated masses. All stages in this fusion process can be followed in living material. The filaments are not visibly altered and remain uniformly distributed even after the granules have clumped into one large body. On the basis of the similarity of this behavior of the granules to the known reaction of nucleoli of other organisms to radiation, Kimball[1] tentatively concluded that they were nucleoli and the filaments were chromosomes.

Confirmation has been obtained for this interpretation by staining reactions. Animals of stock 90 of variety 1 were exposed to ultra-violet from a germicidal lamp and fixed in one per cent osmic acid after observations on living animals showed that the granules had fused into large masses Controls were also fixed at this time. Osmic acid was used as the fixative since observations under the phase microscope showed that, of all the fixatives tried, only osmic acid did not seriously alter the vacuolated fusion masses. The fixed material was dehydrated and embedded in paraffin. Two-micron-thick sections were cut and stained either with the Feulgen-light green procedure following Rafalco[3] and Conn and Darrow[4] or the pyronin-methyl green procedure according to Lee.[5]

Examination of the stained sections of the irradiated animals showed that the fusion masses were stained with light green or pyronin, while the rest of the macronucleus was uniformly stained with Feulgen or methyl green. In control animals, light-green- or pyronin-stained material appeared to be scattered throughout the macronucleus, giving the Feulgen or methyl-green staining a spongy appearance quite different from the uniform texture in the irradiated macronucleus. However, it was not possible to recognize with certainty distinct granules stained with the acid dye. Thus

the granules, which were so clearly visible in the living macronucleus, were no longer clear in the fixed nucleus, and the only evidence for them was scattered distribution of the acid staining. However, this scattered distribution and the results from the observations on living animals and on irradiated animals combine to make it clear that there are many small nucleoli scattered throughout the macronucleus. Apparently, the rest of its volume is largely occupied by many small chromosomes.

It is of interest that an essentially identical interpretation of the structure of the macronucleus was reached by Breitschneider[6] on the basis of electron-microscope observations of sections of *Paramecium caudatum*. He saw many irregularly spherical bodies, connected by thin strands, and fewer larger bodies approximately 1 μ in diameter. He interpreted the former as chromosomes, and the latter as nucleoli. No proof was offered for these identifications.

The macronucleus has been considered polyploid (see Sonneborn[7] for review) or a multiple structure consisting of a number of subunits each of which is, perhaps, diploid.[8] The latter interpretation was based upon evidence from macronuclear regeneration taken in conjunction with genetic considerations. It is supported by Moses' evidence[9] that there is only about 40× as much DNA in the macronucleus as in the micronucleus of *Paramecium caudatum* and by Nanney's work on mating types as given by Sonneborn.[10] In the present work, no evidence was found for subunits, and all the observations were consistent with the hypothesis of polyploidy with no subunits. It is not clear whether this means that the connections between the chromosomes of a subunit are too fine and diffuse to be observed with the techniques which have been used or whether the evidence which suggests subunits must be reinterpreted.

The published observations on the ciliate macronucleus suggest at least two kinds of structure. In a number of cases, scattered acid-stained granules are reported more or less as in the present paper. However, another group of observations indicate that large Feulgen-positive bodies are scattered throughout the nucleus, e.g., Turner[11] for *Euplotes*. These large Feulgen-positive bodies are not readily homologized with the structures seen in the vegetative macronucleus of Paramecium. Commonly used fixatives, such as Schaudinn's, produce considerable alteration in the structure of the macronucleus. Thus final judgment about Feulgen-positive bodies must be reserved until careful comparisons have been made between living and fixed material. Nevertheless, it seems probable that such bodies exist and must be taken into account in any generalized scheme of the structure and function of the macronucleus. The writer is unable to offer a satisfactory hypothesis to account for them.

* Work performed under Contract No. W-7405-eng-26 for the Atomic Energy Commission.

[1] Kimball, R. F., *Anat. Rec.*, **105,** 543 (1949).

[2] Kimball, R. F., and Gaither, N., *J. Cell. Comp. Physiol.* **37,** 211–234 (1951).

[3] Rafalco, J. S., *Stain Technol.*, **21,** 91–93 (1946).

[4] Conn, H. J., and Darrow, M. A., *Staining Procedures Used by the Biological Stain Commission, Inc.*, Biotech Publications, Geneva, N. Y., IIB-14I–IB-15, (1946).

[5] Lee, A. B., *The Microtomist's Vade-Mecum*, 10th ed., The Blakiston Co., Philadelphia, 165, (1937).

[6] Breitschneider, L. H., *Mikroskopie*, **5,** 257–269 (1950).

[7] Sonneborn, T. M., *Ann. Rev. Microbiology*, **3,** 55–80 (1949).

[8] Sonneborn, T. M., *Adv. in Genetics*, **1,** 263–358 (1947).

[9] Moses, M. J., *J. Morphol.*, **87,** 493–536 (1950).

[10] Sonneborn, T. M., *Cold Spring Harbor Symposia*, **16,** 481–503 (1951).

[11] Turner, J. P., *Univ. Calif. Publ. Zool.*, **33,** 193–258 (1930).

INFORMATION TO CONTRIBUTORS

THE PROCEEDINGS is the official organ of the NATIONAL ACADEMY OF SCIENCES and of the NATIONAL RESEARCH COUNCIL for the publication of brief accounts of important current researches of members of the ACADEMY and of the COUNCIL and of other American investigators. The PROCEEDINGS will aim especially to secure prompt publication of original announcements of discoveries and wide circulation of the results of American research among investigators in other countries and in all branches of science.

ARTICLES should be brief. The viewpoint should be comprehensive in giving the relation of the paper to previous publications of the author or of others and in exhibiting, where practicable, the significance of the work for other branches of science. Elaborate technical details of the work and long tables of data should be avoided, but authors should be precise in making clear the new results and should give some record of the methods and data upon which they are based.

MANUSCRIPTS should be prepared with a current number of the PROCEEDINGS as a model in matters of form, and should be typewritten in duplicate with double spacing, the author retaining one copy. Illustrations should be confined to text figures of simple character, though more elaborate illustration may be allowed in special instances to authors willing to pay for their preparation and insertion. Particular attention should be given to arranging tabular matter in a simple and concise manner.

REFERENCES to literature, numbered consecutively, will be placed at the end of the article and short footnotes should be avoided. It is suggested that references to periodicals be furnished in some detail and in general in accordance with the standard adopted for the Subject Catalogue of the International Catalog of Scientific Literature, viz., name of author, with initials following (ordinarily omitting title of paper), abbreviated name of Journal, with place of publication, series (if any), volume, inclusive pages, year. For example: Montgomery, T. H., *J. Morph.*, Boston, 22, 731–815 (1911); or, Wheeler, W. M., *Konigsberg, Schr. physik. Ges.*, 25, 1–142 (1914).

MANUSCRIPTS will be accepted only from members of the Academy or from chairmen of the divisions of the National Research Council who will assume responsibility for the propriety and scientific standards of the paper and should be addressed to *Proceedings of the* NATIONAL ACADEMY OF SCIENCES, *2101 Constitution Ave., Washington, 25, D. C. Articles of which a member of the Academy is author or a co-author may extend to twelve printed pages, those by non-members only to six printed pages; space above these limits will be billed to the author at $17.50 per page.*

PROOF will ordinarily be sent,—with the understanding that charges for an author's correction shall be billed to him. Authors are therefore requested to make final revisions on the typewritten manuscripts.

REPRINTS should be ordered at the time of submission of manuscript They will be furnished to authors at cost, approximately as follows:

SCHEDULE OF RATES FOR REPRINTS, CARRIAGE CHARGES EXTRA

No. Copies	50	100	150	200	250
4 pp.	4.90	5.60	6.30	7.00	7.70
8 pp.	9.80	11.20	12.60	14.00	15.40
Covers	3.75	4.80	5.85	6.90	7.95

CONTENTS

Page

BACTERIOLOGY.—OXIDATION OF INTERMEDIATES OF THE TRICARBOXYLIC ACID CYCLE BY EXTRACTS OF *Azotobacter Agile*. . . . . *By Roy Repaske and P. W. Wilson* 225

BIOCHEMISTRY.—A BIOCHEMICALLY SPECIFIC METHOD FOR ENZYME ISOLATION . . . . . *By Leonard S. Lerman* 232

CHEMISTRY.—THE SOLUBILITY OF THE DIMETHYLETHERATE OF ALUMINUM BROMIDE IN METHYL BROMIDE IN THE PRESENCE OF SATURATED HYDROCARBONS . . . . . *By Luther M. Foster and Charles A. Kraus* 236

CHEMISTRY.—THE POTENTIAL USEFULNESS OF NATURAL TRITIUM . . . . . *By W. F. Libby* 245

CHEMISTRY.—TWO PLEATED-SHEET CONFIGURATIONS OF POLYPEPTIDE CHAINS INVOLVING BOTH CIS AND TRANS AMIDE GROUPS . . . . . *By Linus Pauling and Robert B. Corey* 247

CHEMISTRY.—TWO RIPPLED-SHEET CONFIGURATIONS OF POLYPEPTIDE CHAINS, AND A NOTE ABOUT THE PLEATED SHEETS. . . . . *By Linus Pauling and Robert B. Corey* 253

ENGINEERING.—ON THE INCLINATION OF PLASTIC SLIP BANDS IN FLAT BARS IN TENSION TESTS . . . . . *By T. Y. Thomas* 257

ENGINEERING.—THE EFFECT OF COMPRESSIBILITY ON THE INCLINATION OF PLASTIC SLIP BANDS IN FLAT BARS . . . . . *By T. Y. Thomas* 266

ENGINEERING.—NONLINEAR MULTIPOLES . . . . . *By L. A. Zadeh* 274

GENETICS.—A STUDY OF MUTABILITY IN STREPTOMYCIN-DEPENDENT STRAINS OF *Escherichia Coli*. . . . . *By Edgar L. Labrum* 280

GENETICS.—INDUCED POLLEN LETHALS FROM SEEDS OF *Datura Stramonium* TREATED WITH THERMAL NEUTRONS . . . . . *By J. L. Spencer, W. R. Singleton, and A. F. Blakeslee* 288

GENETICS.—THE EFFECT OF THERMAL NEUTRON RADIATION ON THE CHROMOSOMES OF *Datura* . . . . . *By Henry T. Yost, Jr., W. R. Singleton, and A. F. Blakeslee* 292

MATHEMATICS.—ON SOME VARIATIONAL PROBLEMS OCCURRING IN THE THEORY OF DYNAMIC PROGRAMMING . . . . . *By Richard Bellman, Irving Glicksberg, and Oliver Gross* 298

MATHEMATICS.—FOURIER TRANSFORMS OF TIME SERIES . . *By S. Bochner* 302

MATHEMATICS.—ON THE BASIS THEOREM FOR FINITE ABELIAN GROUPS: IV . . . . . *By Jesse Douglas* 307

MATHEMATICS.—GAMES WITH EQUILIBRIUM POINTS . . . . . *By Richard Otter and John Dunne* 310

MATHEMATICS.—ON THE NUMBER OF HUSIMI TREES, I. . . . . *By Frank Harary and George E. Uhlenbeck* 315

MATHEMATICS.—STUDIES IN THE CONFORMAL MAPPING OF RIEMANN SURFACES, I. . . . . *By Maurice Heins* 322

MATHEMATICS.—THE PARAMETRISATION AND ELEMENT OF VOLUME OF THE UNITARY SYMPLECTIC GROUP . . . . . *By F. D. Murnaghan* 324

MATHEMATICS.—HEAT CONDUCTION ON ARBITRARY RIEMANNIAN MANIFOLDS . . . . . *By D. C. Spencer* 327

MATHEMATICS.—ABSOLUTE VALUED ALGEBRAS . . . . *By Fred B. Wright* 330

ZOOLOGY.—AN ANALYSIS OF THE SYNTHESIS AND DISTRIBUTION OF THE CONTRACTILE PROTEIN, MYOSIN, IN THE DEVELOPMENT OF THE HEART . . . . . *By James D. Ebert* 333

ZOOLOGY.—THE STRUCTURE OF THE MACRONUCLEUS OF *Paramecium Aurelia* . . . . . *By R. F. Kimball* 345